

INSTITUTO UNIVERSITÁRIO DE LISBOA

Development of integraded platform for planning terrestrial and satellite communication systems

Eduardo Filipe da Cruz Mota Ferreira

Masters in Computer Engineering

Supervisor:

Doctor Pedro Joaquim Amaro Sebastião, Assistant Professor Iscte - Instituto Universitário de Lisboa

Co-Supervisor:

Doctor Francisco António Bucho Cercas, Full Professor Iscte - Instituto Universitário de Lisboa

October, 2022



Department of Information Science and Technology

Development of integraded platform for planning terrestrial and satellite communication systems

Eduardo Filipe da Cruz Mota Ferreira

Masters in Computer Engineering

Supervisor:

Doctor Pedro Joaquim Amaro Sebastião, Assistant Professor Iscte - Instituto Universitário de Lisboa

Co-Supervisor:

Doctor Francisco António Bucho Cercas, Full Professor Iscte - Instituto Universitário de Lisboa

October, 2022

Acknowledgements

Firstly, I would like to thank my family and specially my parents, for the unconditional support, words of guidance and for always pushing me to be the best I can be.

To my friends at Iscte-iul for the memories shared in this last 5 years and for always being available to create new ones.

I would also like to thank Dr. Pedro Sebastião and Dr. Francisco Cercas for accepting to take this challenge with me and for all the knowledge, guidance and time allocated for this dissertation to be possible.

Lastly, I extend my gratitude to the Portuguese Army Directorate of Communications and Information System, for their contribution in this dissertation with their expertise and openness to help improve the work presented.

Resumo

Esta dissertação tem como principal objetivo o desenvolvimento de uma ferramenta que permite o planeamento de ligações rádio terrestres e espaciais, considerando as recomendações mais recentes da ITU-R e garantindo os requisitos internacionais.

A ferramenta desenvolvida apresenta elevado valor educacional, tendo sido desenvolvida com o objetivo de ajudar os alunos de engenharia a melhor compreender os efeitos que as suas escolhas apresentam no planeamento destes projetos, estabelecendo as sinergias necessárias entre o que é aprendido nas aulas com o planeamento de projetos no mundo profissional.

No processo de desenvolvimento, a utilização desta ferramenta no setor profissional foi considerada, pretendendo reduzir o tempo consumido no planeamento destes sistemas, que consideram vários efeitos para o um projeto eficaz a ser implementado. Para assegurar a facilidade de utilização da ferramenta proposta, testes de usabilidade foram realizados com a ajuda da Direção de Comunicações e Sistemas de Informação do Exército português, que também propôs a adição de funcionalidades, consideradas vantajosas para o uso no setor profissional.

A ferramenta apresenta um dimensionamento passo-a-passo, distribuídos em blocos interconectados entre si, permitindo perceber a influência de cada passo no planeamento do sistema por completo.

A ferramenta foi desenvolvida usando tecnologias Web, oferecendo uma visualização 3-Dimensional do mundo, permitindo fazer a análise de caraterísticas especificas de cada ligação utilizando a informação obtida através de algoritmos de ray-tracing inovadores, que analisam todos os elementos presentes no trajeto.

Recorrendo informação distribuída pela CelesTrak, esta ferramenta permite a planificação de sistemas de comunicação espacial utilizando mais de 3000 orbitas de satélite.

Palavras-Chave: Propagação Radio, Ferramenta de Planeamento, Ligações Satélite, Ligações Terrestres.

Abstract

The main goal of this dissertation is the development of a software tool that allows the design of terrestrial and spacial microwave radio link, implementing the most recent ITU-R recommendations and meeting the international standards.

The presented tool upholds a strong educational value, being developed having a goal to help engineering students the effects of their choices on a project design, establishing the synergies between the classroom and the methods learned inside it and the design of link projects in the professional sector.

The development process also took in mind the possibility of the presented tool being used in the professional sector, having the goal to decrease the time taken to design this complex systems. In order to assure that the proposed tool is easy to use, usability testing was done with the help of the Portuguese Army Directorate of Communications and Information Systems, who also helped with suggestions for additional features, that were found helpful for professional users.

The tool presents a step-by-step project design layout, having each step being integrated inside blocks that interconnect with each other to evaluate the influence of a step in the entire system design.

This tool was developed using Web programming languages, providing a 3-Dimensional world view and is capable to analyze site specific characteristics with the help of developed innovative ray-tracing algorithms that analyze all elements presented in a project site.

Using information distributed by CelesTrak, the presented tool allows the design of spacial communication systems with over 3000 satellite orbits.

Keywords: Radio Propagation, Software Planning Tool, Terrestrial Microwave Link, Spacial Microwave Link.

Contents

Acknowledgements	i
Resumo	iii
Abstract	v
List of Figures	ix
List of Tables	xiii
Acronyms	xv
Chapter 1. Introduction	1
1.1. Motivation	2
1.2. Research Questions	2
1.3. Objectives	3
1.4. Methodology	3
1.5. Dissertation Structure	5
1.6. Research Plan	5
1.7. Contributions	6
Chapter 2. Related Work	9
2.1. Usability Testing	9
2.2. User Experience	9
2.3. 3-Dimensional World Visualization	10
2.4. Ray Tracing	12
2.5. Literature Review	13
Chapter 3. Radio-Frequency Telecommunication Systems	19

3.1. Terrestrial Communication Systems	21
3.2. Spacial Communication Systems	43
Chapter 4. Tool Development and Optimization	53
4.1. Technologies	53
4.2. Tool Main structure	54
4.3. Project creation	55
4.4. File System Architecture	56
4.5. Terrestrial Communication Systems	57
4.6. Satellite Communication Systems	75
4.7. Tool Optimization	81
Chapter 5. Case Study	87
5.1. Terrestrial project	87
5.2. Spacial project	93
Chapter 6. Conclusions	97
6.1. Main conclusions	97
6.2. Future work	98
References	99

List of Figures

1	DSRM overview based on Peffers, Ken, et al. "A design science research methodology for	
	information systems research." [5]	4
2	Google Earth's visualization of the end of the Vasco da Gama's bridge	11
3	WRDL 3D Maps' visualization of the end of the Vasco da Gama's bridge	11
4	Cesium's visualization of the end of the Vasco da Gama's bridge	12
5	Ray Tracing basic concept - Christen, Martin. "Ray tracing on GPU." Master's thesis,	
	Univ. of Applied Sciences Basel (FHBB), Jan 19 (2005).	13
6	LINKPlanner - Example of a system architecture	14
7	MLinkPlanner demonstration with 2-Dimensional building and terrain detection	15
8	Smart Link Planning Tool initial project page with referred numbered step process (left	
	side)	17
9	Common terrestrial RF communication system [26]	19
10	Common spacial RF communication system [27]	20
11	Example of an antenna radiation pattern in a 3-dimensional view presented by C. A.	
	Balanis in [32]	22
12	Example of antenna radiation pattern divided in 2 separate axis	22
13	Representation of elements for calculation of v [37]	26
14	Elements considered for double isolated edges model [37]	26
15	Signal reflection coordinates system, as presented by C.Salema in [29]]	33
16	Verification process for addition of diversity and equalization	39
17	Orbit Keplerian elements [48]	45

18 TLE elements example for satellite NOAA 6 [49]	45
19 Tool Design prototype	54
20 Flow chart for new project creation process	55
21 Side-menu project selector	5:
22 Example of step window	50
23 Path selection window	58
24 Antenna 3D model	59
25 Flow chart for antenna model addition process	60
26 Point elements for passive repeater addition presented by C.Salema in [29]	60
27 Antenna characteristics step window for terrestrial systems	6
28 Radiation pattern window for terrestrial projects antennas	6.
29 Radio elements dependencies flow chart	62
30 System frequency step window	62
31 Digital signal characteristics step window	63
32 Modulation characteristics step window	6.
33 Example of latitude and longitude tree search	64
34 Example of error found on point clamping algorithm	6.5
35 Elements used to check if a point is inside a Fresnel Ellipsoid	63
36 Elements for approximated normal calculations	6'
37 Results of approximated normals	6
38 Depth search used in complete ray-tracing algorithm	68
39 Relation between number of analyzed deep searched entities and execution time	69
40 Algorithm progress window	70
41 Obstacles attenuation step window for terrestrial projects	70
42 Atmospheric attenuation step window for terrestrial projects	70
43 Rain attenuation step window for terrestrial projects	7

44 Unavailability distribution step window for terrestrial projects	71
45 Fast fading step window for terrestrial projects	71
46 SNR in IPC step window for terrestrial projects	72
47 QoS components of terrestrial projects flow chart	73
48 QoS parameters step window for terrestrial communication systems	73
49 Critical margins step window	74
50 Diversity step window	75
51 Stations characteristics step window for spacial projects	76
52 Possibilities for signal blockage due to earth surface	77
53 Orbit definition step window	78
54 Satellite characteristics step window	78
55 System frequency step window for spacial project	79
56 Digital signal characteristics step window for Spacial projects	79
57 QoS parameters step window for spacial communication systems	80
58 Interference parameters step window	80
59 Satellite project link budget step window	81
60 Invalid input error message	82
61 Step by Step project buttons	82
62 Step by step project layout option	83
63 Professional project layout option	84
64 Project step display feature	85
65 Simulated terrestrial project link	88
66 Radiation pattern selected for terrestrial project demonstration	88
67 Simulated terrestrial project link with passive repeater	89
68 Critical margins evolution through increased communication frequency for simulate	d
terrestrial project	91

List of Tables

l	Research chronogram	5
2	Comparison amongst the researched tools and developed tool	17
3	IEEE frequency bands [28]	20
4	Simulated terrestrial link characteristics	87
5	Weather characteristics in simulated transmission antenna	89
6	Path attenuations for simulated terrestrial system	89
7	Passive repeater characteristics for simulated terrestrial project	90
8	System elements with passive repeater addition for simulated terrestrial project	90
9	Project clauses fulfilment for simulated terrestrial project	90
10	Project clauses critical margins for simulated terrestrial project	91
11	Diversity and Equalization characteristics for simulated terrestrial project	92
12	Project clauses critical margins for simulated terrestrial project using diversity and	
	equalization	92
13	Equipment reliability elements for simulated terrestrial project	93
14	Simulated spacial link characteristics	93
15	Main Keplerian elements of used satellite orbit for simulated spacial project	94
16	Satellite characteristics used in simulated spacial project	94
17	Satellite characteristics for simulated spacial project	94
18	Weather characteristics in antennas positions for simulated spacial project	95
19	Path attenuations for simulated spacial system	95

Acronyms

API Application Programming Interface

BBER Background Block Error Ratio

BER Bit Error Ratio

BPF Bandpass Filter

CAP-EX Capital Expenditure

CSV Comma-Separated Values

CSS Cascading Style Sheets

DSRM Design Science Research Methodology

ECF Earth-Centered Earth-Fixed

ECI Earth-Centered Inertial

EPO Error Performance Objective

ESR Errored Second Ratio

ETA Expected Time of Arrival

HCI Human-Computer Interaction

HTML Hypertext Markup Language

IEEE Institute of Electrical and Electronics Engineers

IFF Intermediate Frequency Filter

IPC Ideal Propagation Conditions

ITU-R International Telecommunication Union Radiocommunication Sector

ITU-T International Telecommunication Union Telecommunication Sector

JSON JavaScript Object Notation

LNA Low Noise Amplifier

LoS Line of Sight

MTBF Mean Time Between Failures

MTTR Mean Time To Repair

NPM Node Package Manager

OP-EX Operational Expenditure

OSM Open Street Maps

OSS Open Source Software

PA Power Amplifier

PSK Phase-shift keying

QAM Quadrature Amplitude Modulation

QoS Quality of Service

RBER Residual Bit Error Ratio

RF Radio-Frequency

SESR Severely Errored Second Ratio

SLPT Smart Link Planning Tool

SNR Signal-Noise Ratio

TIN Triangulated Irregular Networks

TLE Two-Line Element Set

TWTA Traveling-Wave Tube Amplifier

URL Uniform Resource Locators

UX User Experience

CHAPTER 1

Introduction

As the world moves towards an increasing need for connection among each other, systems that provide this possibility have left a major footprint on the day-to-day life. As a consequence, telecommunication and network engineers need access to easy-to-use tools, in a way that provides analyses of the complex systems used [I].

Terrestrial and spacial radio frequency and microwaves systems are commonly used to connect services for radio and television, providing a peer-to-peer link, used to transmit data from one point to another, introducing advantages for long distance communication [2], e.g.:

- High portability
- Easy to install
- Lower installation costs in Capital Expenditure (CAP-EX) and Operational Expenditure (OP-EX)
- Lower Mean Time to Repair (MTTR)
- Lower energy consumption

The design of this type of systems is a methodical and time-consuming process that requires calculations such as attenuation, fading, margins, frequency planning, and evaluation of the Line-of-Sight (LoS) in said link, following the International Telecommunication Union Radiocommunication Sector (ITU-R) recommendations. This recommendations make up a collection of international technical specifications, used to estimate the influence of the link path on the link itself.

To analyse "what if" scenarios, a main estimate of this calculations is made, allowing to evaluate the reliability of the designed link. This estimate is denominated link budget [3]. Since the change of a single characteristic can impose itself in the whole link budget, a recalculation of the ITU-R standard models is in order. As a consequence, a constant manual recalculation of this models becomes impractical for engineering sectors.

In the academic field, the ability to provide an application of the methods studied can be a valuable asset in gaining a greater grasp, not only of the methods themselves, but also how they evolve in a change of scenario. For this reason, being able to provide an easy to understand demonstration of the process required for the design of systems, adds high educational value for engineering academic subjects.

1.1. Motivation

Even though there are tools already on the market that provide the majority of the necessary functions, these programs have several drawbacks, such as:

- Unaffordable licensing for engineering students As the licensing price can go over US \$300 monthly, being unbearable for the common student or academic institutions;
- **Poor User Experience** As a result of trying to fit a higher number of possible features, evolving on the necessity to train users on how to use these tools;
- The need of external software usage Requiring users to face multiple installation processes and to adapt to different layouts and mechanisms;
- **Usage outdated standards** As new standards are published and old ones become deprecated, needing to update the software;
- Reduced outputs Removing educational value.

Furthermore, the majority of this tools are deployed as black boxes, meaning that any of the source code is not available to the customers or the overall public. According to Morgan & Finnegan in [4], open source software (OSS) provides great benefits in terms of reliability, security and performance of the software as it creates a better understanding of how the tool works, as well as raise awareness to some cases of malfunction.

Subsequently, it is found the need for a all-in-one, open source tool, that can provide the principal features needed to assert systems link budgets, available in an affordable price for students and without compromising on the educational value of intermediate computations.

1.2. Research Ouestions

Developing an intuitive tool that can apply complex specifications is a difficult but necessary step in assisting engineers in putting together efficient radio-frequency networks. As a result, it is necessary to respond to the following questions:

- How does this tool reduce the time spend on planning a radio frequency link?
- In the case of complications with the link connection, how does this tool improve the detection and solution of said complications?
- How does the developed tool compare with other tools, commercial and academic? What advantages it upholds?
- How accurate are the results presented?
- How easy is the developed tool to use?

1.3. Objectives

The main purpose of this research is to develop a fully automatic planning tool, able to provide the link budget of designed systems, according to the up-to-date specifications from ITU-R. The goal of this tool is to be able to shorten the time it takes engineers to compute all components of the link budget of a designed link, providing an easy-to-understand graphical user interface to be used by users with little to no instructions. This tool must account for all aspects of the real environment, including topography and urban buildings (when they appear in Line-of-Sight) as they are sometimes neglected in overly simplified models.

To assure the software usability, students and professionals in the telecommunication field were interviewed, caring out an iterative usability and user experience testing.

1.4. Methodology

To accomplish the defined objectives for this dissertation, the Design Science Research Methodology (DSRM) will be used, as it presents important principles, practises and procedures oriented to the creation of successful artifacts [5]. The DSRM, depicted in figure [1], consists of an incremental and iterative method, allowing for multiple evaluations of the artifact created and re-definitions of proposed solutions. The multiple evaluations allows feedback on the designed artifact and a greater grasp of the defined problem, resulting in the design process to be repeated [6].

The first instance of the **DSRM** consists in the problem identification and the motivation definition, providing a concrete presentation of the problem the need of a solution. This step can be seen in the sections [] and [].1]

Secondly, the DSRM proposes the definition of the general objectives of the solution, as well as what are the solution exact requirements, defined by the research questions. This step can be seen in the sections 1.3 and 1.2

In the next phase, the design and development is presented. In this phase, the theoretical methods, presented in Chapter 3, will be applied, defining the artefact. This step can be seen in Chapter 4.

In the fourth step, after presenting the solution design and development, the solution is put into practice, proving that proposed solution can resolve the defined problem. This step can be seen in Chapter 5

The next phase is where the proposed solution is evaluated. This is one of the key points for the success of the artifact created, as it is in this phase that the quality of the artifact created is measured. The transition between the steps "Design and Development" and "Evaluation" will also take into account the agile methodology of software development as proposed by Szalvay in [7], utilizing the feedback received in usability tests and interviews to reiterate the design and development process.

The final step presented in the **DSRM** is the communication of the artefact. This step entails the writing of this dissertation an other contributions carried throughout the artefact creation.

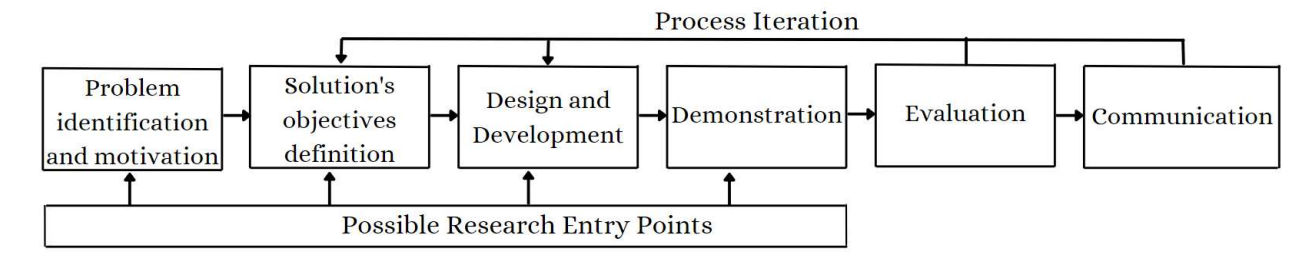


Figure 1. DSRM overview based on Peffers, Ken, et al. "A design science research methodology for information systems research." [5]

1.5. Dissertation Structure

This dissertation is presented in the following structure:

X

 \mathbf{X}

X

- Chapter 2 contains related work and literature review, presenting the softwares already available in the market:
- Chapter 3 contains the theoretical background used for the development of the presented tool, introducing the specifications needed to formulate telecommunication systems, for terrestrial and spacial links;
- Chapter 4 contains a step by step demonstration of the tool development and presentation as well as the results of the usability tests and interviews;
- Chapter 5 presents a case study of a real life system link where the developed tool is used;
- Chapter 6 contains the main conclusions of this dissertation and future work.

1.6. Research Plan

The work developed and presented in the dissertation follows the chronogram of table 1

Description Jul Out | Nov Dec | Jan | Feb | Mar Apr | May Jun Ago | Set Sep Research State of Art \mathbf{X} \mathbf{X} X Development Tool Development \mathbf{X} X X X X X X for Terrestrial Links Tool Development X X X X X X for Spacial Links **Tool Optimization** X \mathbf{X} \mathbf{X} X \mathbf{X} Demonstration and Evaluation User Usability Tests \mathbf{X} \mathbf{X} X Communication Documentation X X X X X X X X X X X X X process Thesis Writing X \mathbf{X} \mathbf{X} X \mathbf{X} X X X Papers Writing X X Supervisors meetings

Table 1. Research chronogram

For a better understanding of table 11 activities, the main goals for each activity is presented in the following list:

X

X

X

X

X

X

X

 \mathbf{X}

 \mathbf{X}

X

- **Research** This represents the first and second phase presented in the **DSRM**, being made up of the research about the tools already available in the market, as well as finding this tools benefits and withdraws;
- Development This represents the third phase of the methodology used. It is divided in the
 development of link budget calculations for terrestrial links feature and the development of
 link budget calculations for spacial links feature. Finally, in this phase is also considered
 the tool optimization, where a refactoring of some points may be done in order to get better
 results;
- **Demonstration and Evaluation** In this phase the usability tests and interviews are conducted. This tests are an essential part to improve, not only the ease-of-use of the tool, but also to acquire additional features that may be presented by the interviewee [8];
- Communication This last phase concludes the tool creation. It is composed by the writing of this dissertation, the documentation of the process allowing providing an easier process of writing this dissertation, additional contributions, through scientific papers publication, and meetings with supervisors, creating a place to change ideas, clarify doubts and receive guidance.

1.7. Contributions

The work developed in this dissertation provides the following contributions:

Papers

- Ferreira E, Sebastião P. and Cercas F., "Simplified 3D Ray Tracing Algorithms for Obstacle Detection, Signal Reflection and Diffraction Calculations in Point-To-Point Microwave Links" (To submit in an international journal)
- Ferreira E, Sebastião P. and Cercas F., "Modern and Optimized Planning Tool for Microwave and Spacial Links Design" (To submit in an international conference)

University pedagogy

Being developed with one of the goals to help engineering students to better understand the methods studied in class and how this methods effect and are effected in the design of a project link, this tool provides a step-by-step design process, allowing a better understanding of the process done in the

professional standpoint.

Technology transfer in the telecommunication industry

CHAPTER 2

Related Work

This section includes project-related work, such as the prerequisites for producing an easy-to-use tool, existing tools that have been built, and significant features to consider.

2.1. Usability Testing

Usability testing is a necessary skill for increasing a product ease-of-use [8]. Usability testing is an evaluation method in which one or more users execute tasks or communicate their objectives while being observed. The test participants are frequently requested to think out loud while executing the test activities in order to obtain information about the users cognitive processes [9]. From this tests, metrics such as "Time on task" and "Success Rate" are measured, obtaining an objective scale that can help pinpoint what areas the users found more confusing, inefficient or frustrating [10]. With this testings, the final product can assure a higher level of ease-of-use, enabling less time spent on training users on how to use the tool.

2.2. User Experience

User Experience (UX) is a concept broadly used in Human-Computer interaction (HCI) and associated with a wide range of meaning, from usability to design beauty [11] [12]. Forlizzi and Battarbee in [11] describe UX as a set of types of user-product interactions and types of experience, relating to the design of interactive systems, as follow:

- Types of user-product interactions:
 - Fluent Automatic and skilled interactions with the product;
 - Cognitive Interactions that focus on the product at hand; result in knowledge or confusion and error;
 - Expressive Interactions that help the user form a relationship to the product.
- Types of Experience:

- Experience Constant stream of "self-talk" that happens when we interact with products;
- An Experience Can be articulated or named; has a beginning and end; inspires behavioral and emotional change;
- Co-Experience Creating meaning and emotion together through product use.

This types of user-product interactions and experience are pivotal point when design a system, as is being the first to implement a technology is no longer enough [13] and the success of an system is highly influence by the experience that it induces on the user. Although [UX] is subjective and can change from user to user, usability tests are also a way to measure the [UX] of the system presented.

Since interactive systems for work use can benefit from a more experience-oriented approach [11], the types of interactions and experiences mentioned will be taken in account when developing the proposed tool.

2.3. 3-Dimensional World Visualization

The first stage in the system design process is to undertake a map analysis to discover the most likely connection locations for new sites to enter the network [14]. In this phase, terrain and buildings positions play a major role in the link reliability, has they create obstacles and signal reflections. Therefore, a simple analyses of a 2-Dimensional map does not provide enough information, creating the need to provide a 3-Dimensional view of the link path.

This visualization relies in real-time streaming of map and location data, capable to provide the user with accurate and robust 3D map of the world. This type of service is already available by many companies that offer an Application Programming Interface (API), allowing development of outside projects using this types of services. The usage of the service is enabled by an API key, that can by paid of free.

Some API's that provide 3-Dimensional world visualization are:

- Google Earth
- WRLD 3D Maps
- Cesium

Google Earth is the oldest of the services researched and also the most developed. It presents a high level of detail in major city and has data updates frequently.



Figure 2. Google Earth's visualization of the end of the Vasco da Gama's bridge

Although this service would be the best to develop the tool 3D world visualization, the Google Earth API has been deprecated since December of 2015.

The WRLD 3D Maps API provides imaging less focus on realism and more oriented on a cartoon feel, being an API developed to be used by game developers.



Figure 3. WRDL 3D Maps' visualization of the end of the Vasco da Gama's bridge

This API also does not provide total camera control to navigate the world, not enabling the user rotate the camera in the x and y-axis. This API does not have an free version able to provide 3D visualization, having a list of pricing beginning at US \$16/month at the time of this research.

Lastly, the Cesium API [15] implements the quantized-mesh-1.0 format, which allows terrains to be represented as Triangulated Irregular Networks (TIN), with the vertices coordinates quantized within the bounding box of the mesh. The complexity of the map (i.e., the number and size of triangles) responds to the variations in elevations in the scene, therefore using a this format instead of a conventional grid is a better representation of the data [16].



Figure 4. Cesium's visualization of the end of the Vasco da Gama's bridge

Even though Cesium visualization has limitations in terms of level of detail, as shown in figure the provided API is available in a free version. Cesium is also open source, enabling the option of further research when developing with this API.

2.4. Ray Tracing

As stated by Roinan Kuchkuda in [17], ray tracing algorithms are one of the most used algorithms for rendering high-quality computer graphics images. The main premise of any ray tracing algorithm is to efficiently detect intersections of a ray with a scene made up of a set of geometric primitives [18].

In telecommunication systems, ray tracing can be used to compute obstructions and reflections of the signal that may occur inside the Fresnel Zone. This concept is described as "Fresnel volume

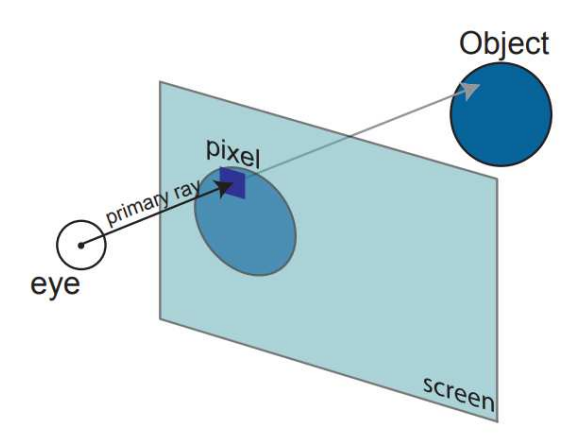


Figure 5. Ray Tracing basic concept - Christen, Martin. "Ray tracing on GPU." Master's thesis, Univ. of Applied Sciences Basel (FHBB), Jan 19 (2005).

ray tracing" by Vlastislav Červený et al. in [19], where the Fresnel volume is the three-dimensional spatial counterpart of the Fresnel zone.

2.5. Literature Review

In order to present an artifact that includes all of the most-important features, it is required a research of the currently available tools for link planning and there benefits and withdraws.

Out of all the tools already developed, the ones that provided a greater value to the tool to develop, both in the academic and engineering world are:

- LINKPlanner
- TAP 7
- MLinkPlanner 2.0
- Feixer
- Smart Link Planning Tool (SLPT)

From the tools presented, LINKPlanner [20], TAP 7 [21] and MLinkPlanner [22] are tools developed for engineering professionals, where the LINKPlanner Tool is the only *Freeware* (free software) and the remaining tools need a licensing with different ranges of price. In the other hand, Feixer [23] and [SLPT] [24] [25] are tools developed in the academic field and, subsequently, free to use.

Firstly, analysing the capabilities of LINKPlanner, this tool provides an great amount of options to create telecommunications architectures, following any structure that the user defines. The user can add "Network Sites" anywhere on the map provided (with online and offline versions) and is required to connect the sites, creating a link connection. Each network site can also be created based on a preexisting antenna configuration containing detailed antenna descriptions, sizes and gains for specific frequencies.

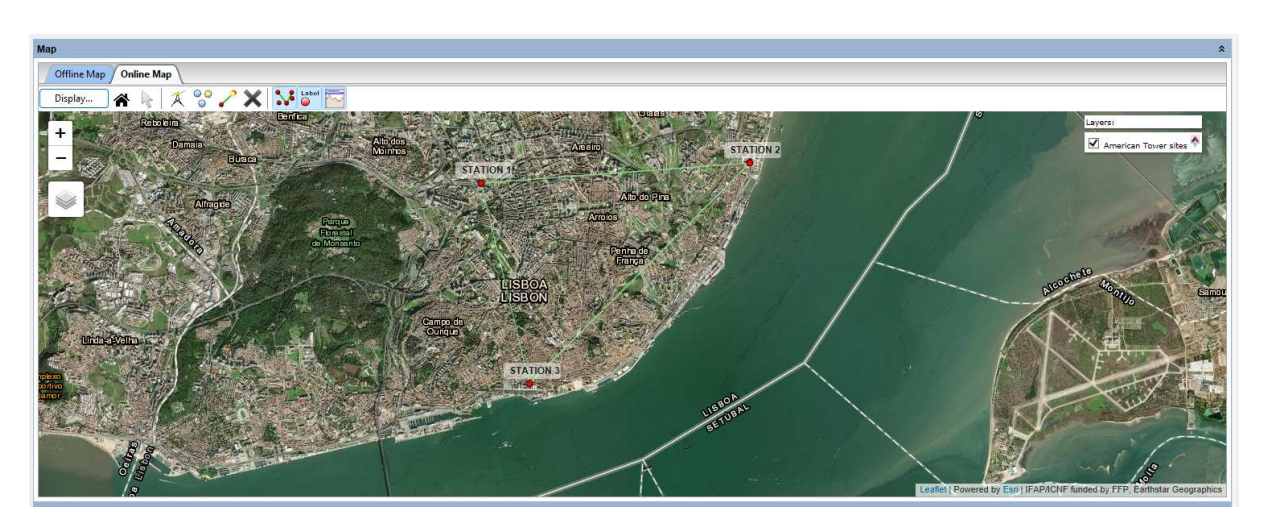


Figure 6. LINKPlanner - Example of a system architecture

Although this tool provides powerful features, it does not provide direct terrain and obstacles detection, inquiring the user to insert them manually. The tool also does not provide a user-friendly layout, making a new user, without any training, search throughout the application to find the features needed to create a site by try and error. Lastly, this tool provides a link report, containing a bill of the materials used and an installation report. Both reports mentioned are generated automatically and can be saved in a PDF file.

Secondly, examining the TAP 7 features, similarly to LINKPlanner, this tool enables the user to add antennas throughout a provided map. 3D world visualization is provided, presenting coverage calculation and obstruction detection, although it requires usage of an external software (TAP Mapper) distributed by the same company. This visualization is accomplished using the Cesium API mentioned in section 2.3 The tool also presents the option to simulate a link connection and coverage, providing the results in the 2D and 3D maps. Comparing with LINKPlanner, MAP 7

presents a friendlier layout, having well labeled feature options, with easy-to-understand icons associated with this options. The TAP 7 tool, as mentioned before, is a licensed tool, having a price range from a 30 day subscription for US \$199 to a annual subscription of US \$1999 at the time of this research, making this tool not affordable for students and academic institutions. The research made on this tool was made based on a demonstration of the software provided by the companies that produces it.

Looking at the features of MLinkPlanner, this tool enables the user to add network sites in a similar manner of the other softwares studied, and, like TAP 7, lets this sites work as part of a network with this its own architecture, while offering a study of point-to-point connections between each station. MLinkPlanner provides obstructions detection with buildings and terrain, relaying on data from open licensing world data providers like Open Street Map (OSM).

Even though building detection is presented, the data offered is limited. This case is prevalent when OSM provides data of a building, but the height of said building is unknown or undefined. In this cases MLinkPlanner lets the user define the default parameter for the height of this buildings.

As shown in figure 7, the buildings presented with the color red are buildings where no height data is given by OSM, being set to 30 meters of height by default.

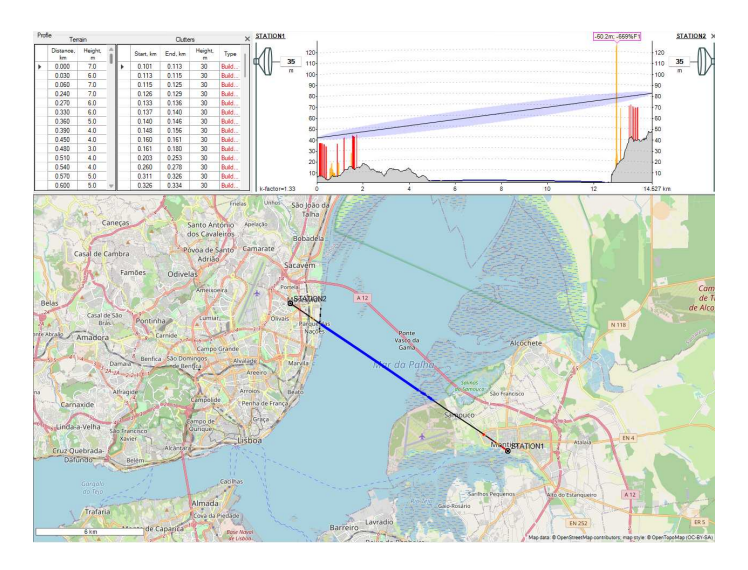


Figure 7. MLinkPlanner demonstration with 2-Dimensional building and terrain detection

Like MAP 7, MLinkPlanner is only available under licensing, with prices ranging US \$399 annually.

Examining tools developed in the academic field, Feixer is a tool developed using the software Wolfram's Mathematica, being Feixer a script meant to run on this software. This is the tool currently used in ISCTE by Telecommunications and Computer Engineering students. Although Mathematica is a licensed software, most students can find free versions of this software so they can use Feixer while in there academic time. Feixer requires the user to provide a text file containing the link path. This text file needs to follow very a specific indentation and it is usually obtained online by the students themselves. Feixer only allows users to add passive signal repeaters and when doing so, the user must acquire a new text file with the link path, passing through the added passive signal repeater. Another drawback of Feixer is that, when an code error is found, it is shown to the user in the interface. Apart from the drawbacks presented, Feixer presents an easy to understand layout, having a scroll-able walk-through of the link design planning.

Lastly, the Smart Link Planning Tool (SLPT), depicted in figure 8, is a tool dependent of the NetBeans IDE to be executed. SLPT follows the same principle of Feixer, where is required to have a text file containing the link path. Although, SLPT provides a script that can be executed by the user outside the tool itself, using the NetBeans IDE, acquiring the necessary text file. However, since the Google changes made to the API used to get the referred data, this script became outdated and can no longer be used. SLPT also provides an easy-to-follow link design workflow, presenting a numbered step process.

As presented by Damião et al. in [25], SLPT also grants numerous default values, asking for a minimum of options or parameters that are needed to characterize and achieve an adequate planning.

Some of the withdraws of SLPT regard the accuracy of the result presented when compared with the calculations following the recommendation models from TU-R In addition, SLPT does not update the results given to the user automatically when a change in the design is made. Since this tool presents the results of separate link characteristics in different windows, the distinction between what window has the updated information becomes difficult to differ.

In conclusion, table 2 summarizes the main features found vital to the tool developed in this dissertation, in comparison with the researched tools.

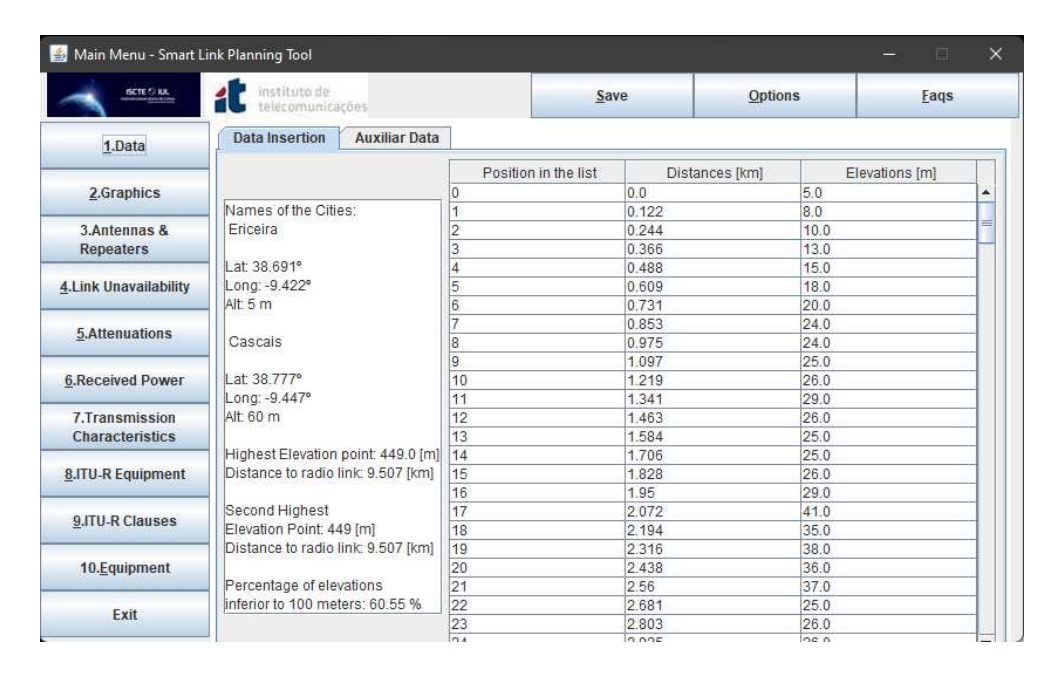


Figure 8. Smart Link Planning Tool initial project page with referred numbered step process (left side)

Table 2. Comparison amongst the researched tools and developed tool

	User- friendly	Automatic obstacle detection	3D Path analyzes	Urban building integration	Updated standards	Single software	Cost per year
LINKPlanner					X	X	Free
TAP 7	X	X	X		X	X	US\$1999
MLink- Planner 2.0		X		X		X	US\$399
Feixer		X					Free*
SLPT	X	X					Free
Developed Tool	X	X	X	X	X	X	Free

^{*}not considering the Wolfram's Mathematica licensing cost

CHAPTER 3

Radio-Frequency Telecommunication Systems

Even-though radio-frequency (RF) communication systems have been used since regularly by the general public since the beginning of the twentieth century, this technology is still broadly used as a means to communicate wirelessly between two or more points, via a one-way or two-way communication. Some examples of today's usage of this systems are:

- Audio Broadcasting of music and entertainment;
- Military and law enforcement communications;
- Television Broadcasting;
- Satellite communications;
- Intercontinental audio and video communications;
- Mobile communications.

Although the specific characteristics of one system may differ between terrestrial and spacial systems, the core of this systems can be defined in 3 parts: a transmission and reception antennas, a propagation path, and radio signal characteristics.

For terrestrial RF systems, the path grants an high level of importance, as it provides a complex problem with terrain level, nature elements (e.g., trees) and urban buildings that take a toll in the emitted signal in the form of signal diffraction and reflection. A typical terrestrial RF system is depicted in figure [9].

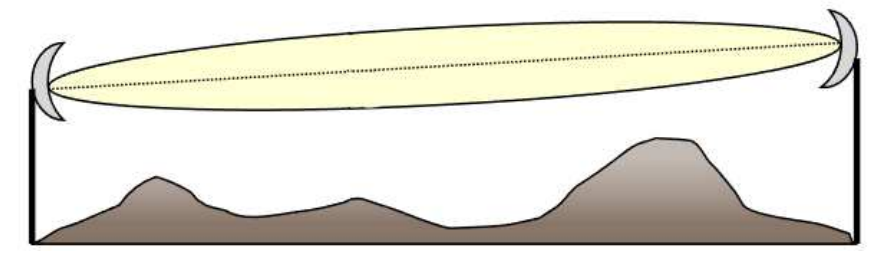


Figure 9. Common terrestrial RF communication system [26]

Contrastingly, in spacial RF systems, depicted in in figure 10, the major variable taken into account in the path pursued is the communication distance, being systems that in general have an higher free space attenuation.

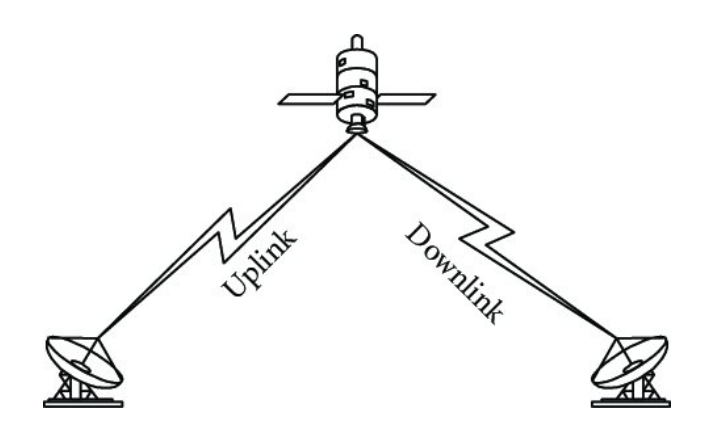


Figure 10. Common spacial RF communication system [27]

Despite the simpler system characteristics, the design of a spacial communication system requires the division of the communication system in 2 separate parts: the ascending link (uplink) and the descending link (downlink), as shown in figure [10].

The final core part of this communication systems, consisting of the radio characteristics, define the signal to be transmitted. Characteristics like bandwidth, modulation and primarily signal frequency, have a major impact in the prediction of attenuations resulted of the path the site defines. The signal frequencies are categorized by IEEE as shown in table 3.

Table 3. **IEEE** frequency bands [28]

Band	Frequency
VHF	30 to 300 MHz
UHF	300 to 1000 MHz
L	1 to 2 GHz
S	2 to 4 GHz
С	4 to 8 GHz
X	8 to 12 GHz
Ku	12 to 18 GHz
K	18 to 27 GHz
Ka	27 to 40 GHz
V	40 to 75 GHz

In the following of this chapter, it will be described the multiple components used to calculate the link budget for terrestrial and spacial communication systems, analysing how the system propagation elements affect the quality of the signal received.

3.1. Terrestrial Communication Systems

In this section, the models used to calculate the link budget for terrestrial RF communication systems will be presented.

3.1.1. Station characteristics

The definition of the characteristics of a station is an important step, as it specifies the course where the signal will be transmitted and how it will be transmitted. The position where a station is situated is optimal when it is in **LoS** with the station who is receiving the signal [29].

An antenna used in a station can be described by the following characteristics:

- Diameter (d_a) ;
- Radiation Efficiency (η) ;
- Effective Area (a_{ef}) ;
- Gain (*G*);
- Directivity.

From the characteristics referred, the gain of both the transmission antenna and receiving antenna are the most important performance parameter in a RF communication system, where small variations can have a significant impact on system overall performance [30]. Given a parabolic antenna, the gain is calculated following the equation:

$$G = 20 \cdot \log_{10} \left(\frac{\pi \cdot d_a \cdot f_{\text{[MHz]}}}{300} \right) + 10 \log_{10}(\eta)$$
 (3.1)

Where f is the communication frequency in Megahertz (MHz), resulting in the gain value in dBi.

Using the antenna efficiency and diameter, the antenna effective area can be approximated using the following equation:

$$a_{ef} \approx \eta \cdot \frac{\pi}{4} \cdot d_a^2 \tag{3.2}$$

Lastly, the antenna directivity is the variation of power density in a certain direction at a fixed distance, in reference to the power density with the same transmit power distributed isotropically, i.e., equally along all axis [30][31].

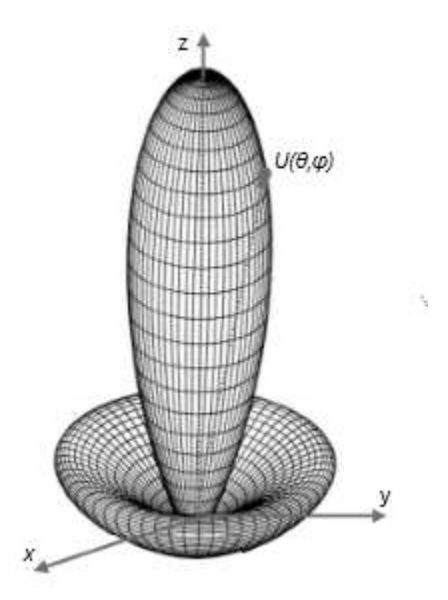


Figure 11. Example of an antenna radiation pattern in a 3-dimensional view presented by C. A. Balanis in [32]

The figure Trepresents an example of an antenna radiation pattern in a 3-Dimensional view. This representation can be viewed in a bi-dimensional plane by separating the variation of power density by orientation and elevation axis, following a polar coordinates system.

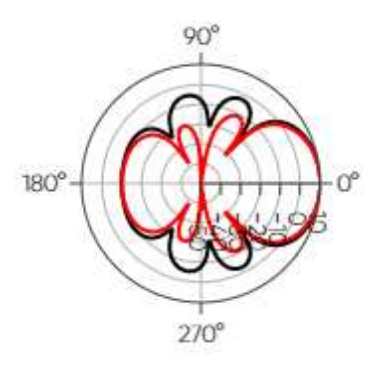


Figure 12. Example of antenna radiation pattern divided in 2 separate axis

The figure 12 represents the variation of transmit power following a orientation axis (in black) and in a elevation axis (in red). The orientation axis value can be represented by an angle θ and the

elevation axis can be represented by an angle φ . Combining this axis, the power transmit by the antenna the referred axis is represented by $U(\theta, \varphi)$, as shown in figure \square

3.1.2. Digital Signal

The characterization of the digital signal provides the definition of the amount of data that can be transmit using the system. Additionally to the signal frequency of which the signal is transmit, bit rate and bandwidth have a major importance on the system usage.

As a consequence of the base frequency used to transmit data (also known as carrier signal) being constant, a need to change the signal emitted to match the data signal is found. This process of transformation is denominated modulation. Although there are multiple types of modulation, in RF systems, the most commonly used modulation types are the Quadrature Amplitude Modulation (QAM) and Phase-shift keying (PSK). To minimize the use of bandwidth, modulations can divide the transmit data in different symbols, typically in bases of 2 (2,4,16,64), where the number of symbols used is commonly represented by m. Therefore, the minimum of bandwidth required to transmit a signal at a given bit rate is obtained by the following equation:

$$b_{rf_{min}} = \frac{f_b}{log_2(m)} \tag{3.3}$$

where f_b represents the bit rate used and m represents the number of symbols used in the modulation process. Since bandwidth is a physical characteristic that is limited and constant, the number of symbols is typically the changing factor to accommodate the system need to transmit data. Algebraically manipulating the equation 3.3, the minimum number of symbols is obtained by the following equation:

$$m_{min} = 2^{\frac{f_b}{b_{rf_{min}}}} \tag{3.4}$$

To assure that inter-symbol interference is minimal or null, an roll-off factor (β) is taken into consideration when defining the bandwidth used in a system [29]. Therefore, the bandwidth used in RF is defined as:

$$b_{rf} = (1+\beta)b_{rf_{min}} \tag{3.5}$$

3.1.3. Equipment Reliability and Availability

The TU-T Recommendation G.602 [33] defines equipment reliability as the probability of an equipment to perform its required function, given a time interval. To qualify equipment reliability, the mean time between failures (MTBF) parameter is used. In this recommendation, availability of a system is defined as the ability to operate at a given time, being influence by the reliability of the equipment that composes the system, maintenance procedures and automatic protection switching.

Given that the elements of emission (of number m) composing the system are connected in series, the MTBF of the system as a whole is obtained by the following equation [29]:

$$\frac{1}{MTBF_s} = \sum_{j=1}^m \frac{1}{MTBF_j} \tag{3.6}$$

Taken the MTBF of the system and the mean time to repair (MTTR) for a given system, the total unavailability of the system is obtained by the following equation [29]:

$$I_s = \frac{MTTR}{MTBF_s} \tag{3.7}$$

In ITU-R Recommendation F.695-0 [34], the availability objective is given by:

$$A = 100 - (0.3 \cdot L/2500)\% \tag{3.8}$$

Where L is the length between the emission antenna and reception antenna in kilometers. L is required to be between 280 km and 2500 km, using those extreme value for L in cases where the link length is lower or higher respectively.

In the cases where the system unavailability does not reach the objective, a solution is the addition of reserve channels. Using n active channels and r reserve channels, the unavailability for this configuration (denominated n+r) is described by C.Salema in [29] as follows:

$$I_p = \sum_{j=r+1}^{n+r} C_{r+1}^{n+r} I^{r+1}$$
(3.9)

3.1.4. Signal Attenuation

An approximation of the signal attenuation (also referred to as path loss) is an important segment in the design of a system, as it provides an understanding of how the path influences the signal received in relation to the signal transmit [35]. In this subsection, different components of the path will be analysed, providing approximation models for the attenuation that said components display on the signal.

3.1.4.1. Free Space Attenuation

As defined in TU-R Recommendation P.525-4 [36] free space propagation is propagation in a perfect path (i.e., without any additional attenuating entity) with an infinite length. This type of propagation is often used as a base-point for analysing a system path. For point-to-point links, the attenuation in free space is defined as:

$$L_{bf} = 32.4 + 20\log(f_{[MHz]}) + 20\log(d_{[km]})$$
(3.10)

3.1.4.2. Diffraction Attenuation

The finding of one or more obstacles is a common occurrence for RF links. Consequently, a need to determinate the losses that said obstacles cause in the signal is found [37]. The models presented in TTU-R Recommendation P.526-15 are divided by the number of obstacles found in the path and are denominated as follow:

- Single knife-edge obstacle
- Double isolated edges
- Bullington model

Firstly, the Single knife-edge obstacle, is used when a single obstacle is found in the path. This model determines that the loss for said obstacle is quantified as:

$$J(v) = -20\log\left(\frac{\sqrt{[1 - C(v) - S(v)]^2 + [C(v) - S(v)]^2}}{2}\right)$$
(3.11)

where v is defined as:

$$v = h\sqrt{\frac{2}{\lambda}\left(\frac{1}{d_1} + \frac{1}{d_2}\right)} \tag{3.12}$$

and λ is the used wavelength and h,d_1 and d_2 can be obtained following figure 13.

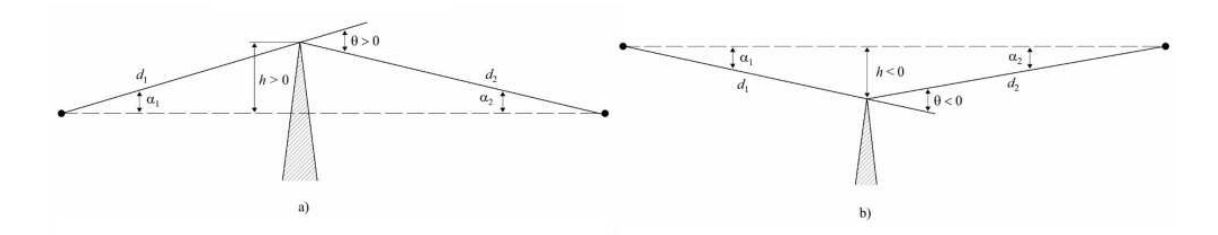


Figure 13. Representation of elements for calculation of v [37]

The functions C(v) and S(v) are defined as:

$$C(v) = \int_0^v \cos\left(\frac{\pi s^2}{2}\right) ds \tag{3.13}$$

$$S(v) = \int_0^v \sin\left(\frac{\pi s^2}{2}\right) ds \tag{3.14}$$

Secondly, the Double Isolated Edges model applies single knife-edge method by dividing the path between the 2 obstacles found, i.e., having the first obstacle act as an obstacle between an imaginary link from the transmission antenna and the second obstacle (L_1) and the second obstacle act as and obstacle between and link between the first obstacle and the reception antenna (L_2) as described in figure 14

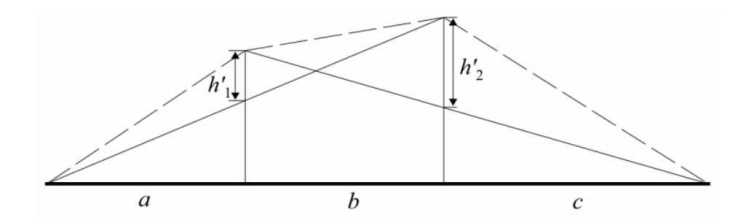


Figure 14. Elements considered for double isolated edges model [37]

In cases where the L_1 and L_2 have a value greater then 15 dB, a correction term is added, resulting in the value of loss provoked by the obstacles to be defined as:

$$L = L_1 + L_2 + L_c (3.15)$$

Where L_c is defined, using the elements provided in figure 14, as:

$$L_c = 10 \log \left[\frac{(a+b)(b+c)}{b(a+b+c)} \right]$$
 (3.16)

To account for the level of separation between both obstacles, a second correction term needs to be considered. This term is obtained by:

$$T_c = \left[12 - 20\log_{10}\left(\frac{2}{1 - \frac{\alpha}{\pi}}\right)\right] \left(\frac{q}{p}\right)^{2p} \tag{3.17}$$

where:

$$p = \left[\frac{2}{\lambda} \frac{(a+b+c)}{(b+c)a} \right]^{1/2} h_1 \tag{3.18}$$

$$q = \left[\frac{2}{\lambda} \frac{(a+b+c)}{(a+b)c} \right]^{1/2} h_2 \tag{3.19}$$

$$\tan \alpha = \left[\frac{b(a+b+c)}{ac} \right]^{1/2} \tag{3.20}$$

and h_1 and h_2 are the obstacles height. In this case, the total diffraction loss is obtained by:

$$L = L_1 + L_2 - T_c (3.21)$$

Lastly, for three or more obstacles the Bullington Model is used to approximate the level of diffraction caused by the obstacles found on the path.

In this model, the first step is to determine the intermediate profile point with the highest slope between the transmitter and the point. This step is obtained following equation [3.22]:

$$S_{tim} = \max \left[\frac{h_i + 500C_e d_i (d - d_i) - h_{ts}}{d_i} \right]$$
 (3.22)

where h_i (in meters) and d_i (in kilometers) are the height and distance of the *i-th* profile point, C_e is the effective Earth curvature (given by $1/r_e$ where r_e is the effective Earth radius in kilometers) and h_{ts} is the height of the transmitter.

Then, the slope from transmitter to receiver considering a LoS path is calculated by the following equation:

$$S_{tr} = \frac{h_{rs} - h_{ts}}{d} \tag{3.23}$$

where h_{rs} is the receiver height and d is the path length.

Given the current steps, the model is divided in two cases:

If $S_{tim} < Str$ (a LoS path) the intermediate profile point with the highest diffraction paramater v needs to be found, using the equation:

$$v_{max} = \max \left\{ \left[h_i + 500C_e d_i (d - d_i) - \frac{h_{ts} (d - d_i) + h_{rs} d_i}{d} \right] \sqrt{\frac{0.002d}{\lambda d_i (d - d_i)}} \right\}$$
(3.24)

For this case, the knife-edge loss, using equation 3.11, is given by:

$$L_{uc} = J(v_{max}) (3.25)$$

If $S_{tim} \geq S_{tr}$ (a trans-horizon path) the intermediate profile point with the highest slope of the line from the receiver to the point needs to be found, by the following equation:

$$S_{rim} = \max \left[\frac{h_i + 500C_e d_i (d - d_i) - h_{rs}}{d_i} \right]$$
 (3.26)

Given this value, the distance from the transmitter to the Bullington point is given by:

$$d_b = \frac{h_{rs} - h_{ts} + S_{rim}d}{S_{tim} + S_{rim}}$$
(3.27)

Using the distance from the transmitter to the Bullington point, the diffraction parameter is obtained by:

$$v_b = \left[h_{ts} + S_{tim} d_b - \frac{h_{ts} (d - d_b) + h_{rs} d_b}{d} \right] \sqrt{\frac{0.002d}{\lambda d_b (d - d_b)}}$$
(3.28)

For this case, the knife-edge loss, using equation 3.11, is given by:

$$L_{uc} = J(v_b) \tag{3.29}$$

For both LoS paths and trans-horizon paths, the total diffraction following the Bullington model is obtained by:

$$L_b = L_{uc} + [1 - \exp(-L_{uc}/6)](10 + 0.02d)$$
(3.30)

3.1.4.3. Atmospheric attenuation

The gases, water vapour and other small particles present in the atmosphere result in signal attenuation which, despite being minimal for smaller frequencies, can effect the system QoS, particularly for paths with a greater length [29].

The model to predict the atmospheric attenuation is described in ITU-R Recommendation P.676-13 [38] and is calculated as:

$$A_a = \gamma \cdot r_0 = 0.1820 \cdot f \cdot (N''_{Oxygen}(f) + N''_{WaterVapour}(f)) \cdot r_0$$
(3.31)

where r_0 represents the path length, $N''_{Oxygen}(f)$ and $N''_{WaterVapour}(f)$ are the imaginary parts of the frequency-dependent complex refractivities, obtained by:

$$N''_{Oxygen}(f) = \sum_{i(Oxygen)} S_i F_i + N''_D(f)$$
(3.32)

$$N_{WaterVapour}^{"}(f) = \sum_{i(WaterVapour)} S_i F_i$$
(3.33)

 S_i and F_i represent the line strength and line shape factor of the *i-th* line of tables 1 and 2 of P.676-13 respectively and is obtained by:

$$S_i = a_1 \cdot 10^{-7} \cdot p \cdot \theta^3 \cdot \exp[a_2 \cdot (1 - \theta)] \quad \text{, for oxygen}$$
 (3.34)

$$S_i = b_1 \cdot 10^{-1} \cdot e \cdot \theta^{3.5} \cdot \exp[b_2 \cdot (1 - \theta)] \quad \text{, for water vapour}$$
 (3.35)

where p represents the dry air pressure in hPa, e represents the water vapour partial pressure in hPa, θ represents a ratio of temperature given by T/300 where T represents the temperature in Kelvin.

The water vapour partial pressure is obtained by:

$$e = \frac{\rho \cdot T}{216.7} \tag{3.36}$$

where ρ represents the water vapour density

The value of F_i is given by:

$$F_i = \frac{f}{f_i} \cdot \left[\frac{\Delta f - \delta(f_i - f)}{(f_i - f)^2 + \Delta f^2} + \frac{\Delta f - \delta(f_i + f)}{(f_i + f)^2 + \Delta f^2} \right]$$
(3.37)

where f_i represents the oxygen and water vapour line frequency presented in table 1 and table 2 in ITU-R Recommendation P.676-13 and Δf represents the line width obtained by:

$$\Delta f = a_3 \cdot 10^{-4} (p \cdot \theta^{(0.8-a_4)} + 1.1 \cdot e \cdot \theta)$$
, for oxygen (3.38)

$$\Delta f = b_3 \cdot 10^{-4} (p \cdot \theta^{b_4} + b_5 \cdot e \cdot \theta^{b_6}) \quad \text{, for water vapour}$$
 (3.39)

Taking into account the Zeeman splitting of oxygen lines and Doppler broadening of water vapour lines the value of the line width is modified to:

$$\Delta f = \sqrt{\Delta f^2 + 2.25 \cdot 10^{-6}}$$
 , for oxygen (3.40)

$$\Delta f = 0.535 \Delta f + \sqrt{0.217 \Delta f^2 + \frac{2.1316 \cdot 10^{-12} f_i^2}{\theta}} \quad \text{, for water vapour} \qquad (3.41)$$

 δ represents the correction factor due to interference effects in oxygen lines, obtained by:

$$\delta = (a_5 + a_6 \cdot \theta) \cdot 10^{-4} \cdot (p + e) \cdot \theta^{0.8}$$
 , for oxygen (3.42)

For Water Vapour lines, the value of δ is equal to zero.

In equation 3.32, the element $N_D''(f)$ represents the dry continuum due to pressure-induced nitrogen absorption and the Debye spectrum and is calculated as:

$$N_D''(f) = f \cdot p \cdot \theta^2 \cdot \left[\frac{6.14 \cdot 10^{-5}}{d \cdot \left[1 + \left(\frac{f}{d} \right)^2 \right]} + \frac{1.4 \cdot 10^{-12} \cdot p \cdot \theta^{1.5}}{1 + 1.9 \cdot 10^{-5} \cdot f^{1.5}} \right]$$
(3.43)

where d represents the width parameter for Debye spectrum and is obtained by:

$$d = 5.6 \cdot 10^{-4} \cdot (p+e) \cdot \theta^{0.8} \tag{3.44}$$

The values of a_1 through a_6 and b_1 through b_6 can be found in table 1 and table 2 of P.676-13.

3.1.4.4. Rain Attenuation

As defined in $\boxed{\text{TU-R}}$ Recommendation P.838-3 $\boxed{39}$, the attenuation due to rain in relation to rain rate R is obtained by:

$$A_r = d \cdot \gamma_R = d \cdot kR^{\alpha} \tag{3.45}$$

where the coefficients k and α are obtained, in cases of frequencies between 1 and 1 000 GHz, as:

$$\log_{10} k = \sum_{j=1}^{4} \left(a_j \exp\left[-\left(\frac{\log_{10} f - b_j}{c_j} \right)^2 \right] \right) + m_k \log_{10} f + c_k$$
 (3.46)

$$\alpha = \sum_{j=1}^{5} \left(a_j \exp \left[-\left(\frac{\log_{10} f - b_j}{c_j} \right)^2 \right] \right) + m_\alpha \log_{10} f + c_\alpha$$
 (3.47)

The values to the constants a_j , b_j , c_j , m_k , m_α , c_k and c_α follow the tables 1 through 4 in Recommendation P.838-3[39].

3.1.4.5. Signal Fading

In order to obtain the percentage of time where any fade depth is exceeded it was used the method for all percentages of time defined in ITU-R Recommendation P.530-18 [40]. Firstly, the method for small percentages of time is taken to account, defining the magnitude of the path inclination $|\varepsilon_p|$ and mean path terrain clearance h_c as:

$$|\varepsilon_p| - \frac{|h_r - h_e|}{d} \tag{3.48}$$

$$h_c = \frac{h_r + h_e}{2} - \frac{d^2}{102} - h_t \tag{3.49}$$

where h_e and h_r are the emission and reception antenna height (respectively), d is the path length in km and h_t the mean terrain elevation along the path. Given the mean path terrain clearance, the subrefractive parameter v_{sr} is given by:

$$v_{sr} = \min\left\{ \left(\frac{dN_{75}}{50} \right)^{1.8} \exp\left[-\frac{h_c}{2.5\sqrt{d}} \right], v_{srlimit} \right\}$$
 (3.50)

being limited by a minimum value described as:

$$v_{sr-limit} = \frac{dN_{75}d^{1.5}f^{0.5}}{24730} \tag{3.51}$$

Parameter dN_{75} represents an empirical prediction of 0.1% increase of refractivity for the average worst month, with a minimum height of 75 meters. The values for this parameter can be found in a digital map, provided in the P.530-18 Recommendation.

As a parameter influenced by the subrefractive parameter, the multipath occurrence factor is obtained by:

$$p_0 = Kd^{3.51}(f^2 + 13)^{0.447} \cdot 10^{-0.376 \tanh\left(\frac{h_c - 147}{125}\right) - 0.3345|\varepsilon_p|^{0.39} - 0.00027h_L + 17.85v_{sr}}$$
(3.52)

Following, the value of fade depth A_t is calculated using the following equation:

$$A_t = 25 + 1.2\log p_0 \tag{3.53}$$

Given a required fade depth A (typically between 25dB and 35dB [29]), the method divides in two cases.

If $A \ge A_t$, the percentage of time where depth fade A is exceeded in the worst month is calculated by:

$$p_w = p_0 \cdot 10^{-A/10} \tag{3.54}$$

If $A < A_t$, the percentage of time where depth fade A_t is exceeded is calculated by:

$$p_t = p_0 \cdot 10^{-A_t/10} \tag{3.55}$$

Given p_w and p_t , the percentage of time that the fade depth A is exceeded (p_W) is calculated by the following equations:

- Step 1: calculate q'_a

$$q_a' = -20\log_{10} \left\{ -\ln\left[\left(100 - p_t\right) / 100\right] \right\} / A_t \tag{3.56}$$

- Step 2: calculate q_t

$$q_t = (q_a' - 2) / \left[\left(1 + 0.3 \cdot 10^{-A_t/20} \right) 10^{-0.016A_t} \right] - 4.3 \left(10^{-A_t/20} + A_t/800 \right)$$
 (3.57)

- Step 3: calculate q_a

$$q_a = 2 + \left[1 + 0.3 \cdot 10^{-A/20}\right] \left[10^{-0.016A}\right] \left[q_t + 4.3\left(10^{-A/20} + A/800\right)\right]$$
(3.58)

- Step 4: calculate p_W

$$p_W = 100 \left[1 - \exp\left(-10^{-q_a A/20}\right) \right] \tag{3.59}$$

3.1.4.6. Signal Reflection

The existence of obstacles in a path can lead to signal reflections that can reach the receiving antenna, which may destructively aggregate to the received signal. The presence of terrain in direct line of site can also provoke this phenomenon. Given the transmission and reception antennas gains g_E and g_R , a system frequency f and emission power p_E , the dispersed power dp_s for a given point P, categorised by the coordinates system presented in figure 15, with an area element of dxdy, is calculated, as presents by C.Salema in 29, by:

$$dp_s = p_E \cdot \frac{\lambda^2}{4\pi} \cdot \frac{g_E^P}{4\pi(x^2 + y^2 + h_E^2)} \cdot \frac{g_R^P}{4\pi[(d - x)^2 + y^2 + h_R^2]} \cdot \sigma \cdot dxdy$$
 (3.60)

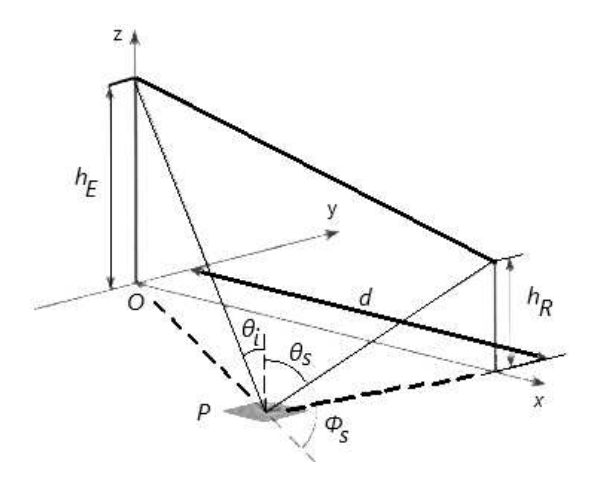


Figure 15. Signal reflection coordinates system, as presented by C.Salema in [29]

where σ represents the effective dispersion section on the reception antenna direction. As it is common in RF systems for the distance between the antennas and the soil to be far less than the distance between both antennas [29], the effective dispersion section can be obtained following a simplified equation:

$$\sigma = \frac{1}{s^2} \exp\left(\frac{\tan^2 \gamma}{s^2}\right) \tag{3.61}$$

where s represents the roughness inclination of surface parameter and $\tan^2 \gamma$ is obtained by:

$$\tan^2 \gamma = \frac{\sin^2 \theta_i - 2\sin \theta_i \sin \theta_s \cos \phi_s + \sin^2 \theta_s}{(\cos \theta_i + \cos \theta_s)^2}$$
(3.62)

Although equation 3.60 does not represent the signal attenuation due to reflection, the ratio between dispersed power and received power (commonly represented as p_R), it gives a rough estimate of the level of effectiveness that the dispersed radiation reflects on the received signal, having values above -10 dB to be considered prejudicial to a system QoS.

Equation 3.60 contains restriction to grant a level of accuracy, being used in cases where:

- Path wavelength is far smaller compared to the rough surface correlation length;
- Multiple dispersion is not considered;
- Surface roughness above average and a Gaussian correlation length.

3.1.5. Parameters for Quality of Service

As presented in TU-R Recommendations F.1668-1 [41], G.826 [42] and F.1491-2 [43], the error performance objectives (EPO) for Severely Errored Second Ratio (SESR), Background Block Error Ratio (BBER) and Errored Second Ratio (ESR) are defined in the following table:

Rate (Mbit/s)	<pre><pre>primary rate</pre></pre>	1.5 to 5	>5 to 15	>15 to 55	>55 to 160	>160 to 400
ESR	$0.04 \cdot X$	$0.04 \cdot X$	$0.05 \cdot X$	$0.075 \cdot X$	$0.16 \cdot X$	Not applicable
SESR	$0.002 \cdot X$	$0.002 \cdot X$				$0.002 \cdot X$
BBER	Not applicable	$2X \cdot 10^{-4}$	$2X \cdot 10^{-4}$	$2X \cdot 10^{-4}$	$2X \cdot 10^{-4}$	$1X \cdot 10^{-4}$

where the value of X is between 0.075 and 0.085 (from 7.5% to 8.5%)

3.1.6. Uniform Fading Margin

The uniform fading margin results from the need to accommodate the system to uniform signal fading. To calculate the uniform fading margin of a system, firstly the relation between signal and

noise (SNR) in ideal propagation conditions (IPC). Consequently, the received power is obtained, in dBm, by:

$$P_{R[dBm]} = P_{E[dBi]} - A_{sup} + G_{E[dBi]} - A_{sup} + G_{R[dBi]} - A_0 - A_{path}$$
(3.63)

where P_E stands for the emission power in dBm, A_{sup} represents supplementary attenuations found in transmission and reception of the signal (from wave guides for example), G_E and G_R represent the transmission and receiving antennas gain (respectively), A_0 represents the free space attenuation as presented in 3.1.4.1 and A_{path} stands for the attenuation found on the path, as presented in 3.1.4.

To calculate an approximation of the noise found in reception antenna, the reference noise and noise factor are analysed.

The reference noise N_0 can be obtained by:

$$N_{0[\text{dBm}]} = -174 + 10\log_{10}\left(b_{rf[\text{MHz}]} \cdot 10^6\right) \tag{3.64}$$

where b_{rf} represents signal bandwidth, in MHz, as defined in 3.3

The noise factor N_f can be approximated, as a function of signal frequency (f), by:

$$N_f = 7.0 + 0.1f \tag{3.65}$$

The noise found in the reception antenna N is determined by the addition of this to parts. Therefore, the signal-noise ratio (SNR) in $IPC(C/N_{ipc})$ is given by:

$$C/N_{ivc} = P_R - N (3.66)$$

Secondly, the SNR needed to consider the SESR value needs to be calculated. This value results on algebraic manipulation of the equations used to calculate the Bit Error Rate (BER), presented by C.Salema in [29]. This equations are in function of the type of modulation.

For systems using BPSK modulation, the SNR needed is obtained by:

$$\frac{C}{N} = \left(\operatorname{erfc}^{-1}\left(2 \cdot ber\right)\right) \tag{3.67}$$

where $\operatorname{erfc}^{-1}(x)$ is the inverse of the complementary error function obtained by:

$$\operatorname{erfc}^{-1}(x) = \operatorname{erf}^{-1}(1-x)$$
 (3.68)

where $erf^{-1}(x)$ is the inverse of error function and can be approximated by [44]:

$$\operatorname{erf}^{-1}(x) \approx \operatorname{sign}(x) \cdot \sqrt{\sqrt{\left(\frac{2}{\pi a} + \frac{\ln(1 - x^2)}{2}\right)^2 - \frac{\ln(1 - x^2)}{a}} - \left(\frac{2}{\pi a} + \frac{\ln(1 - x^2)}{2}\right)}$$
(3.69)

given $a \approx 0.147$ with a maximum relative error of 0.00013 [45].

For systems using a m-PSK modulation, meaning any number of symbols m (different than 2 in this case), the $\boxed{\text{SNR}}$ is obtained by:

$$\frac{C}{N} = \left(\frac{\operatorname{erfc}^{-1}(\operatorname{ber} \cdot \log_2 m)}{\sin(\pi/m)}\right)^2 \tag{3.70}$$

For systems using a m-QAM modulation, the SNR is obtained by:

$$\frac{C}{N} = 2\left[(\sqrt{m} - 1) \cdot \operatorname{erfc}^{-1} \left(\frac{\sqrt{m} \log_2(\sqrt{m}) ber}{2 \cdot (\sqrt{m} - 1)} \right) \right]^2$$
(3.71)

Using the SNR in IPC defined in 3.66 and the minimum SNR to accommodate the value of SESR, the SESR uniform margin is given by:

$$M_u^{\overline{SESR}} = \frac{C}{N|\overline{IPC}|} - \frac{C}{N_{min}}$$
(3.72)

The uniform margin for a given Residual Bit Error Ratio (RBER) is obtained similarly, using equation 3.73:

$$M_u^{\overline{\text{RBER}}} = \frac{C}{N_{\overline{\text{IPC}}}} - \frac{C^{\overline{\text{RBER}}}}{N_{min}}$$
(3.73)

where $C/N_{min}^{\mbox{RBER}}$ is calculated using equations 3.67, 3.70 or 3.71

3.1.7. Selective Fade Margin

In order to accommodate for outage probability due to selective fading, a margin is taken into account preventing this events to take place. As presented in TU-R Recommendations F.1093-1 [46], P.530-18 [40] and by C. Salema in [29], this margin is obtained by:

- Step 1: calculating the deep fade occurrence factor - k_t

$$k_t = 1.4 \cdot 10^{-8} \cdot f_{\text{[GHz]}} \cdot d_{\text{[km]}}^{3.5}$$
 (3.74)

- Step 2: calculating the symbol rate - T_s

$$T_s = \frac{\log_2 m}{f_{b[\text{MHz}]} \cdot 10^6} \tag{3.75}$$

- Step 3: calculating the mean time delay - τ_m

$$\tau_m = 0.7 \left(\frac{d_{\text{[km]}}}{50} \right)^{1.3} \tag{3.76}$$

- Step 4: calculating the multipath activity parameter - η

$$\eta = 1 - \exp\left(-0.2 \cdot k_t^{0.75}\right) \tag{3.77}$$

- Step 5: calculating the probability of outage by intersymbol interference during multipath fading - $P_{s/mp}$

$$P_{s/mp} = 2.16 \cdot k_n \cdot \frac{2 \left(\tau_m \cdot 10^{-9}\right)^2}{T_s^2}$$
 (3.78)

where k_n represents the normalized system parameter found in ITU-R Recommendation F.1093-1.

Using the equations 3.74 through 3.78, the selective fade margin m_s is obtained, in linear values, by:

$$m_s = \frac{k_t}{\eta \cdot P_{s/mp}} \tag{3.79}$$

3.1.8. Diversity and Equalization

Selective fading can severely affect **RF** communication systems, specially systems with a greater level of data flow. To reduce the level of impact selective fading can have in this systems, diversity and/or equalization is used [29].

In terms of diversity, this method is divided in diversity in frequency and diversity in space and the improvement factor applied to the selective fading margin is defined as described in the following subsections.

3.1.8.1. *Diversity in frequency*

Diversity in frequency is described as the usage of a second carrier separated in frequency with the main carrier by a value of Δf . The factor of signal improvement using this type of diversity is defined in [29] as:

$$i_{div} = \frac{80.5}{f_{\text{[GHz]}} d_{\text{[km]}}} \frac{\Delta f_{\text{[GHz]}}}{f_{\text{[GHz]}}} \frac{g_s}{g_p} m_s$$
 (3.80)

where g_s/g_p represents the ratio between the transmission antenna and the diversity antenna and m_s represents the selective fading margin represented in $\boxed{3.79}$.

3.1.8.2. *Diversity in space*

Using diversity in space, a second transmission and receiving antennas are placed with an added height of d_c . The factor of signal improvement using this type of diversity is defined in [29] as:

$$i_{div} = 1.21 \cdot 10^{-3} \frac{d_{c[m]}^2 f_{[GHz]}}{d_{[km]}} \frac{g_s}{g_p} m_s$$
 (3.81)

3.1.8.3. Equalization

The process of using equalization to reduce the affects of selective fading can be divided in two categories. Adaptive frequency domain equalization and adaptive time domain equalization.

Adaptive frequency domain equalization consists of the standardisation of response signal amplitude on the transmission channel following the intermediate frequency on the reception counterpart.

Adaptive time domain equalization is described as the equalization of channel response phase and amplitude, before carrier recovery, using the intermediate frequency.

The signal improvement factor using this methods is characterized as a function of path distance d as presented in the following equation [29]:

$$i_{eq} = \begin{cases} \left(\frac{0.5}{i_{mp}} + \frac{0.5}{i_{nmp}}\right)^{-1} & \text{if } d_{[km]} \ge 40\\ \left(\frac{0.8}{i_{mp}} + \frac{0.2}{i_{nmp}}\right)^{-1} & \text{if } d_{[km]} \ge 20\\ \left(\frac{k_1}{i_{mp}} + \frac{k_2}{i_{nmp}}\right)^{-1} & \text{if } 40 > d_{[km]} > 20 \end{cases}$$
(3.82)

where:

$$k_1 = 0.5 + 0.3 \cdot \frac{40 - d_{[km]}}{20} \tag{3.83}$$

$$k_2 = 0.5 - 0.3 \cdot \frac{40 - d_{\text{[km]}}}{20} \tag{3.84}$$

In summary, the figure 16 presents the process to verify the addition of diversity and/or equalization in order to obtain the selective margin.

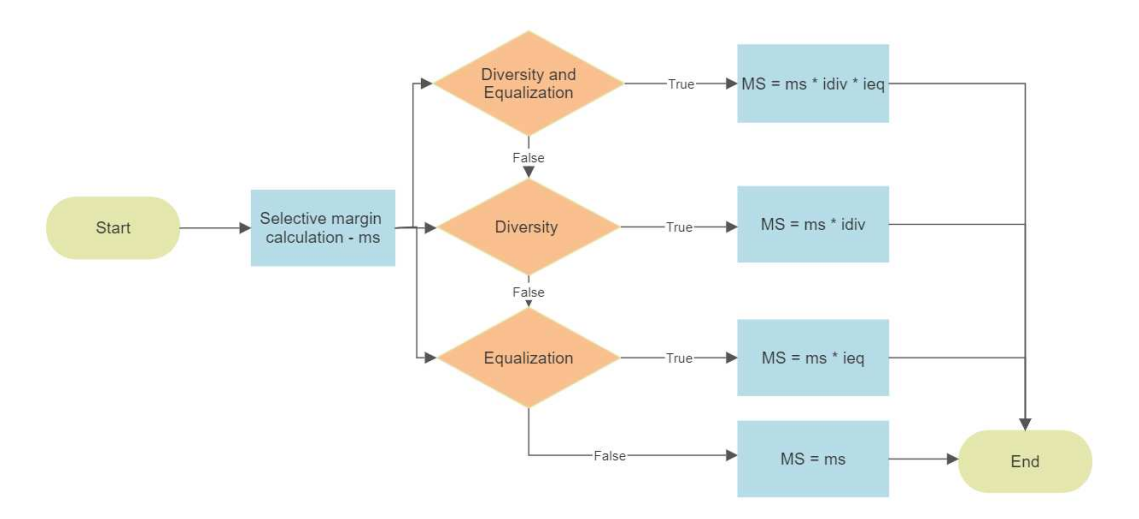


Figure 16. Verification process for addition of diversity and equalization

3.1.9. Critical Margins

In order to analyse a link QoS, four specific metrics are taken into account: SESR, BBER, ESR and Unavailability caused by Precipitation. The performance objectives for SESR, BBER and ESR are presented in section 3.1.5.

In this subsection, methods to calculate the value of SESR, BBER, ESR and unavailability caused by precipitation of a given link are presented, as well as a comparison method with the performance objective already presented.

3.1.9.1. Severely Errored Second Ratio Clause

As defined in ITU-R Recommendation F.1491-2 [43], SESR represents the ratio of severely error second occurrences to total available seconds over a particular measured time interval.

For a specific system, the value of SESR, represented as sesr is calculated as follows:

Firstly, using the uniform fade margin calculated in 3.72, the real margin for SESR is obtained by:

$$m_r^{SESR} = \left(\frac{1}{m_u^{SESR}} + \frac{1}{m_s}\right)^{-1}$$
 (3.85)

where m_u^{SESR} represents the uniform fade margin, in linear value, and m_s represents the selective fading margin in linear value.

Using the real margin for SESR, the value of sesr is obtained by:

$$sesr = \frac{1.4 \cdot 10^{-8} \cdot f_{[GHz]} \cdot d_{[km]}^{3.5}}{m_r^{SESR}}$$
(3.86)

To evaluate the impact of the path in the system QoS, a clause is presented where, if not fulfilled, the system is considered unreliable.

For SESR the clause determines that a safety margin must be complied. To calculate the safety margin, the minimum real margin for SESR must be calculated by:

$$M_{r_{min}}^{SESR} = 10 \cdot \log_{10} \left(\frac{1.4 \cdot 10^{-8} \cdot f_{\text{[GHz]}} \cdot d_{\text{[km]}}^{3.5}}{SESR} \right)$$
(3.87)

where SESR represents the performance objective for this parameter.

Using the minimum real margin for SESR, the safety margin ${\cal M}^{SESR}_{seg}$ is obtained by:

$$M_{seg}^{SESR} = M_r^{SESR} - M_{r_{min}}^{SESR} ag{3.88}$$

Given the value for M_{seg}^{SESR} , the clause for this parameter is fulfilled if the value of safety margin is greater than zero.

The critical margin for this parameter is obtained by:

$$M_{crit}^{SESR} = 10 \cdot \log_{10} \left(\frac{SESR}{sesr} \right)$$
 (3.89)

3.1.9.2. Background Block Error Ratio Clause

As defined in TU-R Recommendation F.1491-2 [43], BBER represents the proportion of background block error occurrences to all blocks (excluding blocks generated during severely errored second occurrences) in the available time within a defined time interval measurement.

To calculate the value of BBER for a specific system *bber*, firstly the real margin for BBER must be obtained by:

$$m_r^{BBER} = \left(\frac{1}{m_u^{rber}} + \frac{1}{m_s}\right)^{-1}$$
 (3.90)

where m_u^{rber} represents the uniform fading margin for RBER, as presented in 3.73 (in linear values).

Using the real margin for BBER, the probability of a given RBER Prber is obtained as follows:

$$P_{rber} = \frac{1.4 \cdot 10^{-8} \cdot f_{[GHz]} \cdot d_{[km]}^{3.5}}{m_r^{rber}}$$
(3.91)

Using equations 3.86 and 3.91 the value of absolute margin m_{abs} is obtained by:

$$m_{abs} = \left| \frac{\log_{10} \left(\frac{rber}{ber_{SESR}} \right)}{\log_{10} \left(\frac{Prber}{sesr} \right)} \right|$$
(3.92)

Following, the value of BBER for a specific system bber is given by:

$$bber = sesr \cdot \frac{\alpha_1}{2.8 \cdot \alpha_2 \cdot (m_{abs} - 1)} + \frac{N_b \cdot rber}{\alpha_3}$$
(3.93)

where:

- α_1 represents the number of errors per burst within the range of $1 \cdot 10^{-3}$ and ber_{SESR} (defined in ITU-R Recommendation P.530-9 [47]). α_1 takes values between 10 and 30;
- α_2 represents the number of errors per burst within the range of ber_{SESR} to RBER, taking values between 1 and 10;
- α_3 represents the number of errors per burst lower then RBER and takes the value of 1;
- N_b represents the number of bits per block

To fulfill the clause imposed for BBER, the value of bber must be lower than the value of BBER. The critical margin for this parameter is obtained by:

$$M_{crit}^{BBER} = 10 \cdot \log_{10} \left(\frac{BBER}{bber} \right) \tag{3.94}$$

3.1.9.3. Errored Second Ratio Clause

The ESR is defined in ITU-R Recommendation F.1491-2 [43] as the ratio of error second occurrences to total available seconds over a particular measured time interval.

The value of **ESR** for a particular system *esr* is obtained by:

$$esr = sesr \cdot {}^{m_{abs}}\sqrt{n} + \frac{n \cdot N_b \cdot rber}{\alpha_3}$$
(3.95)

where n represents the number of blocks per second provided by the system, as defined in ITU-R Recommendation 530-9 [47].

For the clause for $\overline{\text{ESR}}$ to be fulfilled, the value of esr must be equal or lower than the value of $\overline{\text{ESR}}$

The critical margin for this parameter is obtained by:

$$M_{crit}^{ESR} = 10 \cdot \log_{10} \left(\frac{ESR}{esr} \right) \tag{3.96}$$

3.1.9.4. Unavailability caused by Precipitation

To analyse the unavailability caused by precipitation of a system, firstly the safety margin for this phenomenon must be calculated. The safety margin to accommodate the levels of unavailability caused by precipitation of a system M_{seq}^{ind} is obtained by:

$$M_{seq}^{ind} = C/N_{ipc} - C/N_{min}^{ind} - A_{rain}^{ind}$$
(3.97)

where C/N_{ipc} is obtained by equation 3.66, C/N_{min}^{ind} represents the signal to noise ratio needed to accommodate a BER of 10^{-3} and A_{rain}^{ind} is obtained by the method described in section 3.1.4.4.

To fulfill the clause imposed in this parameter, the value of safety margin for unavailability caused by precipitation must be greater than zero.

The critical margin for this parameter is obtained by:

$$M_{crit}^{rain} = C/N_{ipc} - C/N_{cin-in}^{ind}$$
(3.98)

where:

$$C/N_{cip_{min}}^{ind} = C/N_{min}^{ind} + A_{rain}^{ind}$$
(3.99)

The equation 3.99 is deduced from equation 3.97, considering $M_{seg}^{ind}=0$

3.1.10. Passive Repeater

Most terrestrial RF systems are designed keeping a LoS between the transmission and receiving antennas, as it presents lower values of attenuation and a lower overall cost [29]. In some cases, this characteristic can not be accomplished and the usage of signal repeaters is required. Using signal repeaters, the signal is diverged in a different direction of the receiving antenna, to be met with a antenna to allow the signal to be redirected to the location of the receiving antenna. By doing so, major obstacles and reflective entities may be avoided.

Using this method divides the path in two separate paths. By doing so, the methods described in section 3.1.4 are equally divided in two separate paths, one from the transmission antenna to the repeater and a second from the repeater to the receiving antenna.

The introduction of a passive repeater to a system results in the addition of two elements to be considered to calculate the power received in the receiving antenna: the repeater gain and the signal attenuation caused by the repeater.

The repeater gain G_{PR} is obtained by:

$$G_{PR} = 20 \cdot \log_{10} \left[\frac{4\pi}{\lambda^2} \cdot a_{PR} \cdot \cos(\varphi) \right]$$
 (3.100)

where a_{PR} represents the physical area of the passive repeater and φ represents the incidence angle.

The signal attenuation caused by the passive repeater A_{PR} is obtained by:

$$A_{PR} = 10 \cdot \log_{10}(\eta_{PR}) \tag{3.101}$$

where η_{PR} represents the passive repeater radiation efficiency

3.2. Spacial Communication Systems

In this section, the models used to calculate the link budget for Earth-space RF communication systems are presented.

3.2.1. Satellite Orbit

Satellite and Earth stations positions can be described as functions of position vectors and velocity, reflected in a Cartesian coordinates system. Examples of Cartesian coordinates systems used to describe satellite orbits are:

- Earth-centered inertial (ECI)
- Earth-centered Earth Fixed (ECF)

The ECI coordinates system has origin congruent to the earth center, the x-y axis is equal to the equator and the z axis connects the earth center and the geographical north (union point between all meridians).

The ECF coordinates system is defined similarly to the ECI coordinates system, except the x-y axis equatorial plane follows the earth rotation movement. Using this coordinates system, a satellite orbit can be defined using two Keplerian elements groups:

Group 1:

- Longitude of ascending node;
- Inclination;
- Argument of perigee.

Group 2:

- Ellipse larger semi-axis;
- Eccentricity;
- Passage time on perigee.

In order to facilitate the transmission and process of orbit elements, standard coordinates systems are used. An Example of standard coordinates systems used is the Two-Line Element Set (TLE) coordinate system. In this coordinate system the orbit elements are synthesised to 2 lines of 69 digits divided as presented in figure 18.

3.2.2. Signal Attenuation

In this subsection are presented all the methods used to obtain an approximation of the signal attenuation effecting spacial communications.

3.2.2.1. Free Space Attenuation

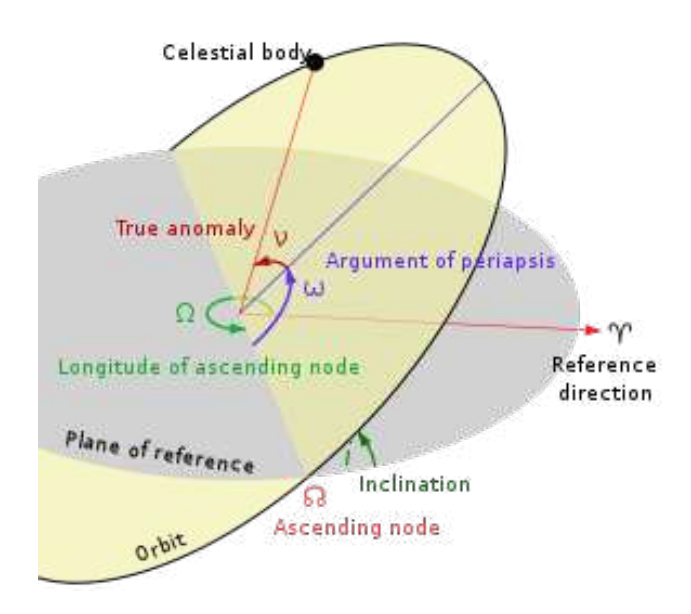


Figure 17. Orbit Keplerian elements [48]

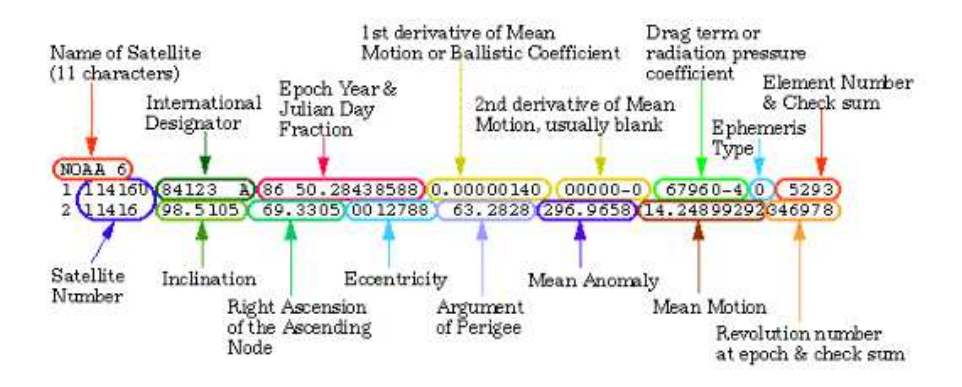


Figure 18. TLE elements example for satellite NOAA 6 [49]

Given that Earth-space communication systems remain a point-to-point communication system, the free space path loss is determined as presented in [3.1.4.1].

3.2.2.2. Atmospheric Attenuation

The ITU-R Recommendation P.618-13 [50] states that atmospheric attenuation may be neglected for communications using frequencies lower than 10 GHz and for frequencies up to 350 GHz can be obtained following the same model described for terrestrial RF communication systems presented in ITU-R Recommendation P.676, as described in 3.1.4.3.

3.2.2.3. Rain Attenuation

The ITU-R Recommendation P.618-13 [50] presents a step-by-step model used to predict the rain attenuation reflected on the system signal. To apply this model, the following parameters are required:

- $R_{0.01}$: Rainfall rate for given location for 0.01% of an average year for given point
- h_s : Earth station height above mean sea level of given point
- h_0 : Isotherm height above mean sea level for given point
- θ : Elevation angle
- φ : Earth station latitude
- f: Communication frequency
- R_e : Effective radius of Earth

The values of $R_{0.01}$, h_s and h_0 are obtained by a digital maps presented in **ITU-R** Recommendations P.837-7 [51], P.1511 [52] and P.839-4 [53] respectively.

To calculate the level of rain attenuation, firstly the slant-path length L_s must be calculated. The slant-path length is obtained by:

$$L_s = \frac{h_R - h_s}{\sin \theta} \quad \text{for } \theta \ge 5^{\circ} \tag{3.102}$$

$$L_s = \frac{2(h_R - h_s)}{\left(\sin^2 \theta + \frac{2(h_R - h_s)}{R_e}\right)^{1/2} + \sin \theta} \quad \text{for } \theta < 5^{\circ}$$
 (3.103)

where h_R represents the rain height of a given point, described in ITU-R Recommendation P.839-4 [53] as:

$$h_R = h_0 + 0.36 \text{ km} \tag{3.104}$$

The horizontal projection of the slant-path L_G is obtained by:

$$L_G = L_s \cdot \cos \theta \tag{3.105}$$

The specific attenuation γ_R used in the presented model is calculated according to the model presented in ITU-R Recommendation P.838-3, as described in 3.1.4.4.

As a result of the value of the specific attenuation and horizontal projection of the slant-path, the horizontal reduction factor for 0.01%, $r_{0.01}$, is obtained by:

$$r_{0.01} = \frac{1}{1 + 0.78 \cdot \sqrt{\frac{L_G \cdot \gamma_R}{f}} - 0.38 \cdot (1 - e^{-2 \cdot L_G})}$$
(3.106)

The vertical adjustment factor for 0.01% of the time, $v_{0.01}$, is obtained by:

$$v_{0.01} = \frac{1}{1 + \sqrt{\sin \theta} \left(31 \cdot \left(1 - e^{(\theta/(1+\chi))} \right) \frac{\sqrt{L_R \cdot \gamma_R}}{f^2} - 0.45 \right)}$$
(3.107)

where:

$$\xi = \tan^{-1} \left(\frac{h_R - h_s}{L_G \cdot r_{0.01}} \right) \tag{3.108}$$

$$L_R = \frac{L_G \cdot r_{0.01}}{\cos \theta} \quad , \text{ for } \xi > \theta \tag{3.109}$$

$$L_R = \frac{h_R - h_s}{\sin \theta}$$
 , for $\xi \ge \theta$ (3.110)

$$\chi = 36 - |\varphi| \quad \text{, for } |\varphi| < 36^{\circ} \tag{3.111}$$

$$\chi = 0$$
 , for $|\varphi| \ge 36^{\circ}$ (3.112)

Resulting of the value of $v_{0.01}$, the effective path length L_E is calculated by:

$$L_E = L_R \cdot v_{0.01} \tag{3.113}$$

allowing to obtain the predicted rain attenuation, exceeded for 0.01% of an average year $A_{0.01}$, as:

$$A_{0.01} = \gamma_R \cdot L_E \tag{3.114}$$

To conclude this model, the value of rain attenuation exceeded for a given percentage p of an average year A_p , where p can take values between 0.001% and 5%, is obtained by:

$$A_p = A_{0.01} \left(\frac{p}{0.01}\right)^{-(0.655 + 0.033 \cdot \ln(p) - 0.045 \cdot \ln(A_{0.01}) - \beta \cdot (1-p) \cdot \sin \theta)}$$
(3.115)

where:

$$\beta = 0$$
 , If $p > 1\%$ or $|\varphi| > 36^{\circ}$ (3.116)

$$\beta = -0.005 \cdot (|\varphi| - 36) \quad \text{, If } p < 1\% \text{ and } |\varphi| < 36^{\circ} \text{and } \theta \ge 25^{\circ} \tag{3.117}$$

$$\beta = -0.005 \cdot (|\varphi| - 36) + 1.8 - 4.25 \sin \theta$$
, otherwise (3.118)

3.2.3. Link Budget

In this subsection, an analysis of the impact of the Earth-space telecommunication system characteristics on the link budget will be made, with the objective of determine the minimal antennas characteristics and signal transmission power to accomplish a successful and reliable communication between two Earth stations, relaying on a satellite. This systems can be divided into two different links, the uplink between the transmission Earth station and the satellite, and the downlink between the satellite and the receiving Earth station.

To analyse a system link budget, firstly the sky noise temperature at the receiving station is studied. Following the ITU-R Recommendation P.618-13 [50], the sky temperature noise at the receiving station T_{sky} , in Kelvin, is obtained by:

$$T_{sky} = T_{mr} \cdot (1 - 10^{-A/10}) + 2.7 \times 10^{-A/10}$$
 (3.119)

where T_{mr} represents the atmospheric mean radiating temperature, and recommended the value of 275 K when in absence of a local surface temperature data. A represents the total atmospheric attenuation applied to the system.

Following, the **SNR** considering rain attenuation for the uplink is obtained by:

$$\left(\frac{C}{N}\right)_{u,r} = \Omega_{sat}^T - BO_i - 10 \cdot \log\left(\frac{4 \cdot \pi}{\lambda^2}\right) - L_{r,u} + \left(\frac{G}{T}\right)^S - 10 \cdot \log(k \cdot B) \tag{3.120}$$

where Ω_{sat}^T represents the satellite power density for transponder saturation, BO_i represents the input back-off of the traveling-wave tube amplifier (TWTA) for clear sky, $L_{r,u}$ stands for the rain attenuation on the uplink connection, $(G/T)^S$ represents the merit factor of the receiving station, k stands for the Boltzmann constant and B represents the system bandwidth.

Given the value of $(C/N)_{u,r}$, the global SNR for the uplink, considering only signal fading from rain attenuation, $(C/N)_{u,r}$ is obtained by:

$$\left(\frac{C}{N}\right)_{u,r} = -10 \cdot \log\left[10^{(C/N)_{u,r}/10} + 10^{(C/I)_{u,r}/10}\right]$$
(3.121)

where $(C/I)_{u,r}$ represents the signal-interference ratio for the uplink considering only signal fading from rain attenuation and, given the value of signal-interference on uplink due to near satellites $(C/I)^{sats}$ and the value of signal-interference due to near channels $(C/I)^{chs}$, the signal-interference ratio is obtained by:

$$\left(\frac{C}{I}\right)_{u,r} = \left(\frac{C}{I}\right)_{u} - A_{p} \tag{3.122}$$

considering:

$$\left(\frac{C}{I}\right)_{u} = -10 \cdot \log \left[10^{-(C/I)^{sats}/10} + 10^{-(C/N)^{chs}/10}\right]$$
(3.123)

Given the value of the global SNR for the uplink considering only signal fading from rain attenuation $((C/N)_{u,r})$, the global SNR for downlink $(C/N)_d$ is obtained by:

$$\left(\frac{C}{N}\right)_{d} = -10 \cdot \log\left[10^{-(C/N)_{global}/10} - 10^{(C/N)_{u,r}}\right]$$
(3.124)

where $(C/N)_{global}$ represents the SNR according to the signal modulation and BER used, as defined in 3.1.6.

Consequently, the SNR for downlink value is obtained by:

$$\left(\frac{C}{N}\right)_{d} = -10 \cdot \log\left[10^{(C/N)_{d}} - 10^{-(C/I)_{d}}\right] \tag{3.125}$$

where $(C/I)_d$ stands for the global signal-interference for downlink. The value of $(C/I)_d$ takes into consideration the signal interference caused by near satellites and channels and the output back-off found on the satellite to the given input back-off. The input back-off found at the satellite takes into consideration the input back-off found with clear sky and the value of signal attenuation caused by rain, specifically for the uplink, as is this connection that impacts the input-back found on the satellite. Given the difference between the input back-off found on the satellite and the input back-off characterized for connection in a clear sky BO_{i-diff} , the global signal-interference for the downlink is obtained by:

$$\left(\frac{C}{I}\right)_{d} = -10 \cdot \log\left[10^{-(C/I)^{sats/10}} + 10^{-(C/N)^{chs/10}}\right] - BO_{i-diff}$$
(3.126)

Given the value for signal-interference for downlink, the receiving station merit factor $(G/T)^T$ is obtained by:

$$\left(\frac{G}{T}\right)^{T} = \left(\frac{C}{N}\right)_{d} + BO_{o} - EIRP_{sat}^{S} + L_{d} + L_{a,d} + 10 \cdot \log(k \cdot B) \tag{3.127}$$

where $EIRP_{sat}^S$ represents the saturated effective isotropic radiated power of the satellite, L_d represents the free space attenuation for downlink and $L_{a,d}$ represents the atmospheric attenuation for downlink.

Succeeding, the **SNR** for downlink calculated by:

$$\left(\frac{C}{N}\right)_{d,r} = -10 \cdot \log\left[10^{-(C/N)_{d,r}/10} - 10^{-(C/I)_d}\right]$$
(3.128)

where:

$$\left(\frac{C}{\mathcal{N}}\right)_{u} = \left(\frac{C}{\mathcal{N}}\right)_{u,r} \tag{3.129}$$

$$\left(\frac{C}{N}\right)_{dx} = -10 \cdot \log\left[10^{-(C/N)_{global}/10} - 10^{-(C/N)_{u}/10}\right]$$
(3.130)

To calculate the merit factor on the receiving station, the sky temperature noise described in 3.119 is taken into account. As a consequence, the merit factor considering the sky temperature noise is obtained by:

$$\left(\frac{G}{T+T_{sky}}\right)_r^T = \left(\frac{C}{N}\right)_{d,r} - EIRP_{sat}^S + BO_o + L_d + L_{a,d} + L_{r,d} + 10 \cdot \log(k \cdot B) \quad (3.131)$$

Given the value of factor merit determined in 3.127, the receiving station temperature T is obtained by:

$$T = \frac{T_{sky}}{1 - 10^{(G/T)_{diff}/10}} \tag{3.132}$$

where

$$\left(\frac{G}{T}\right)_{diff} = \left(\frac{G}{T}\right)^{T} - \left(\frac{G}{T + T_{sky}}\right)_{r}^{T}$$
(3.133)

Using the value of temperature and merit factor, the minimum gain for the receiving station is calculated by the difference between the merit factor and the temperature calculated. Consequently, the minimum antenna diameter for the receiving station is determined using the equation [3.1]

To calculate the minimum gain for the emit antenna the following formula is used:

$$G_E = 20 \cdot \log \left(\frac{f_e}{f_r}\right)^2 + G^T \tag{3.134}$$

To calculate the minimum power used to emit the signal, the effective isotropic radiated power of the transmission station $EIRP^{T}$, considering rain attenuation, is analysed by:

$$EIRP^{T} = \left[\Omega_{sat}^{s} + 10 \cdot \log\left[4 \cdot \pi \cdot d_{u}^{2}\right] + L_{atm-u}\right] - BO_{i}$$
(3.135)

Resulting in calculating the minimum emission power by:

$$P^T = EIRP^T - G^T (3.136)$$

CHAPTER 4

Tool Development and Optimization

In this chapter, the development process for the software is presented. As the software allows the user to simulate two different types of telecommunication systems, the presentation of this software features are described separately. Different instances of telecommunication system simulations are denominated by projects, as a relation to an physical telecommunication project. The file system used to allow the user to save and access a project progress is also presented, as well as different the API's used for additional data and calculations. Lastly, the usability tests and client meetings made for software optimization will be presented and consequently the optimizations done to the software following this tests and client meetings.

4.1. Technologies

To accomplish the goal of creating a flexible and easy to use software tool, as well as containing facilitated access and interaction with third-party software, a Web development approach was used. By doing so, the proposed tool was development using HTML, JavaScript and CSS programming languages. The use of HTML allows the creation of visual structures to be presented and interacted by the user being added functionality using JavaScript, used to define the procedures following the user interactions. Lastly, CSS is used for styling and animation, facilitating the comprehension of the page presented to the user.

To assure a cross-platform client-side software without the direct use of a Web browser, the Electron Framework was used [54]. This Framework uses the Chromium browser to display the developed Web page in a similar manner of most Web browsers and Node.js to simulate a local server to host the developed software. Node.js also allows the integration of modules developed by third-parties (denominated node-modules) with the assistance of a package manager like Node Package Manager (NPM).

For software version control, the Git and GitHub platforms were used. This platforms provide a management and storage of different versions of developed features, useful for software development [55].

4.2. Tool Main structure

In a primary approach on designing the tool, the primary defined objectives were:

- Easy access to save and create new projects;
- Easy access to select and evaluate created projects;
- Visible element to determined the selected project;
- Selected project elements presentation.

To accomplish this objectives, the software and applications designing tool Adobe Xd was used. This software provides drag and drop features to facilitate a visual comprehension of the design to be implemented. Resulting in the mentioned objectives, a prototype design was created as presented in figure [19].

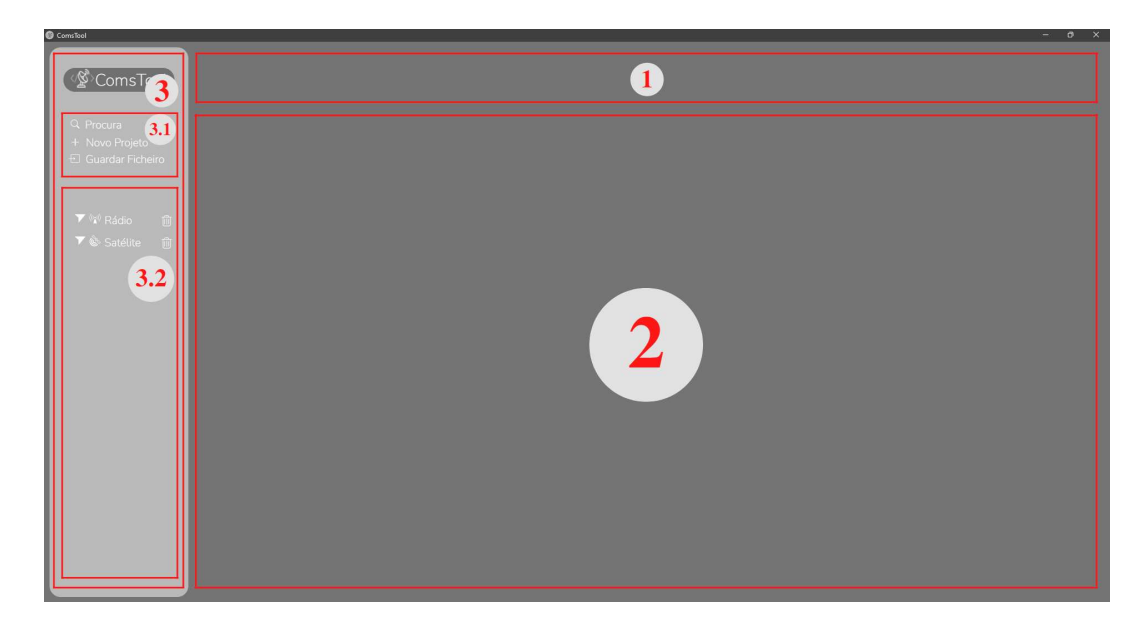


Figure 19. Tool Design prototype

The areas highlighted in figure 19 represent the main objectives previously presented, where area 1 provides the selected project title (defined by the user on the project creation), area 2 presents the selected project content, area 3 contains a side menu containing an easy process for creation

and saving of projects and projects progress in area 3.1 and the presentation the created projects, allowing the user to select or delete a project in area 3.2.

4.3. Project creation

To create a new project, after the user selects the necessary button to initiate this process (presented in figure 20), a pop-up box is presented, allowing the user to select the different types of projects available, the level of data presented and the type of visualization to be presented. The level of data to be presented and type of visualization are two features resulted from client meetings, to be presented.

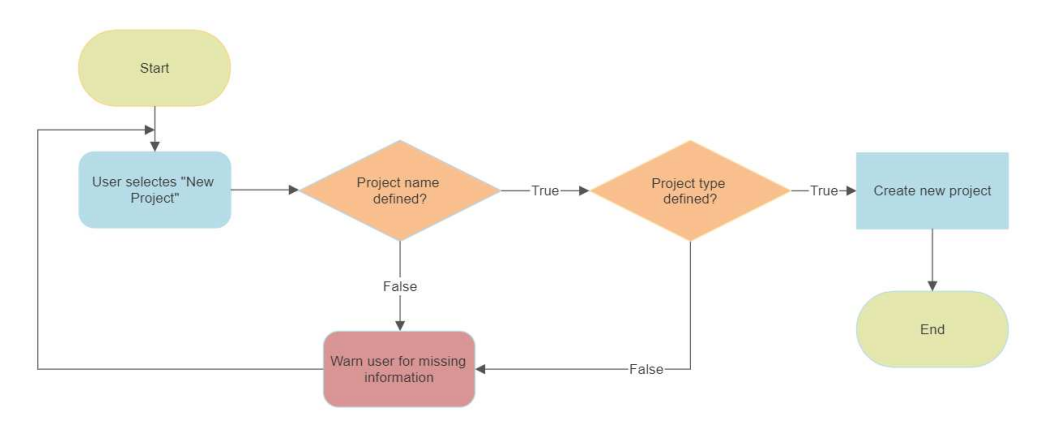


Figure 20. Flow chart for new project creation process

Upon creating a project, an selector element is added to the side-menu, where the user can select the project to load said project. This element contains the project name, an icon to distinguish which type of project it contains, an icon allowing the user to delete the project and an icon that when pressed, provides a window on the side-menu presenting all the steps of said project and an icon that warns the user when the file contains elements that are not saved, being hidden when all project elements defined are saved. These elements are presented as depicted in figure 21.



Figure 21. Side-menu project selector

The different projects content follow an equal design, in order to facilitate the user integration when using a different type of project. This design results in a set of windows analysing distinct

steps of a project creation and analyses. This steps are congruent with the typical order of steps taken in a real communication project. An example of this windows can be visualized in figure 22. In some cases, the step window can be part of another step window, allowing to divide steps into different sub-steps.



Figure 22. Example of step window

The display of input and output elements vary from left to right or in a horizontal grid disposition, depending on the type of values to be input and the type of values to be output as the values vary from option selection, single numbers input and output and output instances of number arrays.

4.4. File System Architecture

In order to allow the user to save the current project progress for further work and re-access this progress, a file system was created. To accomplish this goal, a file folder is automatically created when the software is first ran. This folder is created in the application data directory used by the Operating System which may change for different operation systems (./Library/Application Support for Mac-OS and C:/Users/\$User Name/AppData/Roaming for Windows for example). Therefore, to allow the creation of a cross-platform software by accessing this directory independently of the Operating System, the Electron app API is used.

In this folder, the different projects created by the user are represented in different files with the project name. In order to read and write information in the project files, two different processes were created.

Firstly, text files were used and different project variables were separated by line separator. In order to access the variables, the file is read completely and looped through line by line until the searched variable is found and the project variables progress is save as the user changes said

variable. This process main concern relied in situations were multiple variables were being changed (specially when output were received) and some changes would not be registered due to multiple processes access the same file simultaneously and when said file was saved, one of the processes would have outdated information in the given file, resulting in loss of variable updates.

Given the problems faced, two changes were made to the file system. Due to the level of compatibility between JavaScript and ISON files, this became the file format used to store the projects progress. This change also improved the process to access a specific variable, since ISON files allow to access different elements of the ISON element directly, without the need to loop through all the object entries until the searched variable is found. Furthermore, to account for simultaneous multiple variable changes, the object of the current object became set to be saved in the project process memory, not having to read or write on the project file to access or change a variable. To indicate to the user that a file has not been saved, an icon is demonstrated in the section were the user selected the project and, upon saving the project, this icon is hidden, symbolizing that the project current progress is saved. Finally, only when the user selects to save the file is when the project respective file is re-written. Due to this changes, the file system architecture is similar to a non-relational database, where each project only has saved the variables that have been defined by the user and this saved variables vary between different types of projects (terrestrial or spacial projects).

4.5. Terrestrial Communication Systems

Applying the models presented in 3.1, the steps to simulate a terrestrial RF communication system are presented to the user by the following order:

- Path definition
- Antennas characteristics
- Radio characteristics
- Path Loss
- SNR in IPC
- Diversity
- QoS parameters
- Project margins

In the following sections, the steps development will be further explained.

4.5.1. Path selection

To define the communication path, the Cesium API described in 2.3 is used. The API allows the integration of external 3-dimensional modules imported using a GLB file format. The GLB format is used to exhibit 3D models as it represents a binary structure of data included in GL Transmission Format (glTF) files, using JavaScript Object Notation (JSON). The antennas GLB file was created using the Blender software, a software that allows the creation of 3D models and export said models using the GLB file format.



Figure 23. Path selection window

The 3D model for antennas is composed of two elements: the antenna dish and pool. The dish model is represented using a GLB file with a default radius of 1 meter and the pool uses the Cesium internal entity API with a default height of 1 meter. This difference is due to the fact that the Cesium API only allows the change of scale on a GLB model in all Cartesian coordinate axis. Therefore, when changing the dish diameter, the whole dish can be scaled for that given diameter. The same results are not expected for the antenna pool. When the user desires to increase the pool height, the model should only change the Z-coordinate (without changing the pool width). This feature is only accomplished using the Cesium entities API and changing the model matrix used to represent the

model in frame. By dividing the antenna model in 2 independent parts, it allows to change the pool height and dish rotation independently. The antenna 3D model is depicted in figure 24.



Figure 24. Antenna 3D model

Cesium provides a internal listener for user clicks on the Cesium window. The position where the user clicked can be stored and parsed for a real position in the world presented, using the camera position and projection. Upon clicking the window, the selected position is stored and a 3D model of an antenna is positioned on said position, as well as a label, allowing the user to differentiate the elements used in the communication system. The process of antennas and passive repeater insertion is depicted in figure [25].

Given that Cesium provides a 1:1 measurement of length when compared with the real world, the path length and other measurements required for calculations can be extracted directly from the Cesium API

If both transmission and receiving antennas are in place, a Fresnel Ellipsoid can be represented between both antennas. This ellipsoid provides an estimate of the path that the signal energy travels between. For the ellipsoid to be presented correctly, it is placed in the middle point between the path origin and target and rotated using the Eye-Gaze-Up representation [56].

The process of integrating a passive repeater on the communication system is similar to a station antenna. After the user selects the addition of a passive repeater and indicates the position where it is to be placed a passive repeater model is placed. The model is also divided in two independent parts, where the pool is identical to the station antennas and the dish represents a mirror with a area

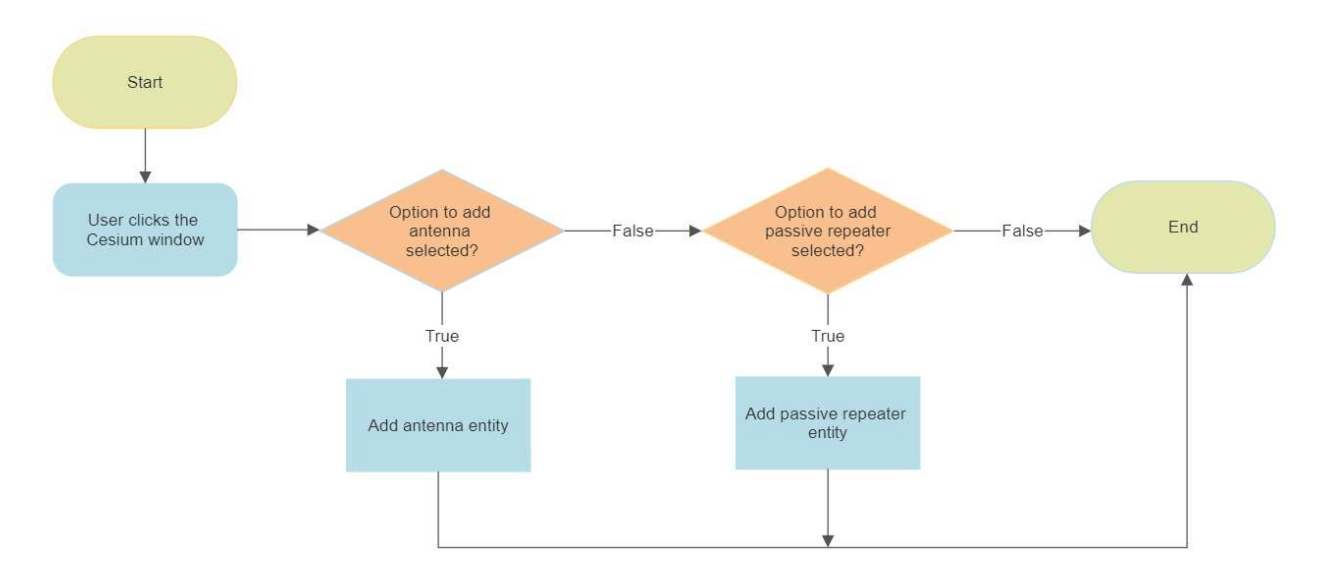


Figure 25. Flow chart for antenna model addition process

of 1 square meter by default. The orientation where the passive repeater is placed requires to be at an angle where the signal post-reflection can be found in the receiving antenna. To do so, the perpendicular vector between the vectors from the repeater position to the transmission and receiving antennas positions respectively (this vectors will be denominated by PO and PT respectively) by calculating the cross product between both vectors. The angle of rotation applied to the vector PO is equal to half of the angle between PO and PT (denominated by φ in figure [26]). Using Rodrigues' rotation formula [57], the orientation point can be found by rotating the PO vector along the perpendicular vector previously mentioned.

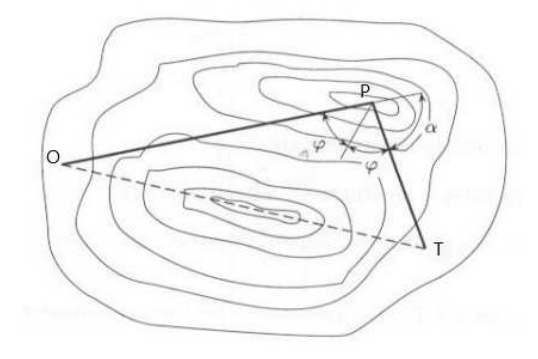


Figure 26. Point elements for passive repeater addition presented by C.Salema in [29]

The user is able to change the antenna pool height, antenna diameter, radiation efficiency, transmission or reception power and the antenna radiation pattern of each station station using the step window presented in figure [27].



Figure 27. Antenna characteristics step window for terrestrial systems

Using the data presented by Telewave in [58], different antennas radiation patterns are presented to the user. The radiation patterns are divided in orientation and elevation angles and are presented to the user using a two-dimensional circular chart. To plot the radiation pattern charts, the Plotly graphing library [59] is used. The user, by selecting the directivity tab, a menu is presented with all available radiation patterns, as depicted in figure [28].

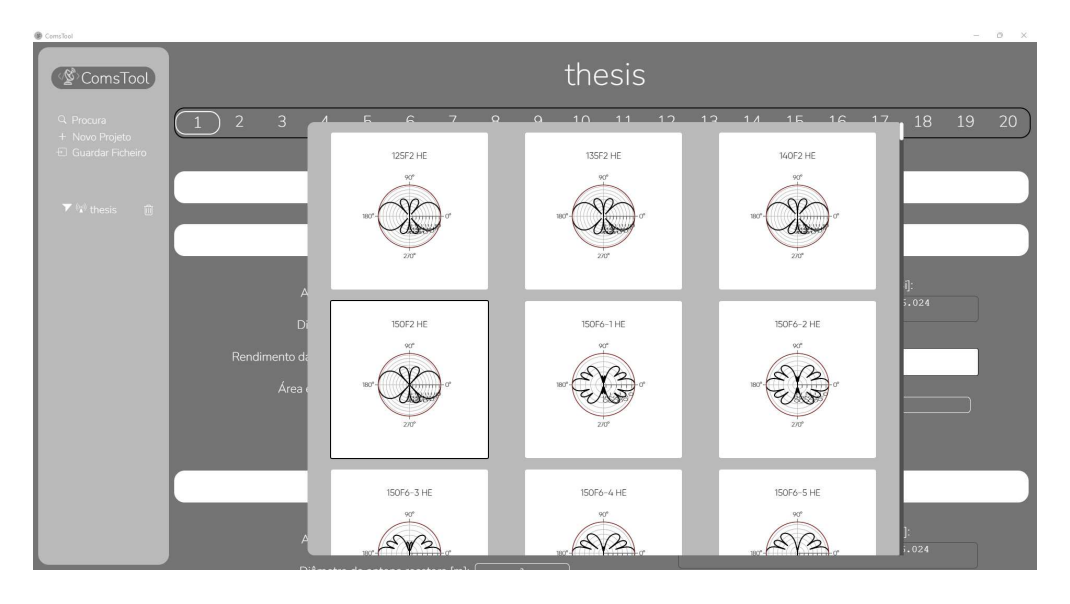


Figure 28. Radiation pattern window for terrestrial projects antennas

4.5.2. Radio characteristics

The radio characteristics influence largely the communication system as a whole, given that the calculations for path loss and margins are a function of frequency and bit ratio for example. Therefore, it is required to accommodate the software for changes of each radio characteristic to perform recalculations with the changed values, as presented in figure [29].

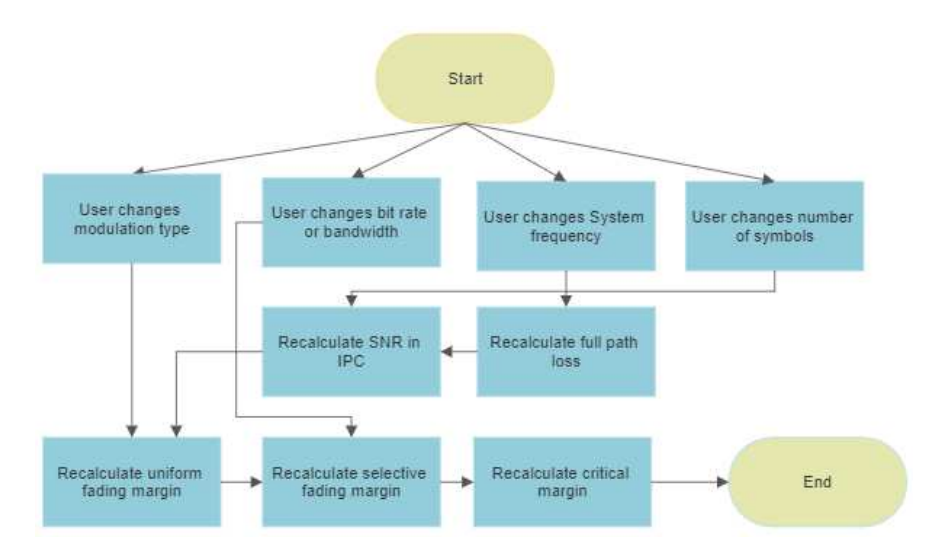


Figure 29. Radio elements dependencies flow chart

To change the system radio elements, 3 step windows are presented, being divided as:

- System frequency;
- Digital signal characteristics;
- Modulation characteristics.

The following figures 30, 31 and 32 depict the step windows presented to the user to change these elements.



Figure 30. System frequency step window

4.2 Sinal Digital	
Ritmo Binário da ligação [Mbits/s]:	34
Largura de Banda [MHz]:	28
Fator de excesso de banda β :	0,142
Número mínimo de níveis de modulação por frequência:	2.61482

Figure 31. Digital signal characteristics step window

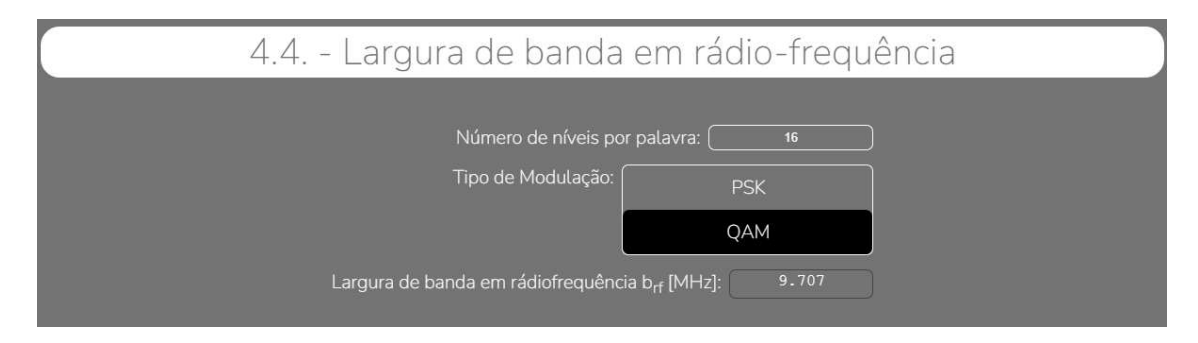


Figure 32. Modulation characteristics step window

4.5.3. Path Loss

The path taken between two antennas has a substantial effect on the signal, to such an extent that, in certain cases, can completely diffract the signal, not allowing a communication to be yield.

To follow the models presented in 3.1.4, real life information is required. The extraction of information for this purpose is done in two manners: through the Cesium API or through pin point data acquired from digital maps originated from TU-R Recommendations.

All the digital maps extracted from Recommendations present a similar data structure. This data structure is composed of three files: a longitude values file, a latitude values file and a specific data file. The files, although being distributed in a text file format (.txt file), are presented similarly to a comma-separated values (CSV) file format. This file sets vary in precision, meaning that although one set of files provides information with leaps of latitude and longitude of 0.75 degrees, a different set of files may provide information with leaps of 1 degree. To provide a faster search of latitude and longitude values, the values are restructured to a tree-search-like structure. In this structure, latitude values are categorized by the integer value it contains. Then, considering the values of longitude available for said latitude value, the longitude value is also categorized by integer value. Finally,

the values contained in each category are inserted bellow their category. The finalised structure of this files can be demonstrated in figure [33].

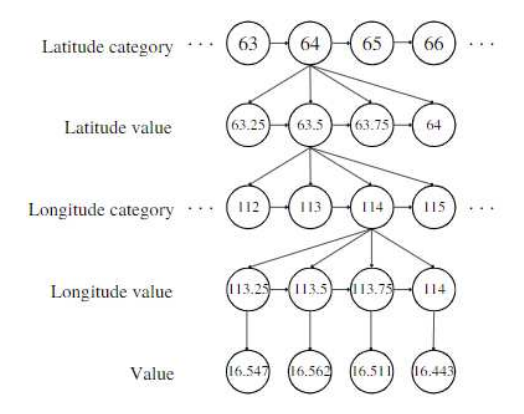


Figure 33. Example of latitude and longitude tree search

The Cesium API is used to extract real life elements that interfere with the link signal. These elements are divided in earth terrain and in urban buildings.

To detect these elements two algorithms were designed. The first algorithm relies on different calculated points situated inside the Fresnel Ellipsoid which were clamped to the height of whatever object is located on that position. By comparing the transmission and receiving antennas height, it can be concluded if in that position a obstacle is found. This method was found to be unreliable, as in some cases the process of clamping points can create high levels of error when compared with the actual height of terrain and buildings found on the path, as displayed in figure 34.

Given this level of unreliability, a second algorithm was designed. This algorithm analyses projections of rays (also known as ray-tracing) from the transmission antenna in order to detect elements on the path. Due to lack of development of the Cesium API for this type of algorithms, the rays used to detect urban buildings can only be originated from the camera placed in the window. Therefore, to be able to ray cast rays from the transmission antenna, the camera is set to travel to the position of the transmission antenna dish. Consequently, the pixels on the Cesium window are looped from top to bottom and left to right. For a faster algorithm, the number of pixels analysed can be minimized by increasing the leap made form each pixel.

At every pixel, after the ray is cast it can be return 2 types of values: undefined value or a Cesium entity object. The undefined value results on rays that do not collide with any objects, therefore can be ignored. If the ray returns an object, the point of collision is firstly analysed as if it

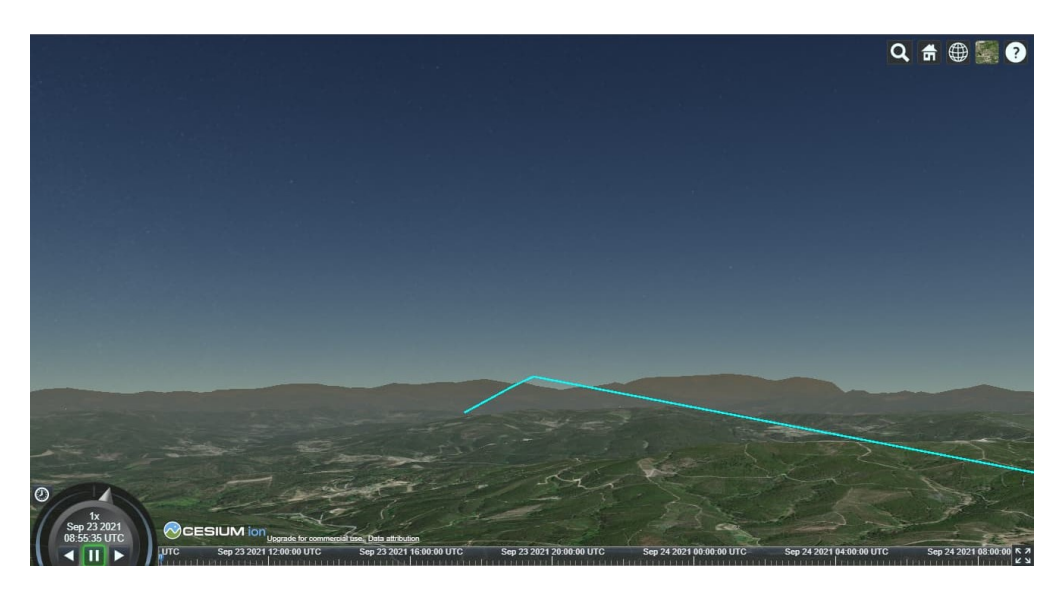


Figure 34. Example of error found on point clamping algorithm

API do not contain the entity model matrix, used to represent the position, rotation and scale of the entity in world coordinates, this verification is made considering only two variables: the distance to the transmission antenna position and the distance to the transposed point in the vector connecting the transmission and receiving antennas (defined as P'(x, y, z) and distance equal to x) and the distance between the verifying point (point P(x, y, z)) and point P' (defined by the value of y). These elements can be visualized in figure 35.

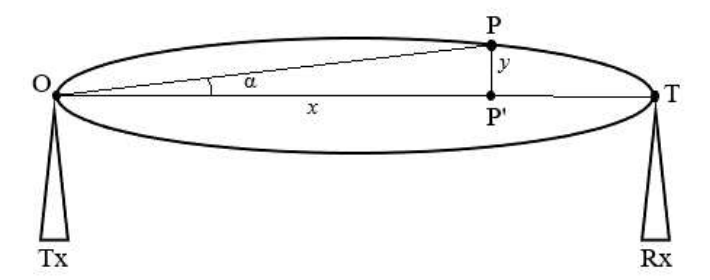


Figure 35. Elements used to check if a point is inside a Fresnel Ellipsoid

Given the transmission antenna point position O(x, y, z), the reception antenna point position T(x, y, z), the middle point between point O and T denominated M(x, y, z), the vertical ellipse

radius r and the arbitrary point P(x, y, z), the stated verification can be obtained, using the ellipse general formula, by:

$$\left(\frac{||\vec{OT}|| \cdot \cos(\alpha) - ||\vec{OM}||}{||\vec{OT}||}\right)^2 + \left(\frac{||\vec{OT}|| \cdot \sin(\alpha)}{r}\right)^2 \le 1$$
(4.1)

This simplification can be applied to a 3-Dimensional problem, since the rotation of point P along \overrightarrow{OT} (that occurs when adding the third dimension) do not change the values of x and y.

By using the ellipse general formula, the verification if point P is inside the first Fresnel Ellipsoid is made. If the point is found to be inside the first Fresnel Ellipsoid, it is stored in a **ISON** object and distinguished by the identifier of the entity object found (denominated by batch id).

To examine if a point can reflect the signal, the normal of the object found on that specific point is required. Although the Cesium API do not return the normal of the triangle of the entity where the point is found, an approximation of this normal can be made. The process of approximating the point normal is done by inquiring the near pixels points, creating a 3D point cloud, and calculating an average cross product of the vectors created by the point in analysis and the inquired points. This approach is similar to the first method presented by Klasing et al. in [60], being differentiated in the process of inquiring the near points used to calculate the approximated normal. Given that an urban building entity can have a multitude of points stored, the calculation of the k-nearest-neighbors, as solicited in [60], becomes a very computationally demanding process added to the process of ray-tracing. To facilitate this inquisition, instead of analysing all the points available for a given entity, 4 additional rays are cast from the 4 pixels around the pixel used to cast the ray, where the results of this ray casts are analysed and verified if the output of the resulting rays obtain the same building entity. If so, these points are used to approximate the normal value as the average normal among the resulting 4 triangles created, as depicted in figure [36].

Given an arbitrary pixel (i, j) the approximated normal for that pixel $\overrightarrow{n_{i,j}}$ is defined as:

$$\overrightarrow{n_{i,j}} = \frac{1}{4} \times \sum_{k=0}^{4} \overrightarrow{OP\left(i - \cos\frac{\pi}{4}k, j - \sin\frac{\pi}{4}k\right)} \cdot \overrightarrow{OP\left(i - \cos\frac{\pi}{4}(k+1), j - \sin\frac{\pi}{4}(k+1)\right)}$$
(4.2)

The results of this process are presented in figure 37.

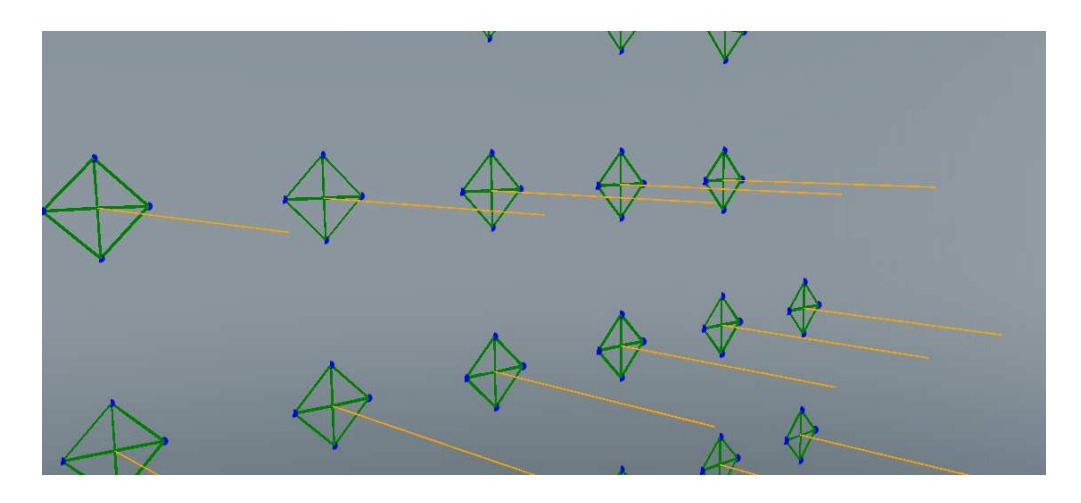


Figure 36. Elements for approximated normal calculations

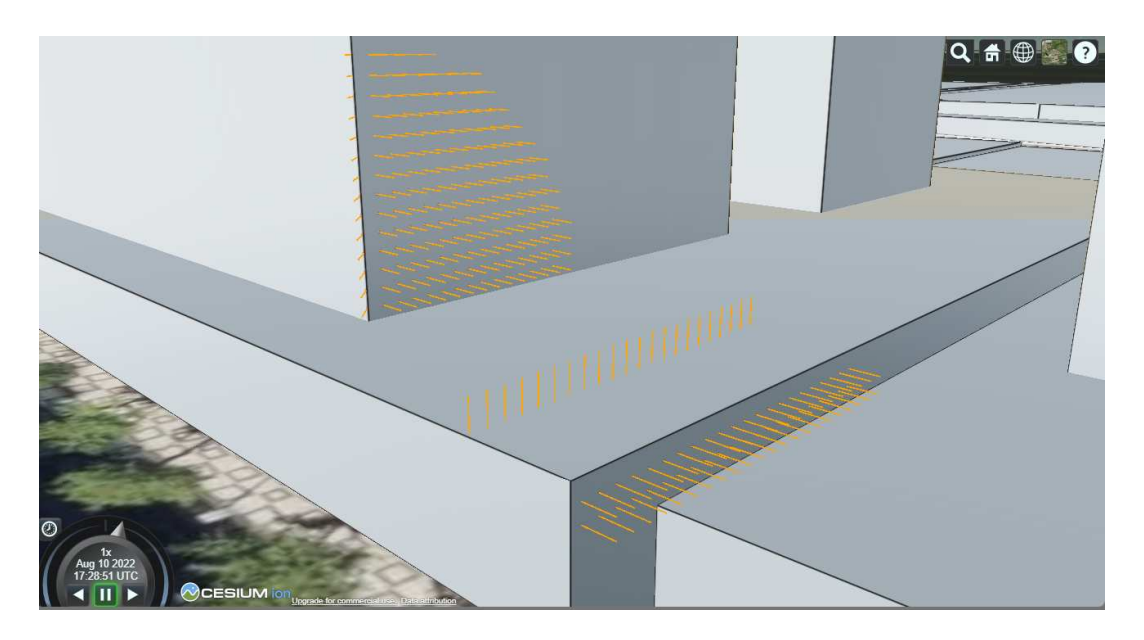


Figure 37. Results of approximated normals

After obtaining the point normal, using the angle of incidence and the approximated normal, the reflected vector is calculated and analysed if it can reach the receiving antenna. If the condition is verified, the point analysed is also stored under a reflective points key inside the JSON object of the building entity whom the point found composes.

In a primary iteration of the ray-tracing algorithm (denominated optical ray-tracing), only the first path elements in LoS were taken into account. To analyse the extra layers that can be found beyond the first obstacle, a second algorithm was developed (denominated complete ray-tracing). In the second algorithm, upon the building entity is returned and the point is stored, the building entity

is hidden and a new ray is cast on the same direction, creating a depth search for path obstacles, as presented in figure [38].

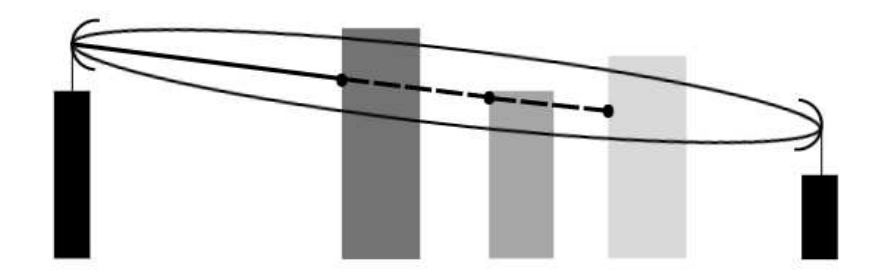


Figure 38. Depth search used in complete ray-tracing algorithm

The depth search stops in two conditions: the following point found is already outside the first Fresnel Ellipsoid or no more points are found (where the ray cast returns a undefined value). To guaranty that the entities are only analysed after the previous entity is hidden, the method of frame request of the Cesium window is change. By default, the Cesium window displays 3D models by rendering frames using a similar process of game engines, requesting new frames at a targeted frame rate [61]. This process can be changed allowing new frames rendering to be requested manually. By doing so, after a found entity is hidden, a frame is manually requested before casting a new ray. After the depth search is completed, all entities hidden are shown and a new frame is requested to be rendered. Lastly, the rendering mode is changed again to the default method as the process of obstacle detection is proceeded.

Although providing a precise analyses of the path obstacles, the ray-casting algorithm execution time can be increased with the level of definition used (the leap size used to loop through the Cesium window pixels) and the number of obstacles found, due to the level of computer power demanded to complete this algorithm. To analyze the developed algorithms performance, both algorithms were executed in 20 different links with various levels of obstruction, from clear LoS to highly obstructed links. All simulated links are located in the Lisbon metropolitan area, since it grants an increased level of terrain and urban elements data.

This study was made using a computer with the following characteristics:

• Operating System: Windows 11;

• CPU: Intel i7-8750H;

• GPU: NVIDIA GeForce GTX 1050 Ti;

• RAM: 16 GB.

Resulting of this study, the optical and complete algorithms average execution time was 5 minutes and 13 seconds and 7 minutes and 22 seconds respectively. The complete ray-tracing algorithm presented an increase of 312.75% obstacles detected. Analysing the effect of deep searched entities analyzed, it is possible to conclude that this is the main factor for increased execution time, having a direct proportion correlation, as presented in the following chart:

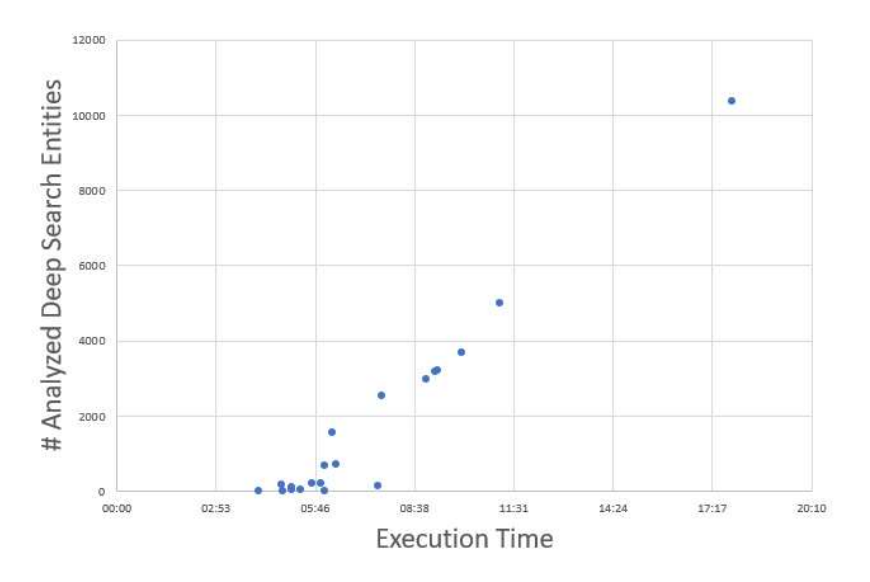


Figure 39. Relation between number of analyzed deep searched entities and execution time

As a result of the high execution time, a new window was created to display the Expected Time of Arrival (ETA). The ETA is calculated by analyzing the execution time to analyze a complete column of pixels (St as step-time) and calculate, using the level of pixel increment and the index of the current pixel, the remaining percentage of pixels to be analyzed (Rp as remaining-percentage). Calculating the percentage corresponding to the current analyzed column (Sp as step-percentage), the ETA is calculated as:

$$\boxed{\text{ETA}} = Rp \cdot \frac{St}{Sp} \tag{4.3}$$

In the window is also presented a progress bar, indicating the current progress on the ray-tracing algorithm completion. This window is presented in figure 40.



Figure 40. Algorithm progress window

To present the result found in the simulated project, the following step windows depicted in figure 41, 42, 43, 44 and 45 are presented.

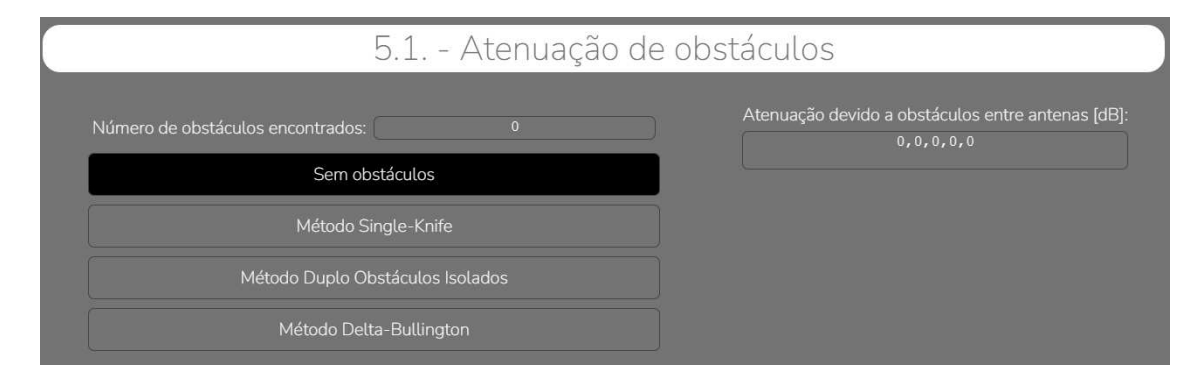


Figure 41. Obstacles attenuation step window for terrestrial projects

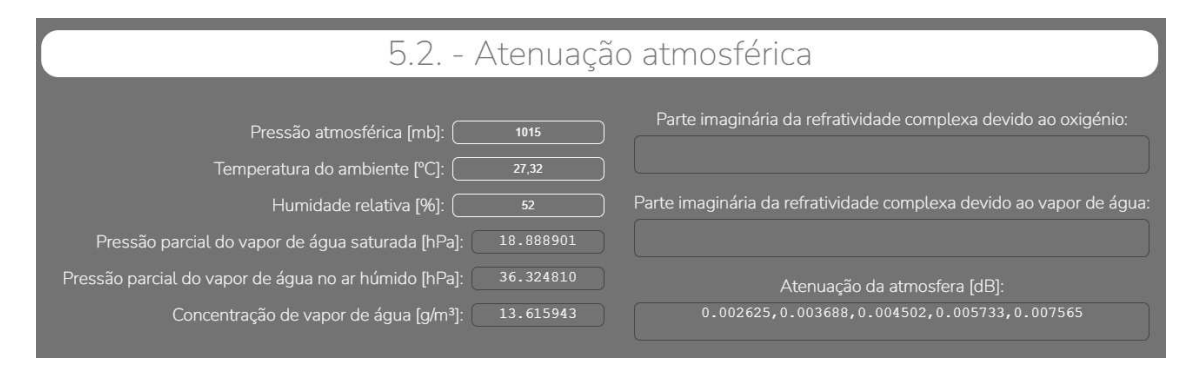


Figure 42. Atmospheric attenuation step window for terrestrial projects

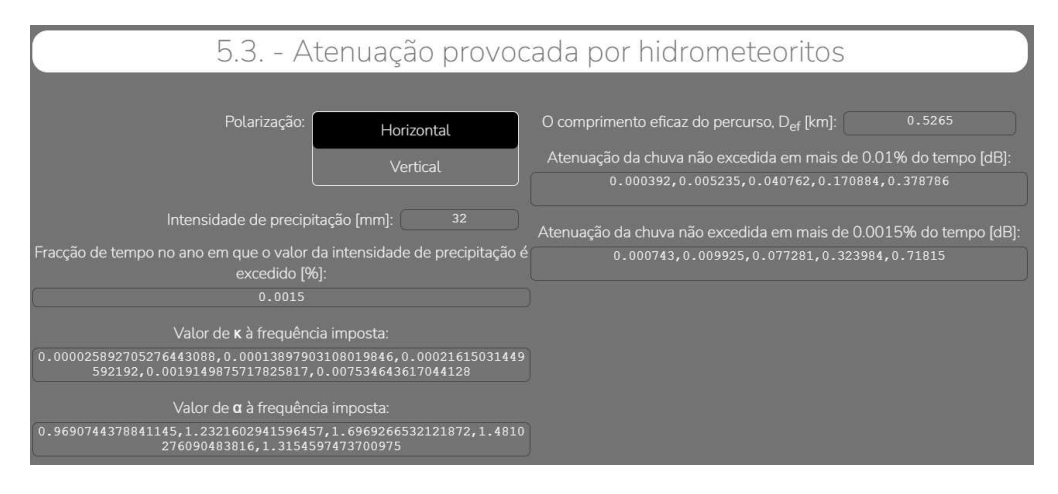


Figure 43. Rain attenuation step window for terrestrial projects

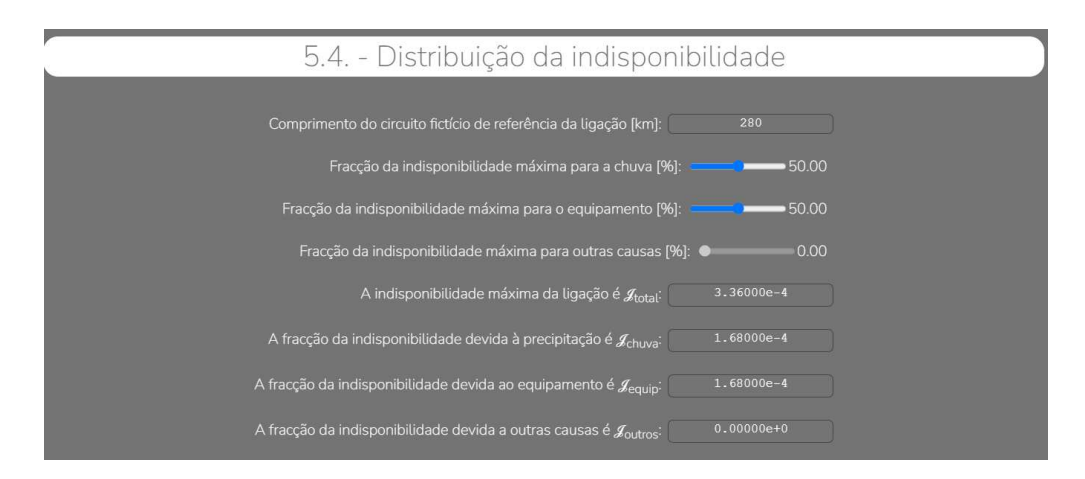


Figure 44. Unavailability distribution step window for terrestrial projects



Figure 45. Fast fading step window for terrestrial projects

To obtain real time weather information used for atmospheric attenuation calculations, the OpenWeatherMap [API [62]] is used. This [API] allows the search of weather variables (including humidity, dry air pressure and temperature) of a given coordinate point. The process to acquire the information starts when the user defines the transmission antenna position. This position is then converted from a Cartesian coordinate system to a geographic coordinate system using the Cesium

API Then, using the position of the antenna in geographic coordinates, an URL is created including the position to be searched, the type of units to be retrieved and an API key that associates the search to a specific user. Using the fetch API incorporated in JavaScript, the information enquired is returned in a JSON object, to be accessed.

4.5.4. **SNR** in **IPC**

To calculate the value of SNR for this section, the following parameters are analysed, as they directly influence the value of SNR:

- Emission power;
- Antennas gains;
- Path loss elements;
- Existence of passive repeater;
- Additional attenuations;
- Number of symbols.

Consequently, upon changes on any of the project elements referred, the SNR may be recalculated and the project elements SNR dependent. The window where the results of this section are presented are depicted in figure 46.



Figure 46. SNR in IPC step window for terrestrial projects

4.5.5. **QoS** parameters

The QoS parameters, although independent from project values, influence further calculations for margins, as they define the quality goals for the project. Therefore, if the user changes the quality objectives, the dependent elements must be recalculated as presented in figure 47.

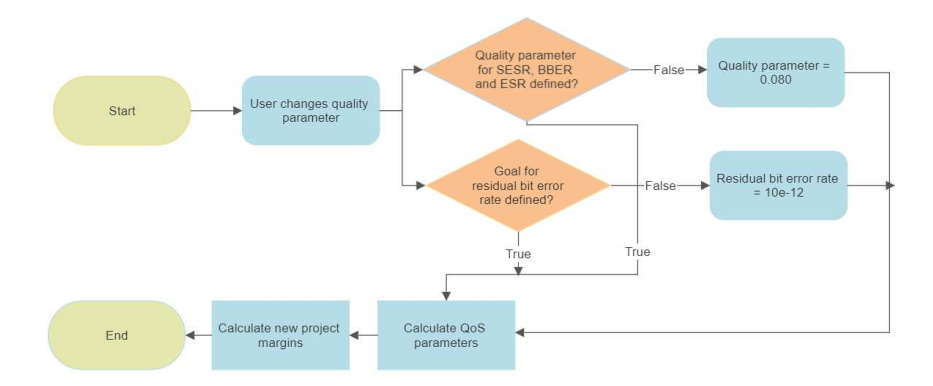


Figure 47. QoS components of terrestrial projects flow chart

The results of this section are presented by the window step depicted in figure 48.

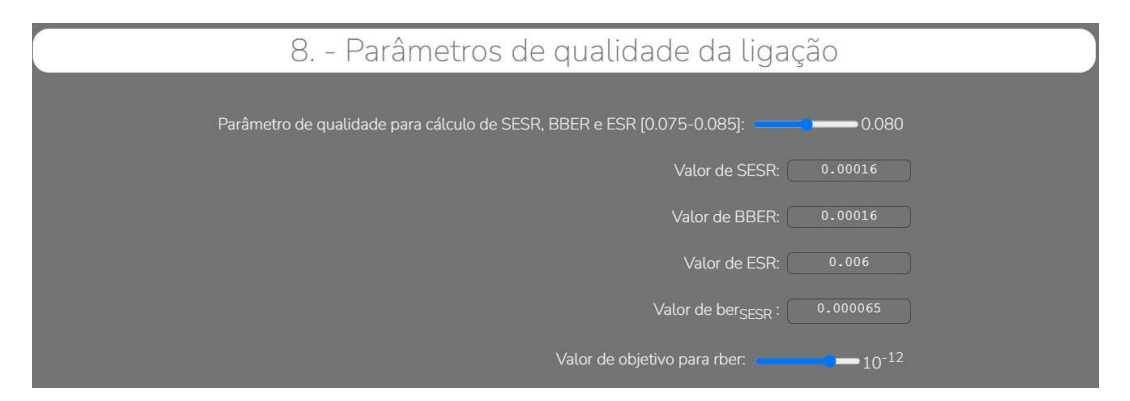


Figure 48. QoS parameters step window for terrestrial communication systems

4.5.6. Project margins

In this section, the uniform fading margin, selective fading margin and critical margins are taken into account. This margins are a method of comparison between the quality objectives defined and the simulated value. Therefore, the margins are dependent of all path elements defined and the objectives defined, needing to be calculated on the occasion that a change on one of these elements occurs.

For a better understanding of the evolution of the system margins due to system frequency change, the margins are presented separately as well as in a two dimensional graph combining the value of said margins with the evolution of system frequency. An example of the step window presented to the user is depicted in figure 49.

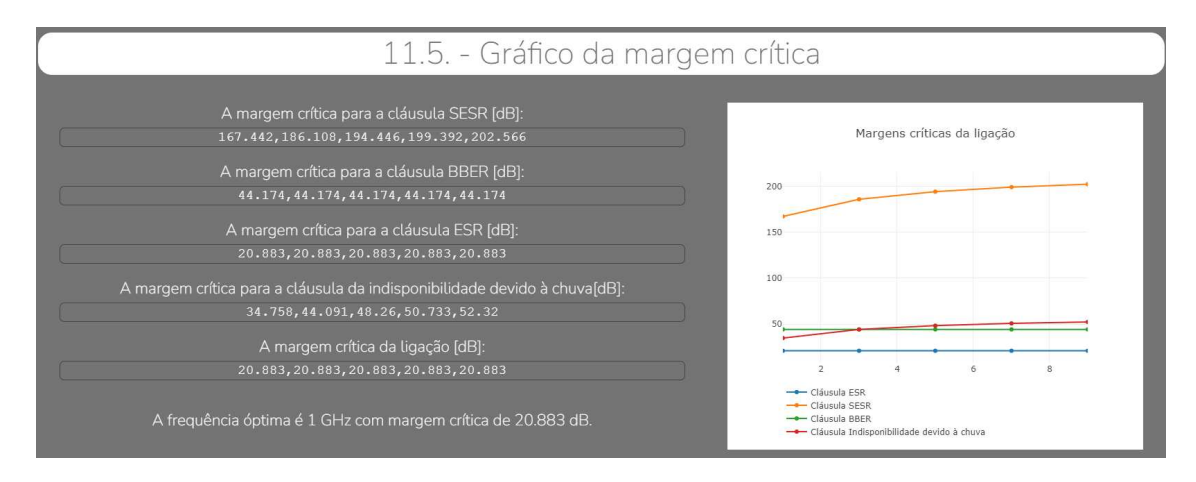


Figure 49. Critical margins step window

4.5.7. Diversity and Equalization

The purpose of adding diversity and equalization is to minimize the effect of selective fading, the addition and removal of diversity and equalization have an impact on the selective fading margin, consequently affecting the rest of system margins calculated. Therefore, the addition, removal and changes made on this techniques require additional calculations to obtain the system margins.

To allow the user to identify the current methods that are being used, different parts of the step window for this section are shown or hidden. The full step window for this section is presented in figure [50].

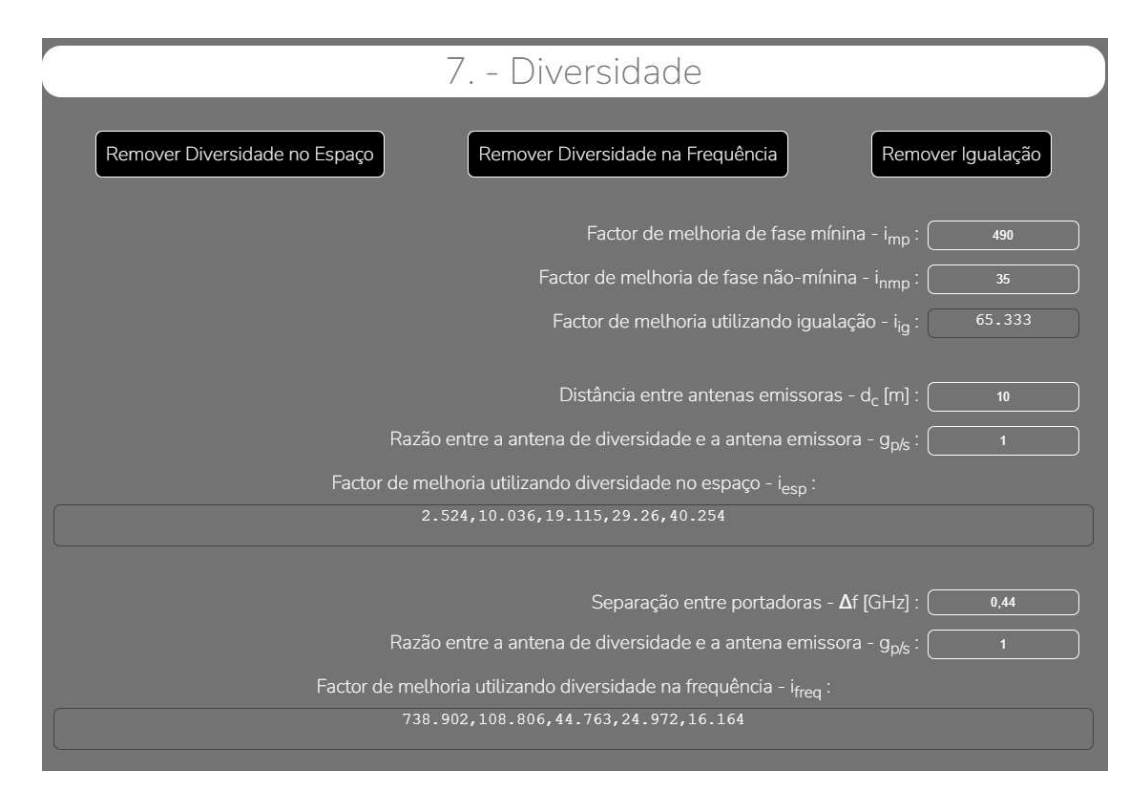


Figure 50. Diversity step window

4.6. Satellite Communication Systems

For satellite communication system projects, to apply the models presented in 3.2, the steps are presented to the user by the following order:

- Transmission and receiving stations characteristics
- Orbit definition
- Satellite characteristics
- Radio characteristics
- QoS parameters
- Path Loss
- Link budget elements

4.6.1. Stations characteristics

In this section, the user defines the stations positions, filling the values presented in figure 51 to create a geographic coordinate. Using this geographic coordinate, a Cartesian coordinate is obtained using the Cesium API and a antenna 3D model equal to the terrestrial communication systems. The

azimuth and elevation angles are calculated using the defined position for the antenna and the current position of the current selected satellite, if said satellite has been defined by the user in section 4.6.2. Additionally, for projects that simulate a communication system singularly with a satellite, the position of the respective station can be defined as equal to the transmission station position by the press of a single button.

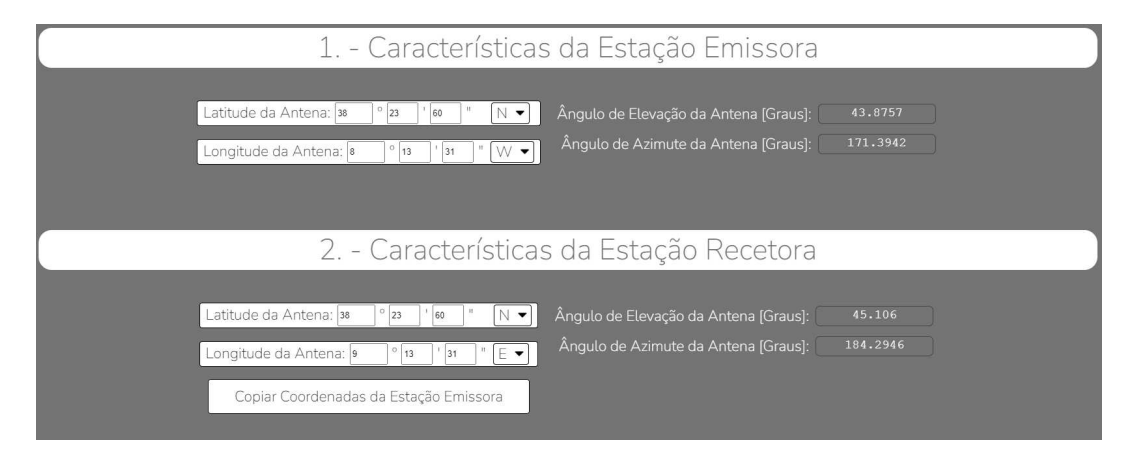


Figure 51. Stations characteristics step window for spacial projects

4.6.2. Orbit definition

To define the orbit of the satellite of which the communication system will relay upon, a set of predefined orbits are presented to the user. This orbits are obtained by using the JavaScript fetch API to return the current active satellites information provided by CelesTrak in http://ce-lestrak.org/NORAD/elements/active.txt. The link provides a text file with over 3000 satellite orbits TLE coordinates that can be displayed in the Cesium window. Upon returning the text file information, a drop-down menu is created to allow the user the select an orbit, identified by the satellite name. When the user selects an orbit, the different TLE components are displayed to the user, as well as a satellite, presented as a Cesium point entity, and an orbital line are displayed in the Cesium window, where the user can see the satellite movement over an one day period. This satellite movement can be stopped and started in the Cesium window by a button provided internally in the Cesium window. The orbital line is created by connecting different points of the selected orbit, using the Cesium polyline entity. These points are obtained by calculating the difference in position that the satellite has every 20 seconds for the entire day that is analysed.

Additionally, 2 lines connecting the satellite position and the stations positions is presented to the user. These lines provide a visual component indicating to the user if the connection is possible to be had or if it is blocked by the earth surface, displaying the color green if there is no blockage and red if otherwise. To inquire if blockage is found, the intersection between a circle (with the earth radius) and the connecting lines found. From this intersection, 2 cases can occur: only one point is found or two points are found. In the case of one point is found, this symbolises that the connecting line between the station and the satellite create a tangent to the earth surface, therefore no blockage is found (case a). In the case where 2 points are found, one point is the station position and the second point is the possible blockage point. By calculating the distance of each point to the satellite, in the case where the possible blockage point is closer to the satellite position than the station position, signal blockage occurs (case b) and, consequently, in the case where the station position is closer to the satellite, no blockage is found (case c). The different cases are described in figure [52].

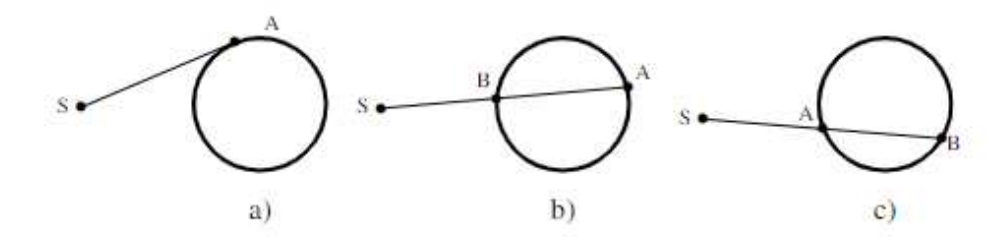


Figure 52. Possibilities for signal blockage due to earth surface

The step window for this section is depicted in figure [53].

4.6.3. Satellite characteristics

In this section, the user is required to enter the satellite characteristics, as this characteristics influence the link budget calculations, having to consequently recalculate the link budget every time a change on this characteristics occurs. The window step presented to the user for this objective is presented in figure [54].



Figure 53. Orbit definition step window



Figure 54. Satellite characteristics step window

4.6.4. Radio characteristics

Similarly to terrestrial communication systems, in this section the user defines the radio characteristics, which are reflected in the entire system. This section differs from terrestrial communication systems in the case where the user is allowed to define different frequencies for the uplink and downlink connections. Consequently, this feature divides the need for recalculations in the different links, meaning that when radio characteristics changes for the uplink only require recalculations for the uplink counterparts or joined counterparts and vice versa. The elements separated by uplink

and downlink are presented as a sub-step, being conjugated in a major step. The step windows for this section are depicted in figures 55 and 56

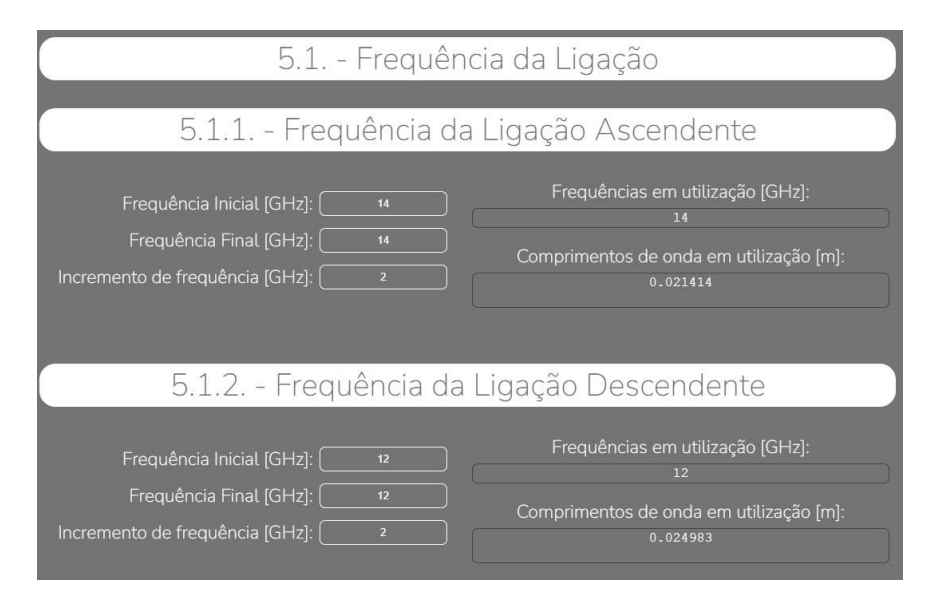


Figure 55. System frequency step window for spacial project



Figure 56. Digital signal characteristics step window for Spacial projects

4.6.5. **QoS** parameters

In this section, the user is required to define the maximum BER to be accomplished by the system, as well as the annual maximum time percentage of outage goal. This parameters influence, not only the path loss calculations (in particular the rain attenuation) but the calculations for the link budget as a whole. Therefore, upon changes, these elements are recalculated, presenting an updated result.

The following figure depicts the step window presented to the user for this section.

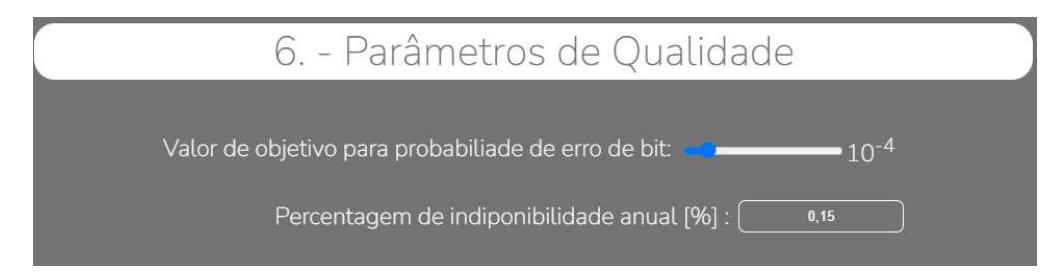


Figure 57. QoS parameters step window for spacial communication systems

4.6.6. Path loss

This step allows the user to analyse the path loss found in the simulated system, being divided in two separate links, the uplink and downlink, as previously mentioned. Departing from the separation in links, the layout of the different subsections is equal to the terrestrial, as the methods of calculation required the same inputs and give the same outputs between the different communication system types.

The spacial communications require an additional step in order to accommodate for interference caused by near communication systems. This step requires the user to input the values of interference to be expected in later calculations for the system link budget. The step window for this subsection is presented in figure [58].



Figure 58. Interference parameters step window

4.6.7. Link budget

In this section, the system elements composing the link budget are presented to the user. Since this section is a reflection of all elements of the system, recalculations must be made upon any element change.

The step window for this section is presented in figure 59.



Figure 59. Satellite project link budget step window

4.7. Tool Optimization

In this section, the optimization process and changes made to the developed tool are presented. This changes are a result of a combined effort with the Portuguese Army Directorate of Communications and Information Systems (DCSI) that partook in usability testing and meetings, allowing to encounter problems in the software workflow and additional features useful for the user.

A total of 2 separate meeting occurred. In the first meeting the following problems were brought up:

- 1 The process of adding antennas and passive repeaters in Terrestrial projects was found to be difficult, since in a first iteration the addition of these elements was not made using different buttons but using the right and left click of a mouse, were the transmission and receiving antennas were added, by order (meaning first the transmission and the receiving secondly, looping this order to change antenna positions), using the left mouse click and the passive repeater by using the right mouse click. To facilitate this process, the buttons presented at the bottom of figure 23 were created;
- 2 Users found difficult to differentiate from an input and an output elements. Therefore, the layout of the different elements was changes, where input elements have a white outline and output elements have a black outline;
- 3 It was requested to add a numerical element for each step window, allowing the user to understand the project progress made. This feature was added in the title of each step window.

Following, in the second meeting the main problems and requests brought up were:

1 - The software allowed the user to input elements without being verified. The input of negative values and different decimal separation elements (. or ,) became not valuable inputs are would display an error to the user as presented in figure 60;



Figure 60. Invalid input error message

2 - A step by step layout was suggested in order to visualise each step independently of the remaining steps, verifying if all inputs of a given step are correctly defined before moving to the next step. This creates a methodical process to define the project elements, contrarily to being allow to define different parts of a given step without a particular order. To accomplish this request, a additional option was added to the project creation window, that when selected, a "next" and "previous" buttons are added to the bottom of the project window that changes the step presented to the user to the next or previous when clicked, as presented in figure [61].

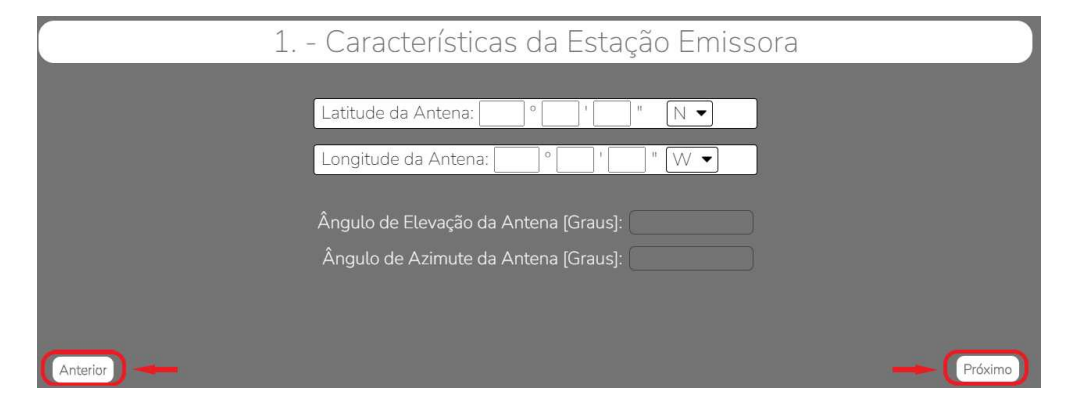


Figure 61. Step by Step project buttons

The figure 62 presents the project creation window with the mentioned feature highlighted;

3 - To facilitate the project design for professional users, it was requested to reduce the number of outputs given by the software. In order to fulfil this request without removing academic value on the project design, an additional project layout was created. In this project, the outputs considered unnecessary to professional usage were hidden from the user, presenting fewer steps to complete the project design.

For terrestrial projects, the steps hidden are:

• Equipment reliability;

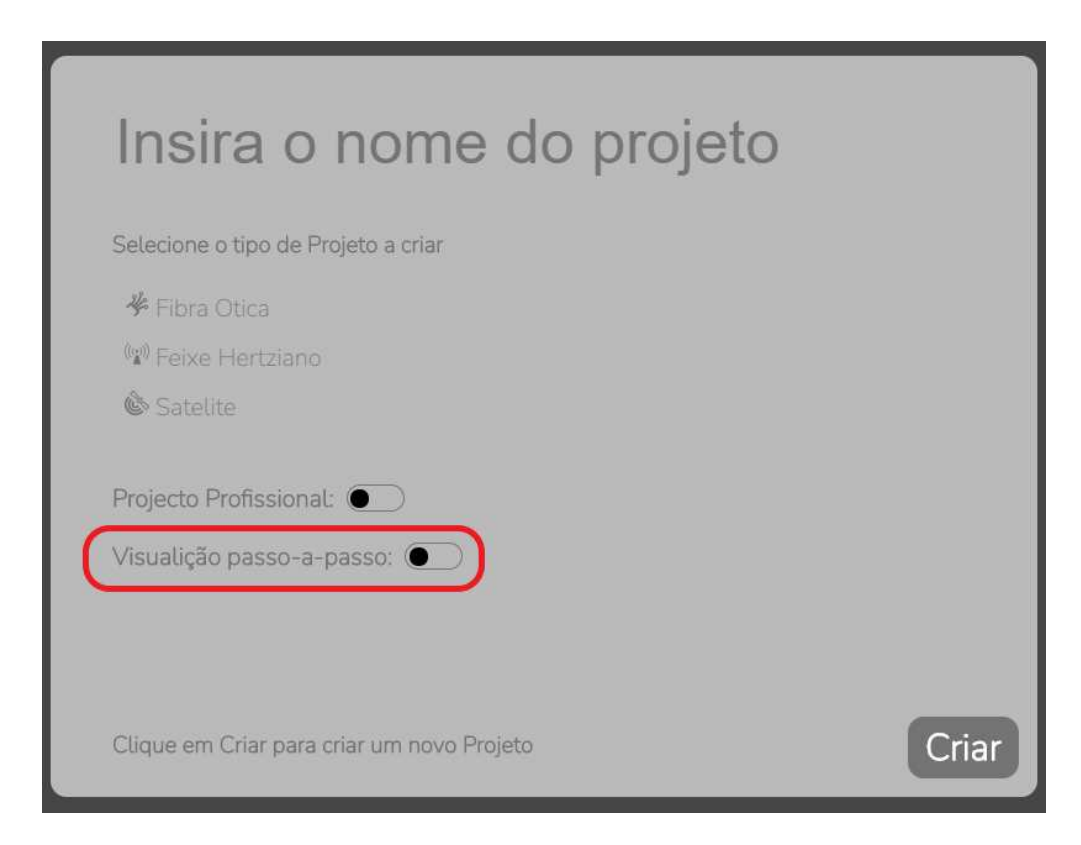


Figure 62. Step by step project layout option

- Obstacle attenuation;
- Atmospheric attenuation;
- Rain attenuation;
- Unavailability distribution;
- Fast fading;
- Signal reflections;
- SNR in IPC:
- Uniform fading margin;
- Selective fading margin.

For spacial projects, the steps hidden are:

- Free space attenuation;
- Atmospheric attenuation;
- Rain attenuation.

To select this project layout, upon creating a project, the user is presented with the option to create a professional project, as seen in figure 63;

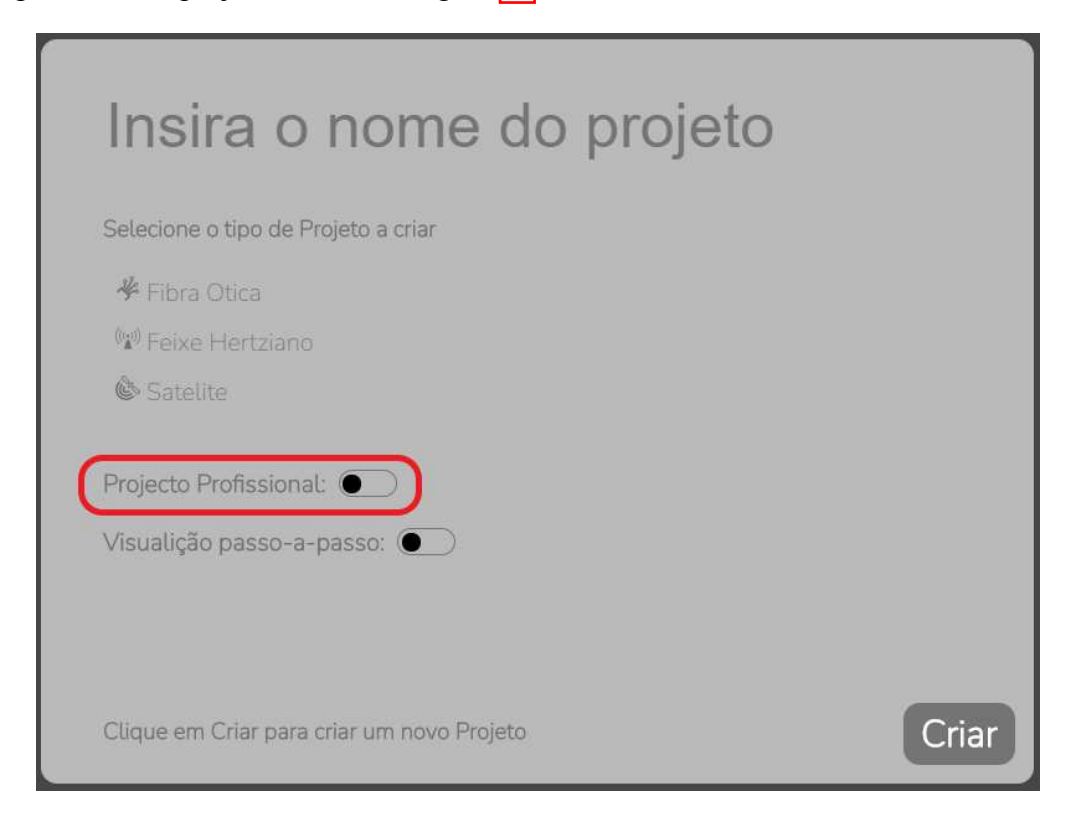


Figure 63. Professional project layout option

4 - It was requested to create a mechanism that allowed the user to identify in which step it is currently being displayed, in relation to the total steps presented in the project design. To accomplish this goal, a slider was added to the top of the project window, indicating the steps that the current project has and the step currently being presented to the user. The slider also displays what step each element represent by hovering the mouse on each step number and allows the user to select said step, scrolling or skipping to the selected step in a normal project or with a step by step layout respectively. The developed feature is presented in figure 64.

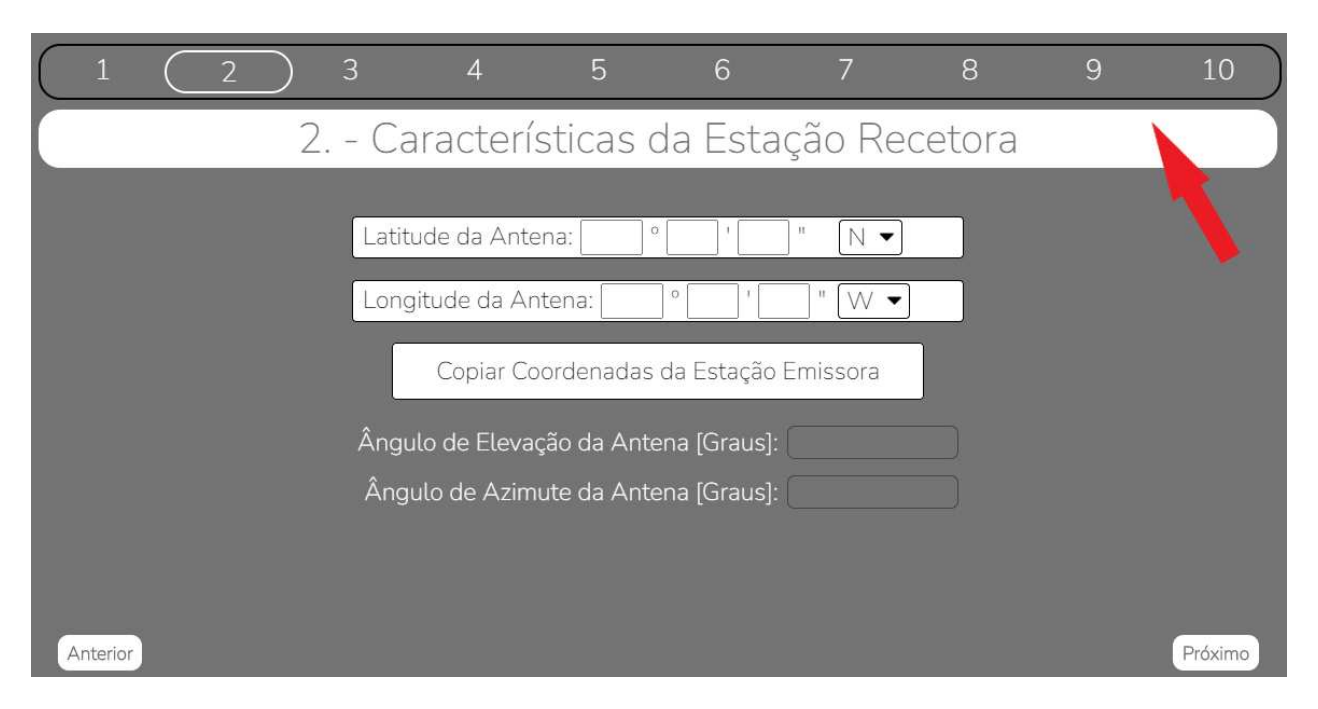


Figure 64. Project step display feature

CHAPTER 5

Case Study

In this chapter, it is designed a terrestrial and a spacial project using the software developed. The system parameters will be presented as well as the results outputted by the tool.

5.1. Terrestrial project

This section presents the design of a terrestrial RF communication project between a station located in Moscavide (Lisbon, Portugal) and a station located in Palmela (Setúbal, Portugal), using the characteristics shown in table 4.

Table 4. Simulated terrestrial link characteristics

Frequencies [GHz]	1,3,5,7,9
Antennas Radiation Efficiency [%]	50
Transmission Power [W]	20
Transmission rate [Mbits/s]	140
Bandwidth [MHz]	34
Roll-of factor	0.142
Modulation	64-QAM
Polarization	Horizontal
RBER	$1 \cdot 10^{-12}$
QoS parameter	X = 0.08
Additional attenuations [dB]	0

5.1.1. Path selection

To position the antennas, 2 buildings were selected in each location to place the antennas as presented in figure 65.

Upon defining the antennas positions, the default values of pool height was not changed, resulting both antennas having a pool of 1 meter of length. The antenna diameter was set to 3 meters resulting in a effective antenna area outputted of 3.5343 m². The calculated gain for both antennas are 26.939 dBi for 1 GHz, 36.481 dBi for 3 GHz, 40.918 dBi for 5 GHz, 43.841 dBi for 7 GHz and



Figure 65. Simulated terrestrial project link

46.024 dBi for 9 GHz. It was selected the same antenna radiation pattern for both transmission and receiving antennas, as depicted in figure 66.

150F2 HE

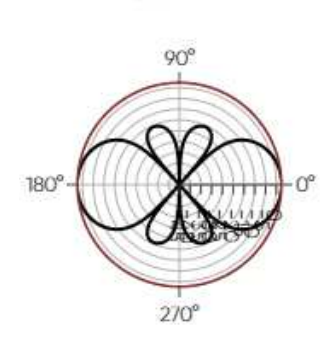


Figure 66. Radiation pattern selected for terrestrial project demonstration

5.1.2. Path loss

Firstly, to detect any obstacles on the chosen path, the ray-tracing algorithm was ran using the optical method, outputting 2 obstacles in the path. Therefore, the double isolated edges calculation method was used.

Using the OpenWeatherMap API, it was determined that, at the time the project simulation occurred, the weather properties found in the transmission antenna were as presented in table 5.

As a result, the path loss found in the system path and consequent SNR in IPC are defined as presented in table 6.

Table 5. Weather characteristics in simulated transmission antenna

Temperature [°C]	23.39
Relative Humidity [%]	69
Dry air pressure [mb]	1015

Table 6. Path attenuations for simulated terrestrial system

Frequency [GHz]	1	3	5	7	9
Free space attenuation [dB]	121.3	120.9	135.3	138.2	140.4
Obstacles attenuation [dB]	3.4	3.4	3.4	3.4	3.4
Atmospheric attenuation [dB]	0.1	0.3	0.5	0.8	1.2
Rain attenuation [dB]	0.03	0.03	2.7	11.2	24.96
Signal Reflections [dB]	-65.9	-17.0	12.9	29.7	38.97
SNR in IPC [dB]	65.2	74.1	75.8	69.6	57.4

Analysing the system signal reflections, the path contains a high level of signal reflections when frequencies equal or above 5 GHz are used, resulting in the need to redirect the signal for the system to provide a reliable connection.

5.1.3. Passive repeater introduction

Resulting on the level of signal reflection found in the simulated communication system, an passive repeater was added to the system. The new communication path is depicted in figure 67.

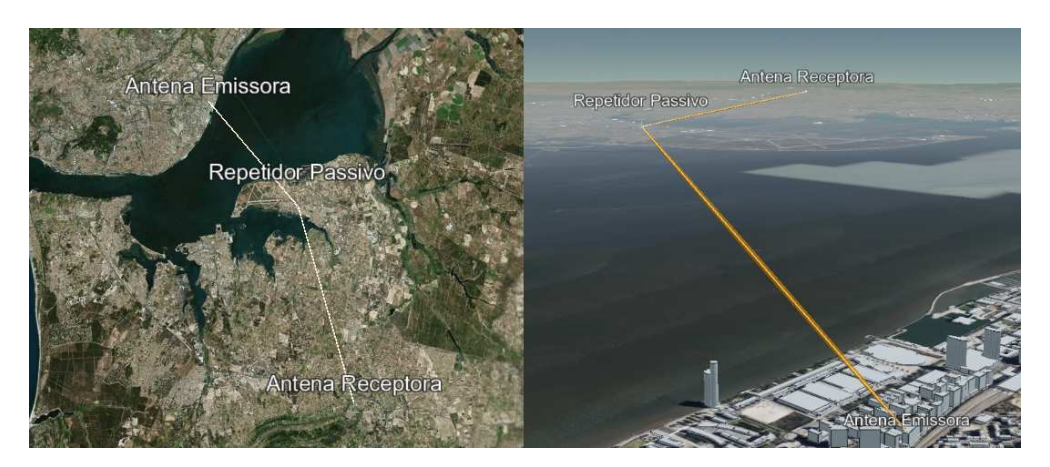


Figure 67. Simulated terrestrial project link with passive repeater

The passive repeater characteristics used are presented in table 7.

To minimize the obstacle attenuation, the antennas heights were also increased to 10 meters for both transmission and reception antennas.

Table 7. Passive repeater characteristics for simulated terrestrial project

Pool height [m]	20
Dish area [m ²]	80
Passive repeater radiation efficiency [%]	95

As a result of the passive repeater addition, the attenuation factors are recalculated, resulting in the output parameters presented in table 8.

Table 8. System elements with passive repeater addition for simulated terrestrial project

Frequency [GHz]	1	3	5	7	9
Free space attenuation [dB]	230.7	249.8	258.7	264.5	268.9
Obstacles attenuation [dB]	0	0	0	0	0
Atmospheric attenuation [dB]	0.1	0.3	0.5	0.8	1.2671
Rain attenuation [dB]	0.03	0.4	2.7	11.4	25.3
Signal Reflections [dB]	$-\infty$	$-\infty$	$-\infty$	$-\infty$	$-\infty$
Passive repeater gains [dB]	67.5	86.6	95.5	101.3	105.7
SNR in IPC [dB]	26.8	45.3	51.3	47.98	37.8

Analysing the outputted results, the signal reflection is no longer a degrading element to the system.

5.1.4. Project margins

To uphold a reliable communication system, it is required to the system to verify all defined margin, as well as having a system critical margin above 3 dB [24]. For the simulated project, the clauses verification is presented in table 9.

Table 9. Project clauses fulfilment for simulated terrestrial project

Frequency [GHz]	1	3	5	7	9
SESR clause fulfilment	False	True	True	True	False
BBER clause fulfilment	False	False	True	False	False
ESR clause fulfilment	True	True	True	True	True
Unavailability due to rain clause fulfilment	True	True	True	True	False

As a result of the clauses analysis, the critical margins calculated for this clauses is presented in table 10.

The critical margins evolution through every analysed communication frequency is presented to the user also using a line graph, as presented in figure 68.

Table 10. Project clauses critical margins for simulated terrestrial project

Frequency [GHz]	1	3	5	7	9
SESR critical margin [dB]	-11.96	1.7	5.6	0.7	-10.6
BBER critical margin [dB]	-16.3	-2.6	1.2	-3.6	-14.9
ESR critical margin [dB]	4.2	15.6	17.2	15.0	5.5
Unavailibility due to rain critical margin [dB]	1.3	19.5	23.7	13.6	-7.4
Project critical margin [dB]	-16.3	-2.6	1.2	-3.6	-14.9



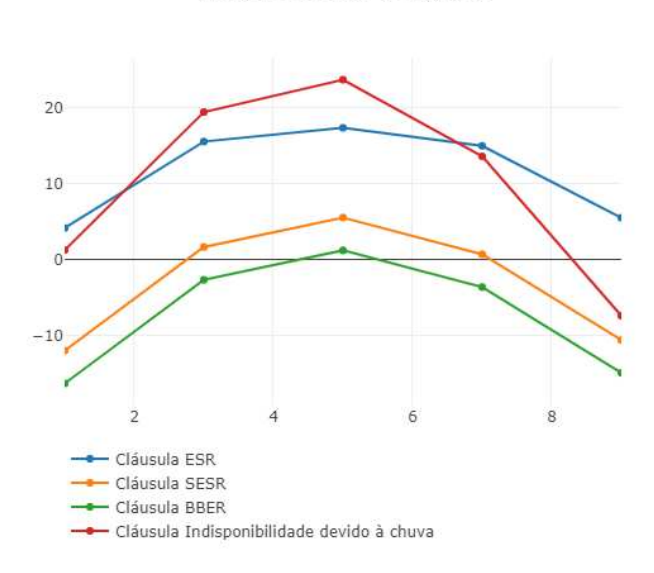


Figure 68. Critical margins evolution through increased communication frequency for simulated terrestrial project

As presented in both tables and 10, as well as in figure 68, all clauses are fulfilled only when frequency of 5 GHz is used. Conversely, using this system frequency does not fulfil a project critical margin of 3 dB (having a 1.2 dB project critical margin), as previously mentioned. Subsequently, diversity and signal equalization is used.

5.1.5. Diversity and equalization introduction

The introduction of diversity and equalization results in the requirement to meet the 3 dB threshold for project critical margin. For this system, both methods of diversity will be implemented, as well as signal equalization. This methods will be implemented using the characteristics shown in table

Table 11. Diversity and Equalization characteristics for simulated terrestrial project

	Distance between space diversity	10
Space diversity	antenna and transmission antenna [m]	10
	Gain ratio between space diversity	1
	antenna and transmission antenna	1
Frequency diversity	Carriers frequency separation [GHz]	4
rrequency diversity	Gain ratio between frequency diversity	1
	antenna and transmission antenna	1
Signal equalization	Minimum phase gain factor	490
Signai equalization	Non-minimum phase gain factor	35

As a result of diversity and equalization implementations, after recalculating the project critical margins, the values obtained are presented in table [12].

Table 12. Project clauses critical margins for simulated terrestrial project using diversity and equalization

Frequency [GHz]	1	3	5	7	9
SESR critical margin [dB]	-37.3	-0.5	11.7	4.97	-15.4
BBER critical margin [dB]	-44.98	-8.2	4.0	-2.7	-23.1
ESR critical margin [dB]	-23.8	12.13	18.3	15.9	-1.9
Unavailibility due to rain critical margin [dB]	1.3	19.454	23.7	13.6	-7.4
Project critical margin [dB]	-44.99	-8.2	4.02	-2.7	-23.1

Using this methods, the project critical margin using 5 GHz communication frequency is increased to 4.0 dB, creating a reliable communication system using the elements and characteristics described throughout this project design.

5.1.6. Equipment reliability

In this section, the **TU-R** standards for equipment reliability are analysed. For the simulated project, the elements presented in table **13** are considered.

Using these elements results in a maximum unavailability of $1.344 \cdot 10^{-4}$ and an unavailability caused by the equipment of $3.057 \cdot 10^{-4}$, not fulfilling the ITU-R Recommendation. Consequently, a reserve channel was added, having a 1+1 configuration. The MTBF for a commutator 1+1 was defined as 90 000 hours, resulting in a unavailability caused by the equipment of $1.334 \cdot 10^{-4}$, fulfilling the ITU-R Recommendation.

Table 13. Equipment reliability elements for simulated terrestrial project

MTBF for transmission [h]	120 000
MTBF for desmodulator [h]	140 000
MTBF for modulator [h]	200 000
MTBF for receptor [h]	200 000
MTTR [h]	6

5.2. Spacial project

In this section, a spacial communication system is simulated using the developed tool. The tool, in the design conclusion, is to output the necessary antennas characteristics required to ensure a reliable connection.

The simulated spacial system characteristics are presented in table 14.

Table 14. Simulated spacial link characteristics

Transmission antenna coordinates	39° 23′ 59" N - 8° 1′ 0" W
Receptive antenna coordinates	16° 0' 7" N - 24° 0' 0" W
Uplink frequencies [GHz]	2,4,6,8,10
Downlink frequencies [GHz]	2,4,6,8,10
Transmission rate [Mbits/s]	60
Bandwidth [MHz]	36
RBER	10^{-4}
Unavailability year percentage [%]	0.15
Modulation	4-QAM
Uplink polarization	Horizontal
Downlink polarization	Horizontal

5.2.1. Orbit definition and satellite characteristics

For the present simulation, the orbit of satellite LCS 1 was used, as this orbit enables a direct connection between the transmission and receiving antennas positions simultaneously. This orbit and the transmission and receiving antennas positions are depicted in figure [69].

The orbit main Keplerian elements for the selected satellite orbit are presented, as outputted, in table 15.

Using the satellite position presented in figure [69], the uplink communication distance is outputted as 3441.669 km and the downlink communication distance as 3743.343 km.

The parameters of the satellite are summarized in table 16.

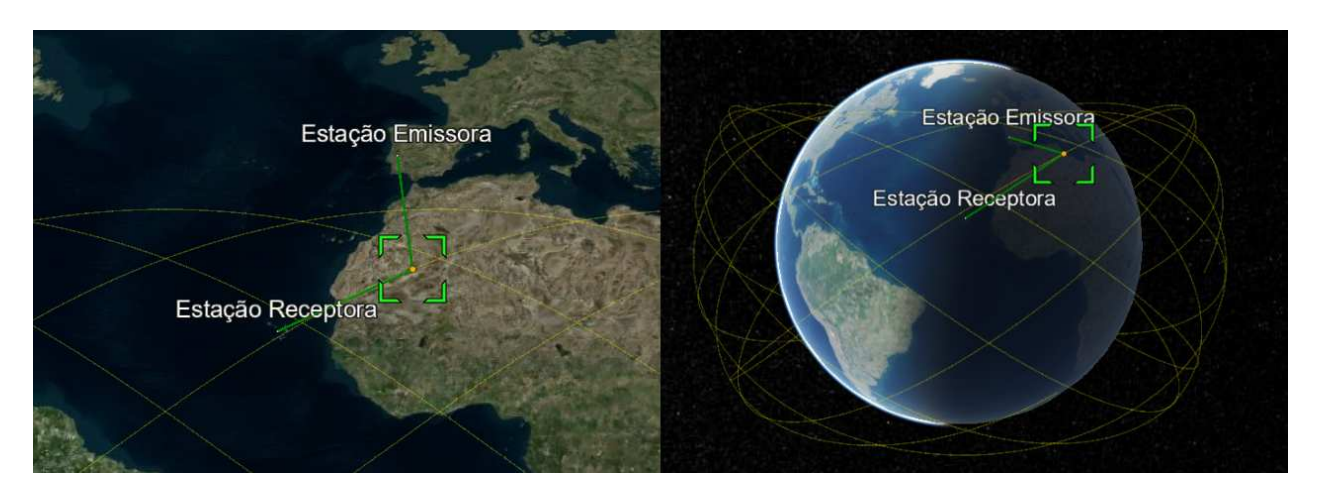


Figure 69. Antennas and satellite positions for simulated spacial project

Table 15. Main Keplerian elements of used satellite orbit for simulated spacial project

Longitude of ascending node [°]	231,55
Orbit inclination [°]	32,14
Argument of perigee[°]	137,36
Ellipse semi-major axis [km]	9166,05744
Eccentricity	0,0012574

Table 16. Satellite characteristics used in simulated spacial project

Power density for transponder saturation [dBW/m2]	-81.5
Receptor merit factor [dB/K]	3.1
Saturated effective isotropic radiated power [dBW]	46.2
Input back-off in clear sky communication [dB]	3
Output back-off in clear sky communication [dB]	0.3

5.2.2. Stations characteristics

To connect the antennas to the satellite, the antennas are required to be rotated following an azimuth and elevation angle. For the simulated project, the angles of rotation outputted are presented in table [17].

Table 17. Satellite characteristics for simulated spacial project

Transmission antenna	Azimuth angle [°]	172.8158
	Elevation angle [°]	44.3478
Receiving antenna	Azimuth angle [°]	61.0633
	Elevation angle [°]	61.9849

This step is used in a practical manner, as it outputs antenna physical characteristics that are applied in the project deployment phase.

5.2.3. Path loss

Similarly to the terrestrial project, the OpenWeatherMap API was used to inquire the weather conditions in the transmission and receiving antennas. The obtained results are presented in table 18.

Table 18. Weather characteristics in antennas positions for simulated spacial project

	Temperature [°C]	26,09
Transmission antenna position	Relative Humidity [%]	45
	Dry air pressure [mb]	1017
Receiving antenna position	Temperature [°C]	25,8
	Relative Humidity [%]	76
	Dry air pressure [mb]	1009

Following the methods presented in section 3.2.2 and using the weather characteristics outputted, the attenuation values outputted are presented in table 19.

Table 19. Path attenuations for simulated spacial system

	Frequency [GHz]	2	4	6	8	10
Uplink	Free space	169.2	175.2	178.7	181.2	183.1
	attenuation [dB]	109.2				
	Atmospheric	0.1	0.2	0.3	0.5	0.7
	attenuation [dB]	0.1				
	Rain attenuation [dB]	0.04	0.3	1.4	3.5	6.1
Downlink	Free space	169.9	175.9	179.4	181.9	183.9
	attenuation [dB]	109.9				
	Atmospheric	0.2	0.4	0.7	1.1	1.6
	attenuation [dB]	0.2				
	Rain attenuation [dB]	0.06	0.4	1.9	4.8	8.6

5.2.4. Link budget

Using all the elements inputted and outputted, in this step the antennas characteristics are outputted allowing to deploy a reliable communication system. Considering the elements presented for this simulation, the antennas characteristics outputted are presented in table 20.

Table 20. Simulated spacial project link budget elements

Transmission antenna	Diameter [m]	1.41
	Radiation effeciency [%]	50
	Minimum gain [dB]	40.4
	Minimum emission power [W]	61.57
Receiving antenna	Diameter [m]	1.41
	Radiation effeciency [%]	50
	Minimum gain [dB]	40.37

CHAPTER 6

Conclusions

6.1. Main conclusions

In this dissertation, a tool able to automatize the process of project design of terrestrial and spacial RF communication systems, minimizing the time spend in this project step, was developed. This tool abides to the most recent ITU-R Recommendations at the time of development.

Apart from performing the needed calculations, the tool also provides processes to warn the user when an element of the project design is detrimental to the project, as well as how can the user fix the found problem.

Even though there are tools currently available for similar use, it was found that the majority of tools available are outdated or bare a large financial investment for engineering students and organizations. Contrarily, the developed tool provide a free to use experience, mostly advantageous to students. Furthermore, the developed tool provide both academic and professional use, providing a greater understanding of design elements for students and a fast and direct approach to professional project designers.

To validate the tool results, independent projects previously designed were simulated using the developed tool, to verify if the results in both instances matched.

By meeting with possible professional users, the features developed were tested, being able to inquire the changes needed, problems that could be unresolved and additional useful features.

A new method for obstacle detection was created. The usage of a simplified ray-tracing algorithm allow, not only to detect obstacles in a link path, but also to predict the signal diffraction and reflection caused by the given obstacles. Despite the level of complexity of this algorithm and having an elevated execution time when compared with two-dimensional algorithms, the developed algorithm presents an increased level of precision, considering all elements in a link path and the path surroundings, granting greater scientific value to the developed tool.

6.2. Future work

In order to further improve the quality of results and experience using the developed tool, some features were unable to be explored, resulting in research points to be carried out in future work:

- Changing the usage of Cesium default engine to using Unreal Engine in conjuncture with the Cesium plugin already developed, as the Unreal Engine is far more developed for ray-tracing algorithms compared with Cesium default engine.
- Expanding the types of projects designs available, for example communication projects using fiber connections;
- Incorporation of data bases of characteristics of real life models of antennas and satellites

References

- [1] D. R. Beering, S. Tseng, J. L. Hayden, *et al.*, "Rf communication data model for satellite networks," in *MILCOM 2009 2009 IEEE Military Communications Conference*, 2009, pp. 1–7. doi: 10.1109/MILCOM.2009.5379814.
- [2] M. Pagani and H. Italia, "Microwave digital radio link transceivers: Historical aspects and trends," in *IEEE MTT-S Int. Microw. Symp., Workshop WMH-4*, 2015.
- [3] W. Gunathilaka, H. Dinesh, and K. Narampanawe, "Semi-automated microwave radio link planning tool," in *2011 6th International Conference on Industrial and Information Systems*, IEEE, 2011, pp. 294–299.
- [4] L. Morgan and P. Finnegan, "Benefits and drawbacks of open source software: An exploratory study of secondary software firms," in *IFIP International Conference on Open Source Systems*, Springer, 2007, pp. 307–312.
- [5] K. Peffers, T. Tuunanen, M. A. Rothenberger, and S. Chatterjee, "A design science research methodology for information systems research," *Journal of management information systems*, vol. 24, no. 3, pp. 45–77, 2007.
- [6] G. L. Geerts, "A design science research methodology and its application to accounting information systems research," *International journal of accounting Information Systems*, vol. 12, no. 2, pp. 142–151, 2011.
- [7] V. Szalvay, "An introduction to agile software development," *Danube technologies*, vol. 3, 2004.
- [8] J. R. Lewis, "Usability testing," *Handbook of human factors and ergonomics*, vol. 12, e30, 2006.
- [9] S. Riihiaho, "Usability testing," *The Wiley Handbook of Human Computer Interaction*, vol. 1, pp. 255–275, 2018.

- [10] B. Albert and T. Tullis, *Measuring the user experience: collecting, analyzing, and presenting usability metrics.* Newnes, 2013.
- [11] J. Forlizzi and K. Battarbee, "Understanding experience in interactive systems," in *Proceedings of the 5th conference on Designing interactive systems: processes, practices, methods, and techniques*, 2004, pp. 261–268.
- [12] M. Hassenzahl and N. Tractinsky, "User experience-a research agenda," *Behaviour & information technology*, vol. 25, no. 2, pp. 91–97, 2006.
- [13] C. Kraft, User experience innovation: User centered design that works. Apress, 2012.
- [14] T. Manning, "Design of terrestrial microwave radio links," in *Proceedings of IEEE*. *AFRICON'96*, IEEE, vol. 2, 1996, pp. 564–569.
- [15] Cesium. "Cesium api documentation." (2022), [Online]. Available: https://cesium.com/learn/cesiumjs/ref-doc/(visited on 08/15/2022).
- [16] R. Campos, J. Quintana, and R. Garcia, "Quantized mesh generator for cesium 3d," *EMODnet High Resolution Seabed Mapping*, 2018.
- [17] R. Kuchkuda, "An introduction to ray tracing," *Theoretical Foundations of Computer Graphics and CAD, Italy*, 1987.
- [18] M. Christen, "Ray tracing on gpu," *Master's thesis, Univ. of Applied Sciences Basel (FHBB), Jan*, vol. 19, 2005.
- [19] V. Červený and J. E. P. Soares, "Fresnel volume ray tracing," *Geophysics*, vol. 57, no. 7, pp. 902–915, 1992.
- [20] C. Networks. "Linkplanner design networks." (2022), [Online]. Available: https://www.cambiumnetworks.com/products/software/linkplanner/ (visited on 09/29/2022).
- [21] Softwright. "Tap 7 demo software." (2022), [Online]. Available: https://www.softwright.com/support/downloads/tap-demo-software/(visited on 09/29/2022).
- [22] C. Planning. "Mlinkplanner 2.0." (2022), [Online]. Available: https://www.wireless-planning.com/mlinkplanner (visited on 09/29/2022).
- [23] L. Chaves and L. Estevam, "Feixer programa de feixes hertzianos," M.S. thesis, Instituto Superior Técnico, 1999.

- [24] M. Damião, "Desenvolvimento e optimização da ferramenta smart link planning tool para o planeamento de feixes hertzianos digitais," M.S. thesis, ISCTE Instituto Universitário de Lisboa, 2013.
- [25] M. Damião, M. Costa, F. Cercas, P. Sebastião, and J. Sanguino, "Modern and optimized planning tool for microwave link design," in 2014 4th International Conference on Wireless Communications, Vehicular Technology, Information Theory and Aerospace & Electronic Systems (VITAE), IEEE, 2014, pp. 1–5.
- [26] P. Queluz and F. Pereira, "Sistemas de telecomunicações feixes hertzianos," 2018. [Online]. Available: https://docplayer.com.br/94042743-Sistemas-de-telecomunicacoes-feixes-hertzianos-sistemas-de-telecomunicacoes.html.
- [27] E. Kofidis, V. Dalakas, Y. Kopsinis, and S. Theodoridis, "A novel efficient cluster-based mlse equalizer for satellite communication channels with-qam signaling," *EURASIP Journal on Advances in Signal Processing*, vol. 2006, pp. 1–16, 2006.
- [28] "Ieee standard letter designations for radar-frequency bands," *IEEE Std 521-2002 (Revision of IEEE Std 521-1984)*, pp. 1–10, 2003. doi: 10.1109/IEEESTD.2003.94224.
- [29] C. Salema, Feixes Hertzianos. IST Press, 1998.
- [30] W. L. Stutzman, "Estimating directivity and gain of antennas," *IEEE Antennas and Propagation Magazine*, vol. 40, no. 4, pp. 7–11, 1998.
- [31] The concept of transmission loss for radio links, P.341-7, ITU-R, 2019. [Online]. Available: https://www.itu.int/rec/R-REC-P.341.
- [32] C. A. Balanis, "Fundamental parameters and definitions for antennas," *Modern Antenna Handbook*, pp. 1–56, 2008.
- [33] Reliability and availability of analogue cable transmission systems and associated equipments, G.602, ITU-R, 1988. [Online]. Available: https://www.itu.int/rec/T-REC-G.602.
- [34] Availability objectives for real digital radio-relay links forming part of a high-grade circuit within an integrated services digital network, F.695-0, ITU-R, 1990. [Online]. Available: https://www.itu.int/rec/R-REC-F.695.
- [35] D. B. Faria *et al.*, "Modeling signal attenuation in ieee 802.11 wireless lans-vol. 1," *Computer Science Department, Stanford University*, vol. 1, 2005.

- [36] Calculation of free-space attenuation, P.525-4, ITU-R, 2019. [Online]. Available: https://www.itu.int/rec/R-REC-P.525.
- [37] Propagation by diffraction, P.526-15, ITU-R, 2019. [Online]. Available: https://www.litu.int/rec/R-REC-P.526.
- [38] Attenuation by atmospheric gases and related effects, P.676-13, IEEE, 2022. [Online]. Available: https://www.itu.int/rec/R-REC-P.676.
- [39] Specific attenuation model for rain for use in prediction methods, P.838-3, ITU-R, 2005. [Online]. Available: https://www.itu.int/rec/R-REC-P.838.
- [40] Propagation data and prediction methods required for the design of terrestrial line-of-sight systems, P.530-18, ITU-R, 2021. [Online]. Available: https://www.itu.int/rec/R-REC-P.530.
- [41] Error performance objectives for real digital fixed wireless links used in 27 500 km hypothetical reference paths and connections, F.1668-1, ITU-R, 2007. [Online]. Available: https://www.itu.int/rec/R-REC-F.1668.
- [42] End-to-end error performance parameters and objectives for international, constant bit-rate digital paths and connections, G.826, ITU-R, 2002. [Online]. Available: https://www.litu.int/rec/T-REC-G.826.
- [43] Error performance objectives for real digital radio links used in the national portion of a 27500 km hypothetical reference path at or above the primary rate, F.1491-2, ITU-R, 2002. [Online]. Available: https://www.itu.int/rec/R-REC-F.1491.
- [44] S. Winitzki, "A handy approximation for the error function and its inverse," *A lecture note obtained through private communication*, 2008.
- [45] W. H. Press, S. A. Teukolsky, W. T. Vetterling, and B. P. Flannery, *Numerical recipes in Fortran 77 the art of parallel scientific computing*. Cambridge university press, 1992.
- [46] Effects of multipath propagation on the design and operation of line-of-sight digital fixed wireless systems, F.1093-1, ITU-R, 2006. [Online]. Available: https://www.itu.int/ rec/R-REC-F.1093.
- [47] Propagation data and prediction methods required for the design of terrestrial line-of-sight systems, P.530-9, ITU-R, 2002. [Online]. Available: https://www.itu.int/rec/R-REC-P.530.

- [48] M. Zamaro, "Coupled orbital and attitude sdre control system for spacecraft formation flying," 2011.
- [49] NASA. "Definition of two-line element set coordinate system." (2022), [Online]. Available: https://web.archive.org/web/20200609193115/https://spaceflight.nasa.gov/realdata/sightings/SSapplications/Post/JavaSSOP/SSOP_Help/tle_def.html.
- [50] Propagation data and prediction methods required for the design of earth-space telecommunication systems, P.618-13, ITU-R, 2017. [Online]. Available: https://www.itu.int/ rec/R-REC-P.618.
- [51] Characteristics of precipitation for propagation modelling, P.837-7, ITU-R, 2017. [Online]. Available: https://www.itu.int/rec/R-REC-P.837/en.
- [52] Topography for earth-space propagation modelling, P.1511-2, ITU-R, 2019. [Online]. Available: https://www.itu.int/rec/R-REC-P.1511/en.
- [53] Rain height model for prediction methods, P.839-4, ITU-R, 2013. [Online]. Available: https://www.itu.int/rec/R-REC-P.839/en.
- [54] Electron. "Electron documentation." (2022), [Online]. Available: https://www.electronjs.org/docs/latest (visited on 09/21/2022).
- [55] V. Cosentino, J. L. Cánovas Izquierdo, and J. Cabot, "A systematic mapping study of software development with github," *IEEE Access*, vol. 5, pp. 7173–7192, 2017. doi: 10.1109/ACCESS.2017.2682323.
- [56] P. Shirley, M. Ashikhmin, and S. Marschner, *Fundamentals of computer graphics*. AK Peters/CRC Press, 2009.
- [57] L. Fraiture, "A history of the description of the three-dimensional finite rotation," *The Journal of the Astronautical Sciences*, vol. 57, no. 1, pp. 207–232, 2009.
- [58] Telewave.io. "Antenna pattern files." (2022), [Online]. Available: https://www.telewave.com/resources/antenna-pattern-files/ (visited on 08/31/2022).
- [59] Plotly. "Plotly documentation." (2022), [Online]. Available: https://plotly.com/javascript/ (visited on 08/31/2022).

- [60] K. Klasing, D. Althoff, D. Wollherr, and M. Buss, "Comparison of surface normal estimation methods for range sensing applications," in *2009 IEEE international conference on robotics and automation*, Ieee, 2009, pp. 3206–3211.
- [61] G. Getz, *Improving performance with explicit rendering*, Jan. 2018. [Online]. Available: https://cesium.com/blog/2018/01/24/cesium-scene-rendering-performance/.
- [62] OpenWeather. "Openweathermap api documentation." (2022), [Online]. Available: https://openweathermap.org/current/(visited on 08/15/2022).